Earthquake Tests on Scale 1:5 RC-Frames

Skjærbæk, P. S.; Nielsen, Søren R. K.; Kirkegaard, Poul Henning

Publication date:
1997

Document Version
Early version, also known as pre-print

INSTITUTTET FOR BYGNINGSTEKNIK
DEPT. OF BUILDING TECHNOLOGY AND STRUCTURAL ENGINEERING
AALBORG UNIVERSITET • AAU • AALBORG • DANMARK

FRACTURE & DYNAMICS
PAPER NO. 86

P.S. SKJÆRBÆK, S.R.K. NIELSEN, P.H. KIRKEGAARD
EARTHQUAKE TESTS ON SCALE 1:5 RC-FRAMES
MAY 1997 ISSN 1395-7953 R9713

The FRACTURE AND DYNAMICS papers are issued for early dissemination of research results from the Structural Fracture and Dynamics Group at the Department of Building Technology and Structural Engineering, University of Aalborg. These papers are generally submitted to scientific meetings, conferences or journals and should therefore not be widely distributed. Whenever possible reference should be given to the final publications (proceedings, journals, etc.) and not to the Fracture and Dynamics papers.

Printed at Aalborg University

Earthquake Tests on Scale 1:5 RC-frames

P.S. Skjærbæk S.R.K. Nielsen and P.H. Kirkegaard

Department of Building Technology and Structural Engineering,
Aalborg University, DK-9000 Aalborg, Denmark

Contents

1 Introduction **1**

2 Definition of the test structure **3**
2.1 Frame structure . . . 3
2.1.1 Reinforcement . . . 3
2.1.2 Concrete . . . 4
2.1.3 Shear reinforcement . . . 4
2.1.4 Beams and columns . . . 5
2.2 Reference specimens . . . 6
2.3 Definition of frames . . . 7

3 Precalculations with SARCOF **9**
3.1 Input parameters . . . 9
3.2 Determined dynamic characteristics . . . 9
3.3 Time analysis . . . 10
3.3.1 Generation of earthquake time series in SARCOF . . . 10
3.3.2 Damage Assessment . . . 12
3.4 Concluding remarks . . . 15

4 Test set-up and conduction of dynamic tests **17**
4.1 Shaking table . . . 17
4.2 Experimental set-up . . . 17
4.2.1 Free Decay Tests . . . 18
4.2.2 Instrumentation of frame AAU1 . . . 18
4.2.3 Instrumentation of frames AAU2 and AAU3 . . . 21
4.2.4 Data aquisition system . . . 21
4.3 Data processing . . . 21
4.3.1 Time integration . . . 21
4.3.2 Estimation of Storey Force-Deformation Curves . . . 22
4.3.3 Examples with simulated data . . . 24

5 Conduction of static tests **29**
5.1 Material testing . . . 29
5.1.1 Compression tests of concrete specimens . . . 29
5.1.2 Tension tests of reinforcement steel . . . 29
5.2 "Cut up" of test frame . . . 29
5.3 Static tests on reference and damaged specimens . . . 29

6 Non-destructive testing **31**
6.1 Data Processing 33
6.2 Non-destructive testing of frame AAU1 33
6.2.1 Free decay tests 33
6.3 Non-destructive testing of frame AAU2 38
6.3.1 Free decay tests 38
6.4 Non-destructive testing of frame AAU3 41
6.4.1 Free decay tests 41

7 Destructive testing **45**
7.1 Results for frame AAU1 46
7.1.1 Processed data 50
7.2 Results for frame AAU2 52
7.2.1 Processed data 55
7.3 Results for frame AAU3 59
7.3.1 Processed data 63

8 Results of reference tests and static bending tests **65**
8.1 Compression tests of reference concrete specimens 65
8.2 Tension tests of reference steel specimens 65
8.2.1 Longitudinal reinforcement steel 65
8.3 Static bending tests of beams and columns 65
8.3.1 Results of Static bending tests 67

9 Results of visual inspection after each run **79**
9.1 Definition of used classifications 79
9.2 Frame AAU1 79
9.3 Frame AAU2 80
9.4 Frame AAU3 81

10 Summary **83**

Bibliography **84**

Appendices

A Photos **89**
A.1 The construction process 89
A.2 Destructive testing and damage evaluation 93
A.3 Static Testing 97
A.4 Visual inspection of AAU2 and AAU3 99

B File Data Sheets **103**

Chapter 1

Introduction

When civil engineering structures are subjected to sufficiently high dynamic loads it is well known that some kind of damage will occur somewhere in the structure. In RC-structures the damage may start as cracking developing into crushing of concrete and yielding of reinforcement. The damage may be highly localized or more spread out in the structure. During an earthquake both types of damage may develop in the structure and there is a need for methods to assess the damage in the structure. The traditional way of assessing damage in RC-structures is by visual inspection of the structure by measuring cracks, permanent deformations, etc. This is often very cumbersome, since panels and other walls covering beams and columns need to be removed. Furthermore, internal damage such as bond slippage can be very difficult to determine by visual inspection. However, a much more attractive method is measuring of the structural response at a given location of the structure. From this response time series, damage indicators based on e.g. changes in dynamic characteristics, accumulated dissipated energy, low cycle fatigue models, stiffness or flexibility changes etc. can be calculated. In the literature several methods for damage assessment from measured responses has been presented during the last 2 decades, see Banon et al. [1] Stubbs et al. [55], Penny et al., [35], Casas [6], DiPasquale et al. [8], Hassiotis et al. [12], Kirkegaard et al. [14], Koh et al. [18], Pandey et al. [30], Park et al. [31], Penny et al. [35], Reinhorn et al. [36], Rodriguez-Gomes [37], Skjærbæk et al. [42], [43], [44], Stephens et al. [52], [53], [54] and Vestroni et al. [60].

The motivation for performing earthquake experiments on a 1:5 scale 6-storey, 2-bay model test frame is to provide data for verification and validation of these methods for non-destructive damage assessment of RC-frames based on one or more measured reponses of the structure. The purpose of this report is to give a presentation of the data collected from a series of test performed on 7 RC-frames in the Autumn 1996/Winter 1996-1997 at the structural laboratory at Aalborg University, Denmark.

The 7 frames are tested in pairs of 2 giving 3 identical experimental set-ups and the last frame is used as spare/reference. Each of the 3 experimental set-ups are equipped with an extensive instrumentation measuring accelerations at all storeys and the base acceleration. Furthermore, after each damaging event is subjected to the frame a detailed inspection is performed of every structural component in the frames.

The report is organized so that chapter 2-4 describe the design of the frames and how the frames and reference specimens are tested both non-destructive and destructive. In chapter 5 it is described how various static tests are performed. Chapter 6 present the results of the non-destructive testing and chapter 7 results from the destructive strong motion experiments.

Chapter 8 present results from material testing and static bending tests of the reference frame as well as the damaged frames. Finally chapter 9 presents the results of the visual inspections performed during the destructive strong motion experiments. Appendix A contains photos taking during the entire process from casting of the frames until the final visual inspection. Appendix B describes the metheodology used for generation of the used ground motions in the shaking table tests.

Chapter 2

Definition of the test structure

For the test series 7 reinforced concrete frames were casted one at a time since only one form was available. For each frame casting reference specimens were casted for determination of compression strength of the concrete used for each of the frames. In the following the design specifications of the frames and the reference specimens are described.

2.1 Frame structure

All the 7 frames considered in the test series were constructed identically. The test frame considered is a 6-storey, 2-bay RC-frame. The dimensions of the test frame is 2400 by 3300 mm. Corresponding to a "real" structure with dimensions 12 by 16.5 m. The test frame is build of 50 by 60 mm RC-sections reinforced with 6 mm KS410. A plane view of the test frame is shown in figure 2.1. The weight of each frame is $\approx$ 2 kN. To model the storey deck, 8 RC beams (0.12*0.12*2.0m) are placed on each storey. The total weight per frame is then $\approx$ 20 kN.

2.1.1 Reinforcement

All longitudinal reinforcement used in the frame and reference specimens are of the type KS410 (ribbed steel) with a characteristic (2% fractile) yield stress of 410 MPa.

The amount of reinforcement used in each frame are listed in table 2.1.

No.	Type	size	Thickness/diameter
24	KS410	2460 mm	6 mm
12	KS410	3300 mm	6 mm
12	flat-steel, type1	50x60 mm	6 mm
1	flat-steel, type2	50x60 mm	6 mm
2	flat-steel	50x55 mm	6 mm
3	flat-steel	100x150 mm	10 mm

Table 2.1: *Amount of steel in each RC-frame.*

The steel used in each frame equal approximately 22 kg.

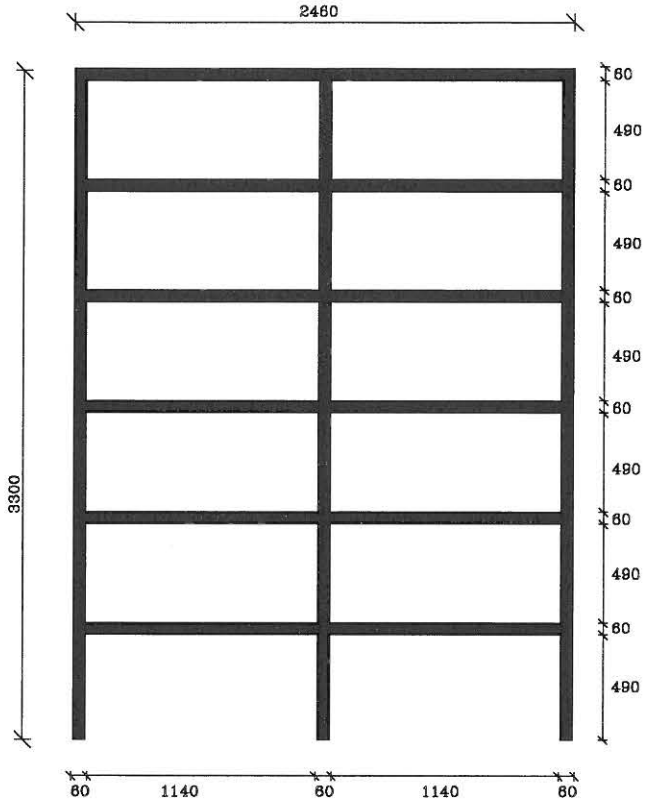

Figure 2.1: Plane view of test frames.

To avoid overlapping longitudinal reinforcement giving uncontrolled changes in bending stiffness and strength the longitudinal reinforcement bars are ended with anchoring steel-plates welded to the reinforcement.

2.1.2 Concrete

The concrete used has a design compression strength of 25 MPa with a maximum aggregate diameter of 5 mm. For each frame is used approximately 80 l concrete.

2.1.3 Shear reinforcement

The columns in the lower storey are reinforced for shear with 3mm steel thread (St37) which has been formed into spirals, see figure 2.3.

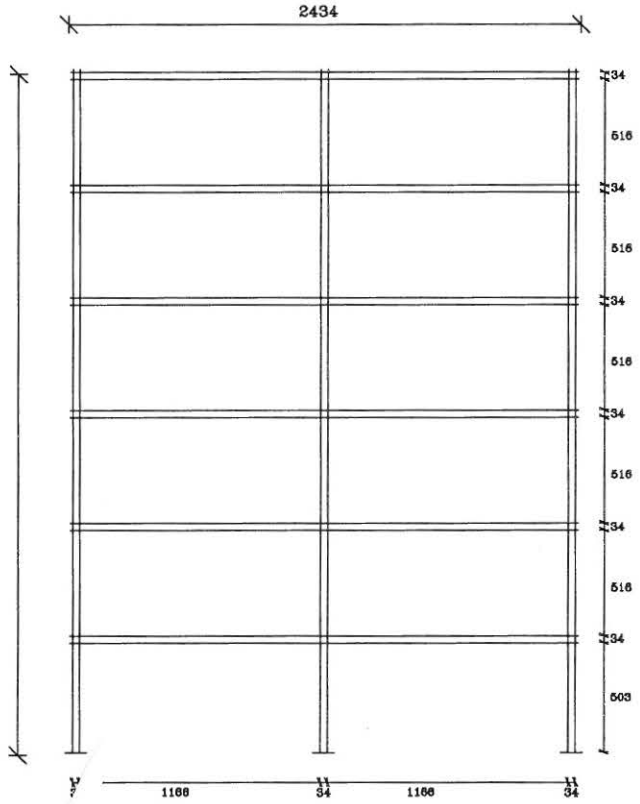

Figure 2.2: Main reinforcement in frame. All measures in mm.

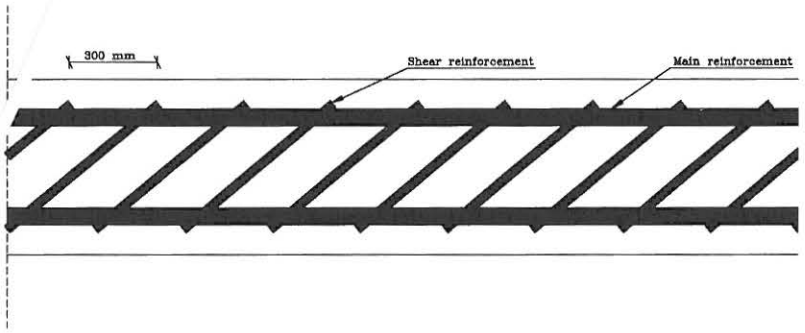

Figure 2.3: Shear reinforcement of columns in the lower storey.

2.1.4 Beams and columns

The dimensions of the beams and columns in the frame are constant all over the frame with outer measures of 50 × 60 mm. Columns are reinforced with 6ø6 KS410 (ribbed steel) and beams with 4ø6 KS410, see figure 2.4.

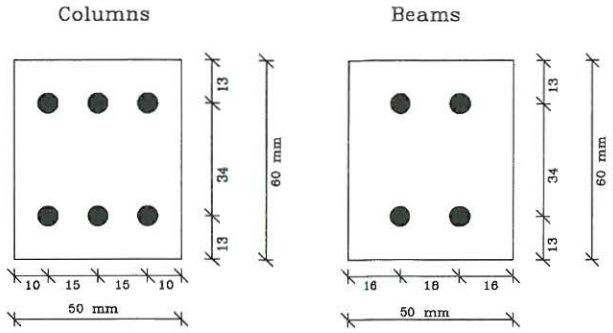

Figure 2.4: Cross-section of beam and columns.

2.2 Reference specimens

For determination of the strength and stiffness parameters of the concrete, 3 circular specimens with dimensions $100 \cdot 200$ compression tests of the concrete are casted. For determination of the strength and stiffness parameters of the reinforcement 3 reinforcement bars with length 500 mm are tested in tension. The reference specimens are shown in figure 2.5.

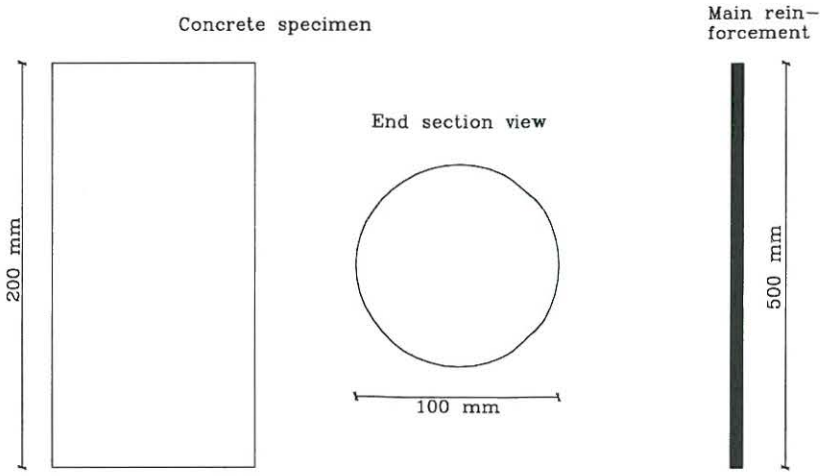

Figure 2.5: Reference specimens.

To provide data for the reference stiffness and strength of the beams and columns in the frames one frame are produced to be cut into pieces as is the case for the frames that have been dynamically tested. These pieces are tested in the same way as the damaged parts.

2.3 Definition of frames

In the tests described in this report three different experimental set-ups are considered. These set-ups are through-out the report referred to as AAU1, AAU2 and AAU3, respectively. Since each set-up consists of two frames which are instrumented independently, these are referred to as e.g. AAU1a and AAU1b.

Chapter 3

Precalculations with SARCOF

To obtain some guidelines for how the structure will be damaged at a certain earthquake magnitude a series of simulations are performed using the non-linear finite element programme SARCOF which have been proven to predict the dynamic characteristics of deteriorating RC structures, Mørk [24]. The programme is based on the implementation of Roufaiel-Mayer hysteretic oscillators the different elements of the structure. The ground motions applied to the structure is generated using amplitude modulated gaussian white noise filtered through a Kanai-Tajimi filter. The programme is troughoutly described in Mørk [25].

3.1 Input parameters

Since no compression or tension tests have been performed at the time of the preliminary SARCOF calculations, the material characteristics has to be roughly estimated for the analysis. In the calculations the cross-section characteristics shown in table 3.1 are used.

	I_{uc} $[10^{-6}m^4]$	I_{cr} $[10^{-6}m^4]$	E_c $[\frac{\mathrm{N}}{\mathrm{m}^2}]$	M_y [Nm]
Column	1.12	0.48	35000	930
Beam	1.00	0.41	35000	820

Table 3.1: *Characteristics of cross-sections.*

3.2 Determined dynamic characteristics

Initially the SARCOF program calculates the damped two lowest eigenfrequencies and correponding mode shapes. In the calculations a damping of 0.05 is assumed in all modes. Since the frames will be partially cracked at the beginning of the tests, the eigenfrequencies and mode shapes are calculated for the undamaged uncracked and cracked structure. In the SARCOF program it is optional whether the $P-\delta$ effect is taken into consideration and the frequencies of the structure is therefore calculated with and without the $P-\delta$ correction. The calculated frequencies for the uncracked and cracked structure are listed in table 3.2.
From table 3.2 it is seen that the P-δ effect influence on the calculated frequencies seems to be relatively limited.

	f_1 [Hz]	f_2 [Hz]
Uncracked (without correction)	2.98	9.47
Cracked (without correction)	1.93	6.13
Uncracked (with correction)	2.96	9.43
Cracked (with correction)	1.90	6.07

Table 3.2: *Calculated eigenfrequencies for the uncracked and cracked structure.*

In figure 3.1 the two lowest modes shapes are shown for the frame structure.

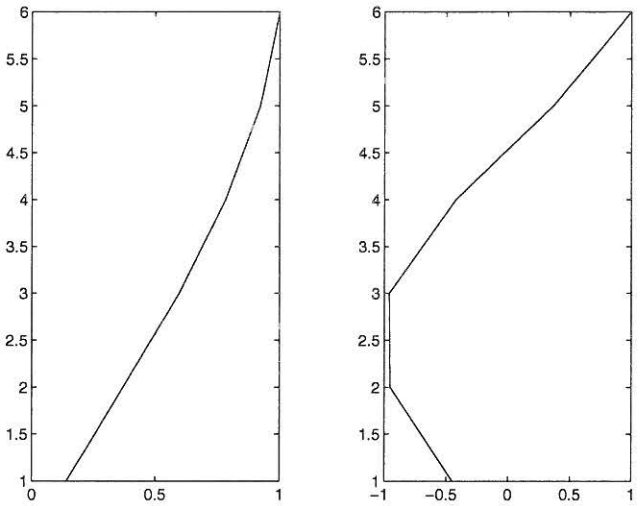

Figure 3.1: The two lowest mode shapes of the undamaged structure

3.3 Time analysis

To obtain some guidelines for how and how much the structure get damaged at different load levels 5 simulations with different load levels are performed. The load level are here defined by the maximum peak acceleration which have been proven to be highly correlated to the damage level of the structure. In each simulation the load time series are applied to the undamaged cracked structure.

3.3.1 Generation of earthquake time series in SARCOF

The acceleration process at the ground surface used in the precalculations are determined as the response process of a intensity modulated Gaussian white noise, filtered through a Kanai-Tajimi filter, Tajimi [57]. A Kanai-Tajimi filter can be visualized as a model of the dynamic response of a sediment layer subjected to earthquake excitations applied at the surface of an underlying bedrock, see figure 3.2a. The mass of the sediment layer is assumed to be infinitely large compared to the mass of the structure, and only a single mode with undamped circular eigenfrequency ω_0 and damping ratio ζ_0 is considered in the modal expansion of the response of the sediment layer. The displacement of the earth surface r_0 relative to the bedrock surface

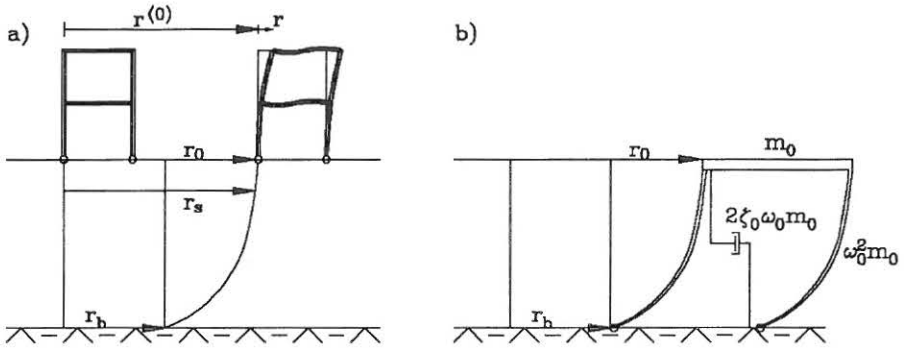

Figure 3.2: Earthquake excitation model. a) Definitions of parameters. b) Mechanical analogy of Kanai-Tajimi filter.

is then related to the bedrock acceleration $\ddot{r}_b$ by the differential equation

$$\ddot{r}_0 + 2\zeta_0\omega_0\dot{r}_0 + \omega_0^2 r_0 = -\ddot{r}_b \tag{3.1}$$

The bedrock acceleration process $\{\ddot{r}_b(t), t \in [0 : \infty[\}$ is modelled as a time modulated unit Gaussian white noise process, i.e.

$$\ddot{r}_b dt = \beta(t) dW(t) \tag{3.2}$$

$\{W(t), t \in [0; \infty[\}$ is a unit Wiener process, which is a Gaussian process with the increment proporties

$$E[dw(t)] = 0, \quad E[dW(t_1)dW(t_2)] = \begin{array}{l} 0, \ t_1 \neq t_2 \\ dt, \ t_1 = t_2 \end{array} \tag{3.3}$$

Realizations of the unit Gaussian white noise process are generated by the method of Ruiz and Penzien [38].

$\beta(t)$ is a deterministic intensity envelope function, defined as

$$\beta(t) = \beta_0 \begin{cases} \left(\frac{t}{t_1}\right)^2 & ,0 \leq t \leq t_1 \\ 1 & ,t_1 \leq t \leq t_0 + t_1 \\ \exp(-c(t - t_0 - t_1)) & ,t_0 + t_1 \leq t \end{cases} \tag{3.4}$$

where β_0 is a given amplitude.
The acceleration at the ground surface is then given as

$$\ddot{\mathbf{r}}_s(t) = \mathbf{R}_s(\ddot{r}_b + \ddot{r}_0) = \mathbf{R}_s(-2\zeta_0\omega_0\dot{r}_0 - \omega_0^2 r_0) \tag{3.5}$$

where $\mathbf{R}_s$ is a two-dimensional amplitude vector.

The structure is exposed to the five time series shown in figure 3.3.

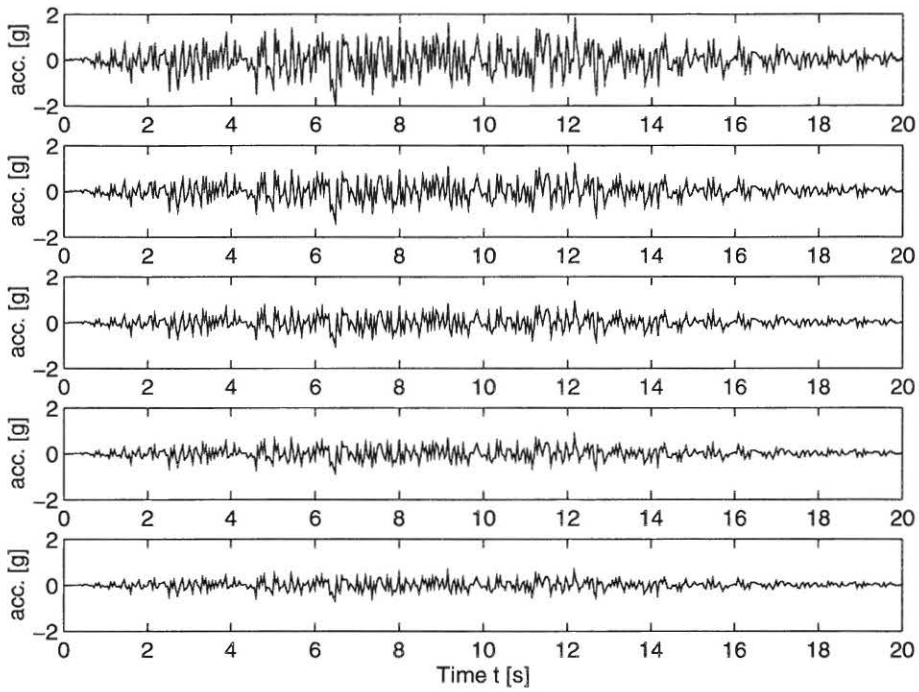

Figure 3.3: The five simulated ground motions exposed to the structure. a) $a_{max} = 0.83 \cdot 9.82 \frac{\mathrm{m}}{\mathrm{s}^2}$, b) $a_{max} = 1.04 \cdot 9.82 \frac{\mathrm{m}}{\mathrm{s}^2}$, c) $a_{max} = 1.25 \cdot 9.82 \frac{\mathrm{m}}{\mathrm{s}^2}$, d) $a_{max} = 1.66 \cdot 9.82 \frac{\mathrm{m}}{\mathrm{s}^2}$, e) $a_{max} = 2.48 \cdot 9.82 \frac{\mathrm{m}}{\mathrm{s}^2}$ $\omega_0 = 10\mathrm{s}^{-1}$, $\zeta_0 = 0.3$, $t_0 = 10\mathrm{s}$, $t_1 = 3\mathrm{s}$ and $c = 0.2$

3.3.2 Damage Assessment

As a measure of damage the socalled maximum softening damage index δ_M is used and it is defined as

$$\delta_M = 1 - \frac{T_{max}}{T_0} \tag{3.6}$$

where T_{max} is the maximum value of the lowest eigenperiod during the seismic event and T_0 is the initial eigenperiod of the undamaged structure.

In figures 3.4-3.8 the top storey response and the development in the maximum softening are shown for the three cases.

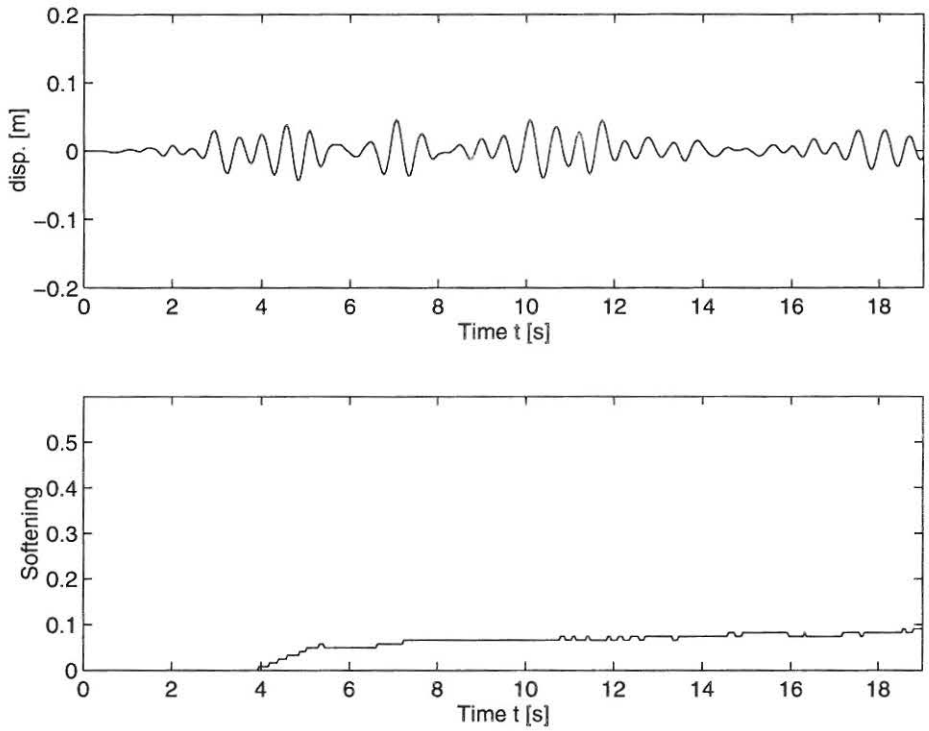

Figure 3.4: Top storey response and development in softening for the first case. $\delta_M = 0.09$.

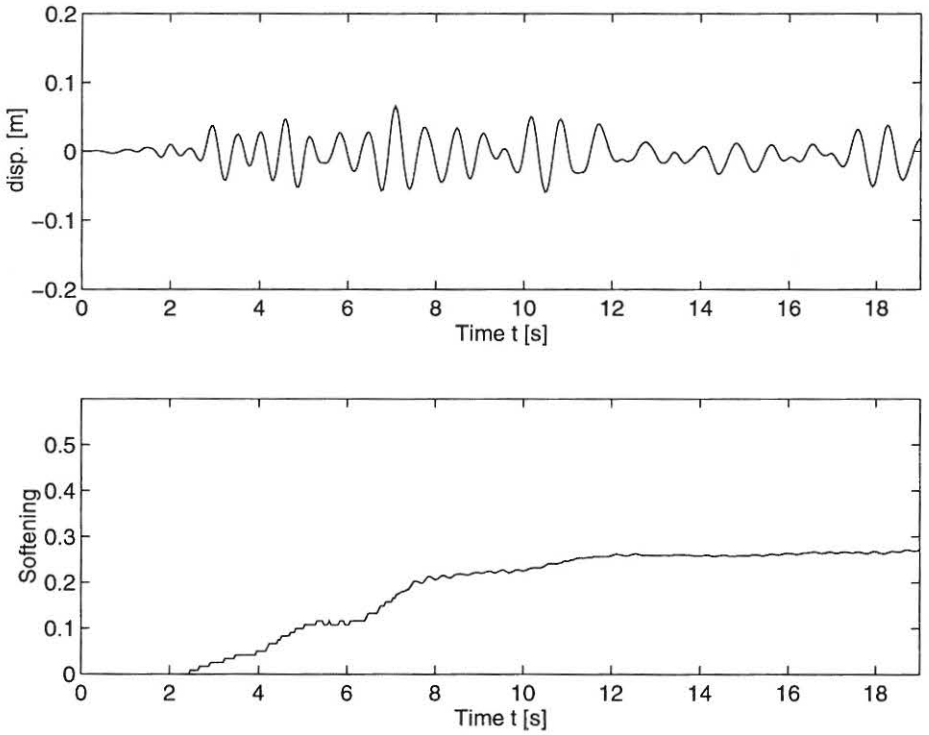

Figure 3.5: Top storey response and development in softening for for the second case. $\delta_M = 0.27$.

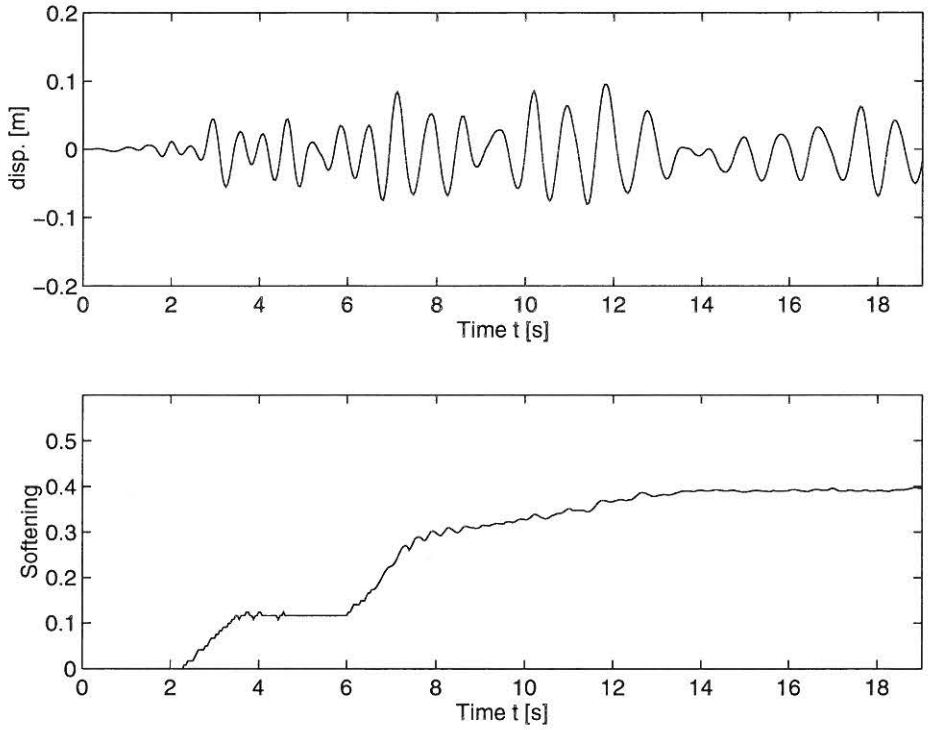

Figure 3.6: Top storey response and development in softening for the third case. $\delta_M = 0.40$.

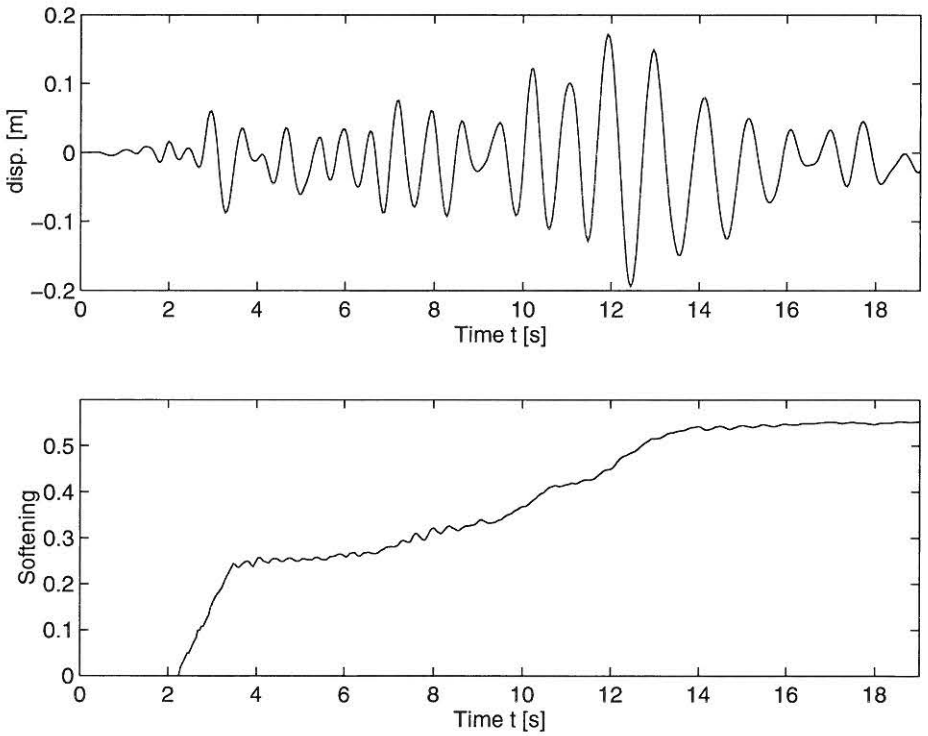

Figure 3.7: Top storey response and development in softening for the fourth case. $\delta_M = 0.56$.

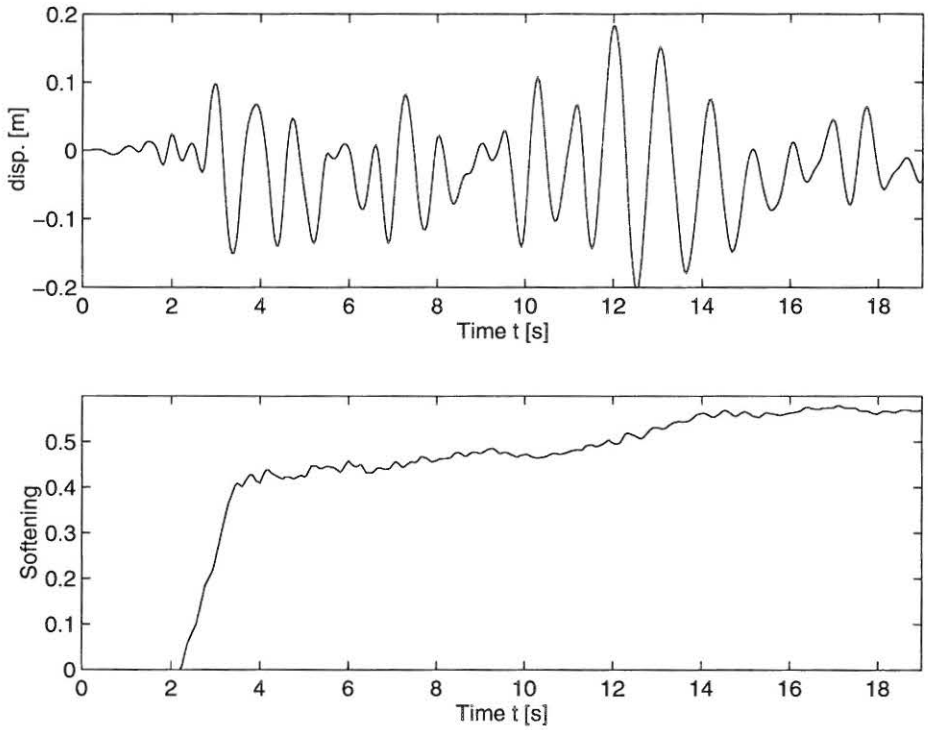

Figure 3.8: Top storey response and development in softening for the fifth case. $\delta_M = 0.58$.

From the figures 3.4-3.8 the maximum softening is extracted and is listed for the five cases in table 3.3

Case	$a_{max}[g]$	δ_M
1	0.83	0.09
2	1.04	0.27
3	1.24	0.40
4	1.66	0.56
5	2.48	0.58

Table 3.3: *Maximum softenings obtained by SARCOF for different maximum peak accelerations.*

3.4 Concluding remarks

From the numerical analysis performed in this chapter it can be concluded that the structure only will suffer minor damage for earthquakes with a peak acceleration less than $1g$. On the other hand it seems as if the damage level increases quite dramatically when the peak acceleration reaches the interval 1 to 1.5 g.

Chapter 4

Test set-up and conduction of dynamic tests

4.1 Shaking table

The shaking table is constructed of two frames of HEB 160 steel profile. The two frames are connected by two linear leaders with a dynamic carring capacity of 9000 N per carriager. The force is produced by a 63 kN HBM cylinder with a ± 20 mm displacement field. A schematic view of the shaking table is shown in figure 4.1.

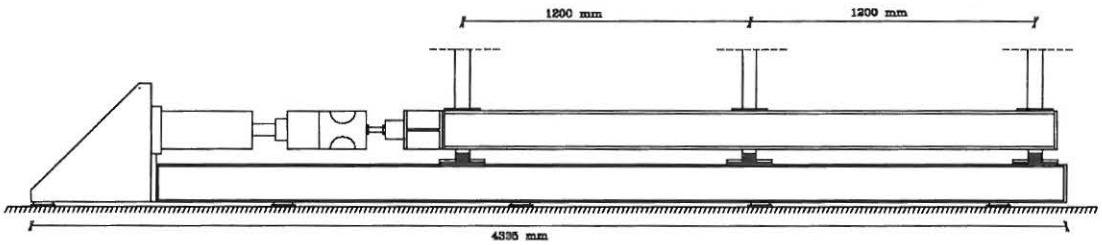

Figure 4.1: Dimensions of shaking table.

4.2 Experimental set-up

The frames are tested in pairs of two where the same ground surface acceleration is applied to the two frames. The frames are placed at the shaking table at a distance of 1000 mm and is stabilized in space by a steel cross at each end.

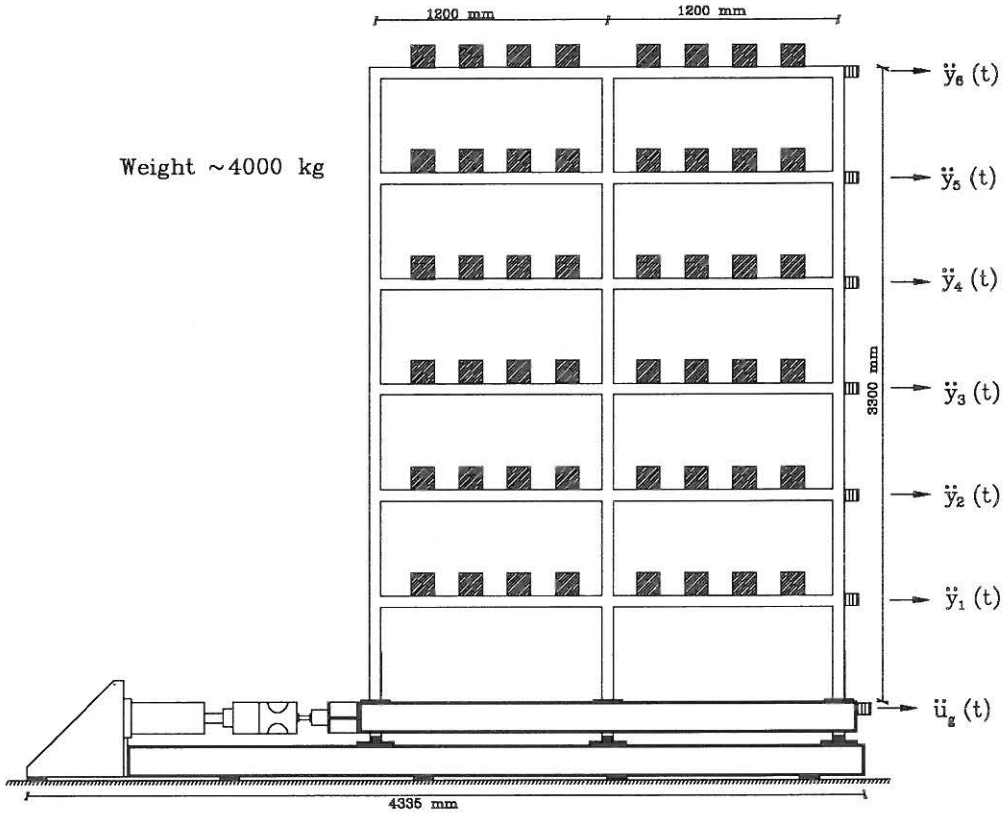

Figure 4.2: Side view of experimental set-up.

The hydraulic cylinder providing the base motions is controlled by a HBM computer system. In the connection between the shaking table and the hydraulic cylinder a load cell is placed to measure the actual cylinder force as a function of time. Furthermore, the cylinder is capable of measuring the cylinder displacements as function of time.

4.2.1 Free Decay Tests

Free decay tests with the frames was in case of frame AAU1 performed by applying a horizontal force at the top storey of the frame. This was done manually by means of a rope.

For the structures AAU2 and AAU3 the pull-out of the top storey was changed to a set-up where a load-cell was used to measure the pull-out force, see figure 4.3.

4.2.2 Instrumentation of frame AAU1

Each storey of the left frame are instrumented with an accelerometer measuring the horizontal acceleration of the storey and the right frame are instrumented with an accelerometer at the 2nd, 4th and 6th storey. Furthermore, the top storey of each of the frames are instrumented with a accelerometer which is analog double integrated on-line. To measure eventually rotations of the structure, the right frame is equipped with 2 accelerometers at the top storey measuring the "out-of-plane" movement of the frames. The total number of accelerometers are 14. The two last channels in the 16 channel data-logger system are used to measure the displacement

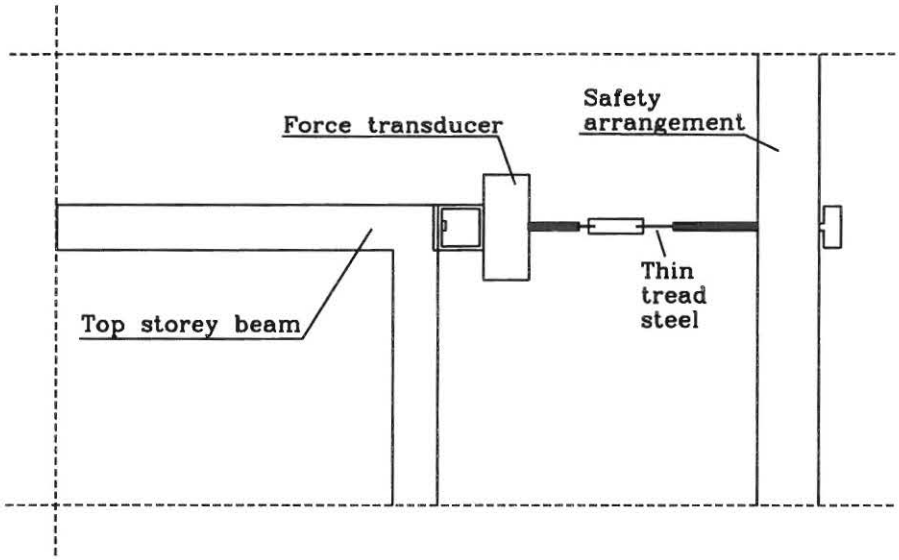

Figure 4.3: Pull out arrangement used for free decay tests.

and the force provided by the hydralic cylinder. The exact location of the measuring devices are shown in figure 4.4 and the number and type of transducers are shown in table 4.1.

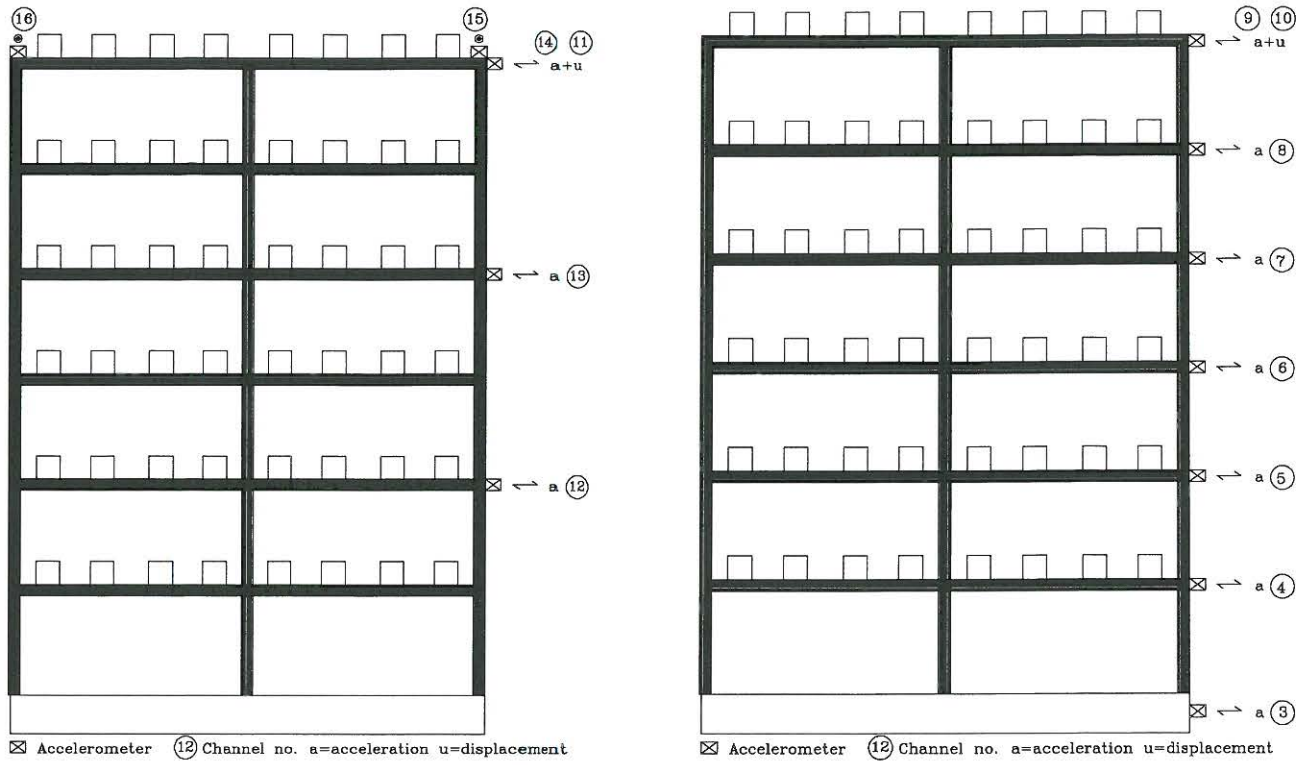

Figure 4.4: Instrumentation of the right and left frame in set-up AAU1.

Channel	Response	Type	Calibration
1	Force	HBM	10V=63kN
2	Displacement	HBM	10V=20mm
3	Acceleration	BK8306	0.991V/ms^{-2}
4	Acceleration	BK8306	0.989V/ms^{-2}
5	Acceleration	BK8306	0.994V/ms^{-2}
6	Acceleration	BK4370	Variable
7	Acceleration	BK4370	-
8	Acceleration	BK4370	-
9	Acceleration	BK4370	-
10	Displacement	BK4370	-
11	Displacement	BK4370	-
13	Acceleration	BK4371	-
14	Acceleration	BK4371	-
12	Acceleration	K8304B2	956mV/g
15	Acceleration	K8304B2	963mV/g
16	Acceleration	K8304B2	1027mV/g

Table 4.1: *The used transducers and calibration factors for frame AAU1. BK=Brüel and Kjær, K=Kistler.*

4.2.3 Instrumentation of frames AAU2 and AAU3

After the shaking table tests with frame AAU1 the instrumentation of the test frames were changed so all storeys at both the right and left frame were equipped with an accelerometer measuring the horizontal acceleration. Due to the experiences from the tests with frame AAU1 the entire set-up was changes in a manner that prevented the frame from making any rotational movements and the accelerometers used in the transverse direction was moved to measure horizontal accelerations at the right frame.
The exact location of the measuring devices on frame AAU2 and AAU3 are shown in figures 4.5 and the number and type of transducers are shown in table 4.2.

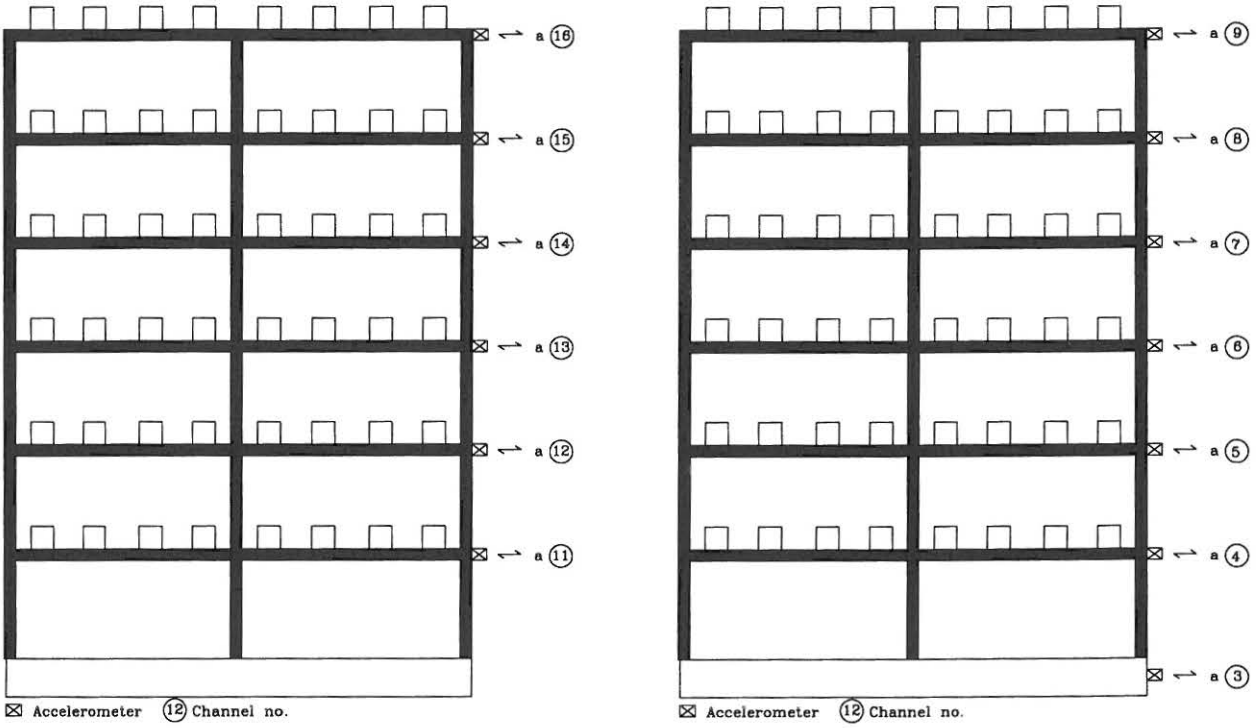

Figure 4.5: Instrumentation of the right and left frame for set-up AAU2 and AAU3.

4.2.4 Data aquisition system

All transducers are connected to a 16-channel HBM data acquisition system where data from all channels are sampled momentary with a rate of 150 Hz.

4.3 Data processing

4.3.1 Time integration

In order to evaluate the displacements or velocities from measured acceleration time-series, one or two time-integrations of the acceleration response becomes necessary. In reality, how-

Channel	Response	Type	Calibration
1	Force	HBM	10V=63kN
2	Displacement	HBM	10V=20mm
3	Acceleration	BK8306	9.86V/g
4	Acceleration	BK8306	9.80V/g
5	Acceleration	BK4370	$1.00V/ms^{-2}$
6	Acceleration	BK4370	$1.00V/ms^{-2}$
7	Acceleration	BK4370	$1.00V/ms^{-2}$
8	Acceleration	BK4370	$1.00V/ms^{-2}$
9	Acceleration	BK4370	$1.00V/ms^{-2}$
10	-	-	-
11	Acceleration	K8304B2	1027mV/g
13	Acceleration	K8304B2	963mV/g
14	Acceleration	K8304B2	956mV/g
12	Acceleration	K8304B2	1008mV/g
15	Acceleration	K8304B2	963mV/g
16	Acceleration	K8304B2	963mV/g

Table 4.2: *The used transducers and calibration factors. BK=Brüel and Kjær, K=Kistler.*

ever, measured acceleration data contain spurious response components caused by 1) uncontrolled phenomenas associated with the structure/system under study and 2) the measurement/recording system itself. These spurious components of the record, called noise, can significantly alter the character of the velocity and displacement histories obtained by succesive integration.
This process was intensively studied by Stephens [54] and he concluded that if the noise filled acceleration signal was used uncritically very misleading results may be obtained. Stephens [54] suggested that the acceleration signal was bandpassfiltered to cut very low and high frequencies components out of the signal before integration. After the first integration the velocity response was obtained and a new bandpassfiltering were performed before the last integration to obtain the displacement response. The suggested procedure to get from acceleration response to displacement response is illustrated in figure 4.6.

4.3.2 Estimation of Storey Force-Deformation Curves

From the acceleration measurement at each storey the force-deformation curve can be estimated for each storey. In the following a short review of a method for estimation of these from storey acceleration measurements of frame structures is given.
Stephens [54] used a relative simple method to estimate the interstorey force-displacement curve using acceleration response information. This method works in three steps. The lateral restoring force are calculated in a spring-mass model of the structure using the acceleration data. The corresponding deformations are obtained from the displacement response which is obtained from noise treatening and integration of the acceleration data. The force-deformation response is estimated from this information using a least squares interpolation technique.
Using a multi degree of freedom mass-spring model assigned one lateral degree of freedom at each measuring point (storey), where the storey mass is lumped. This is illustrated in figure 4.7.

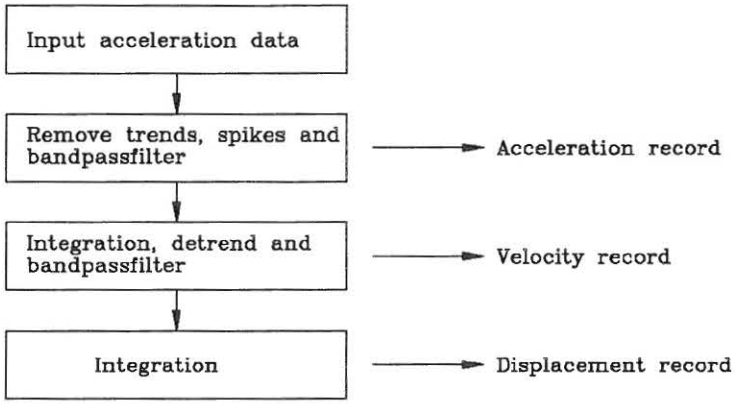

Figure 4.6: The procedure to transform acceleration response to displacement response. From Stephens.

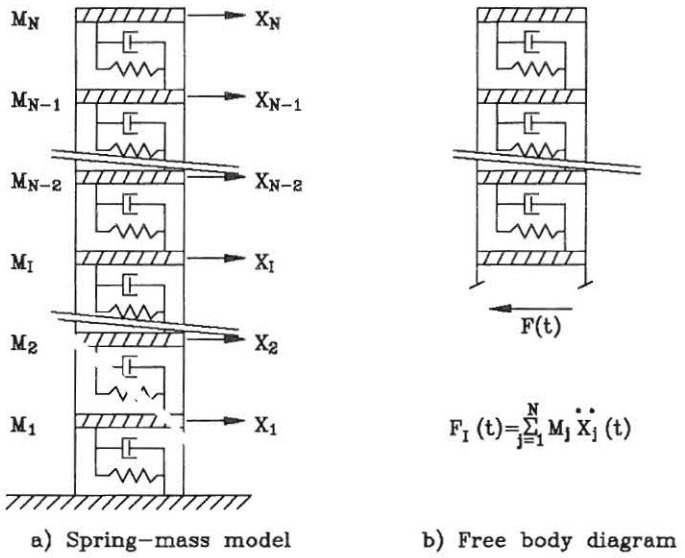

Figure 4.7: Simple spring-mass model.

The dynamical equilibrium expression will then be on the form

$$F_i(t) = \sum_{j=i}^{N} m_j \ddot{x}_j(t) \tag{4.1}$$

for each interval between the storeys. $F_i(t)$ is the restoring force in the storey below mass i, N is the total number of masses, m_j is the mass of storey j and $\ddot{x}_j(t)$ is the measured absolute acceleration at storey j. The restoring forces can the be calculated inserting the measured accelerations into eq. 4.1.
The deformation at each storey are calculated by taking the difference of the corresponding storey displacements obtained from integration of the measured accelerations.
The force-deformation response between adjacent masses of the structure is then estimated by a polynomial piecewise paired force and deformation histories, see figure 4.8.

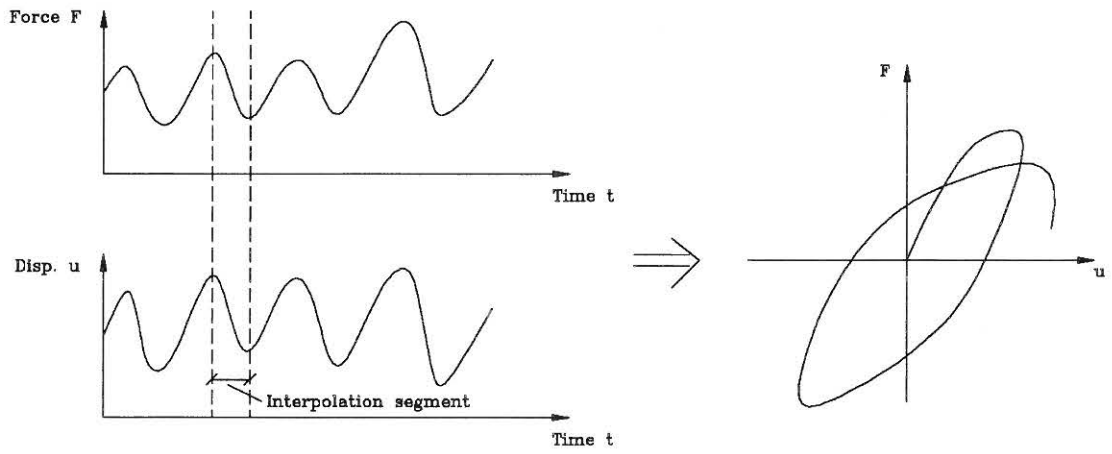

Figure 4.8: Piecewise paired force and deformation giving the force-deformation curve.

I should be noted, that this method is only effective for structures where the relative displacement directly displays the deformation behaviour as in the case of frame structures as illustrated in figure 4.9.

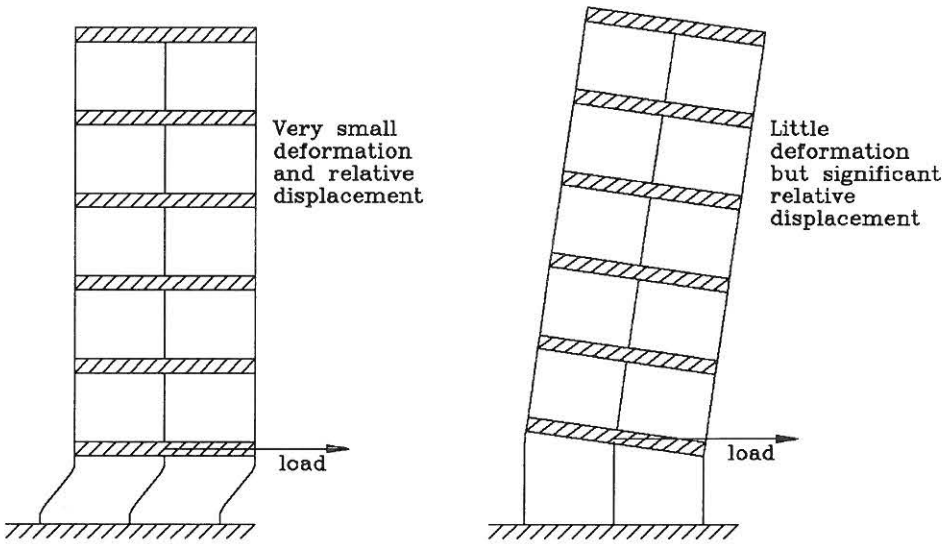

Figure 4.9: Relative displacement versus deformation response of frame and shear wall structure

4.3.3 Examples with simulated data

To illustrate some of the problems discussed in this section, two examples are given , where "perfect data" has been generated by the programme SARCOF, and some artificially generated noise has been added. In the first example the problems connected with integrating noisefilled signals it illustrated, and in the second example the need for the piecewise interpolation of the

force and displacement time series is illustrated.

Example 1: Integration of noise filled acceleration signal

Consider the two acceleration time series illustrated in figure 4.10. The signal in figure 4.10a is perfect noiseless and without trend and the signal shown in figure 4.10b is noisefilled with a slight trend.

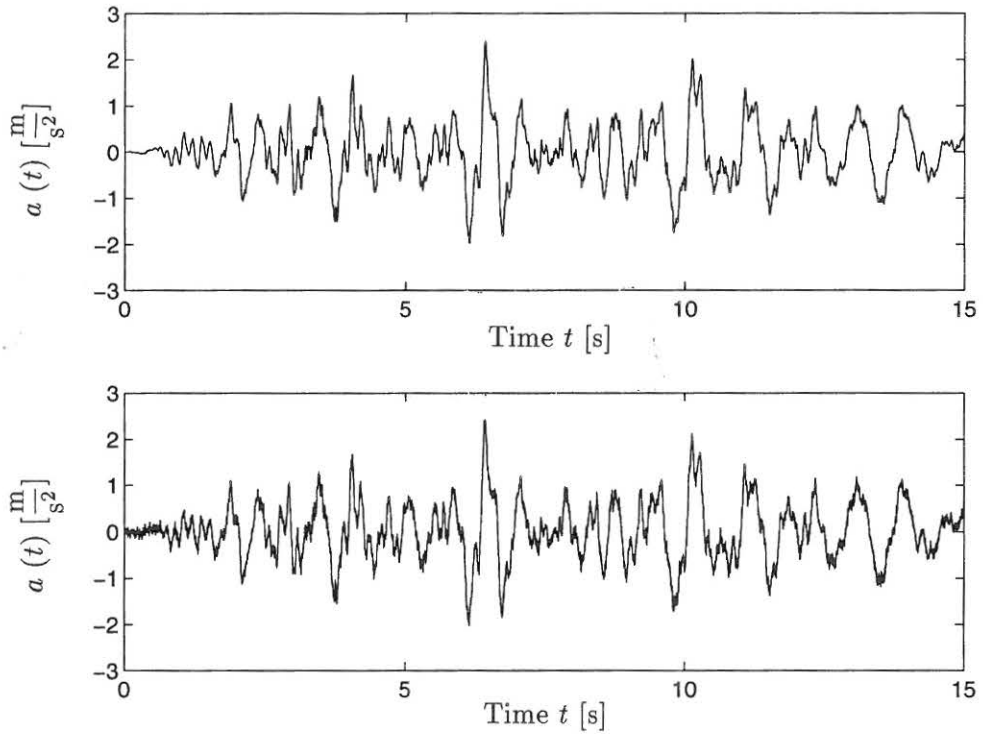

Figure 4.10: Acceleration time series, a) Noisefree and detrended and b) Noisefilled and trended.

It is seen from the presented example, that even little noise and a very sligt trend in the signal can cause a severe drift in the signal.

Example 2: Piecewise interpolation of the force-deformation curve

Even after the integration and filtration performed in the previous example, inaccuracies and noise makes the obtained restoring force timehistory and interstorey displacement time history unsuitable for direct plotting of the force-deformation curve. Consider the noise filled force and displacement time histories shown in figure 4.12 (generated with a noise-to-signal ratio $\frac{\sigma_{noise}}{\sigma_{signal}} = 0.05$. If the noise filled signals is used directly for plotting the force-deformation curve, the result as shown at figure 4.13b is obtained and compared to the correct curve in figure 4.13a it is seen that it is practically useless due to the large fluctuations.
If however, the piecewise interpolation is used, a much better result as shown in figure 4.14b is obtained.

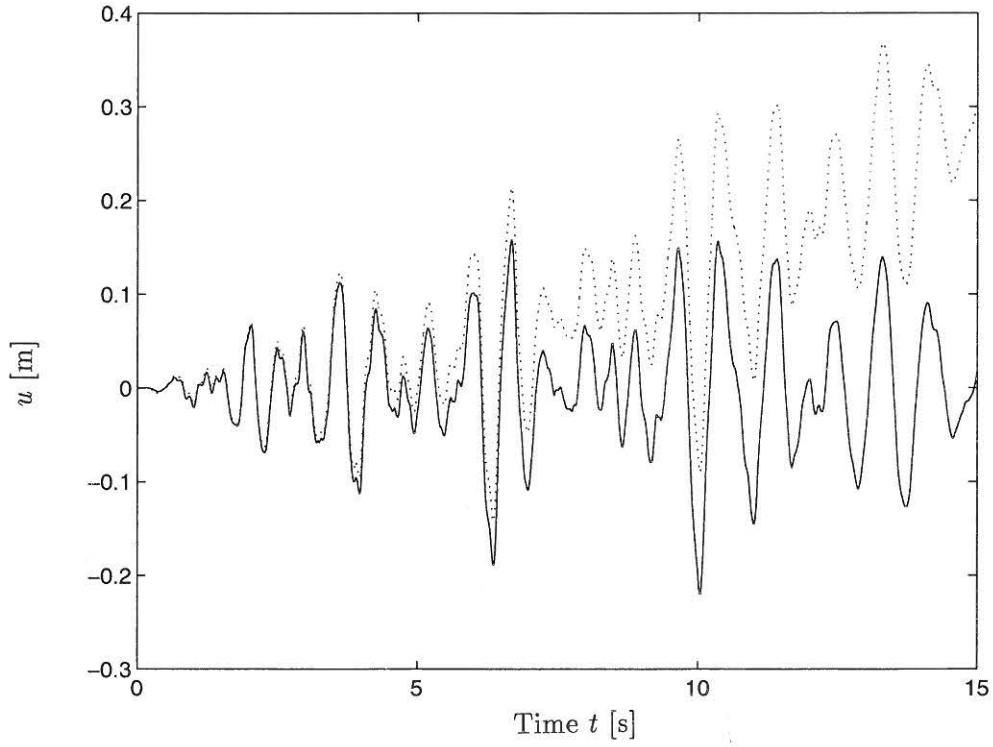

Figure 4.11: Displacement realisations obtained by direct integration of a) noise free and detrended data, and b) using noise poluted and trended data.

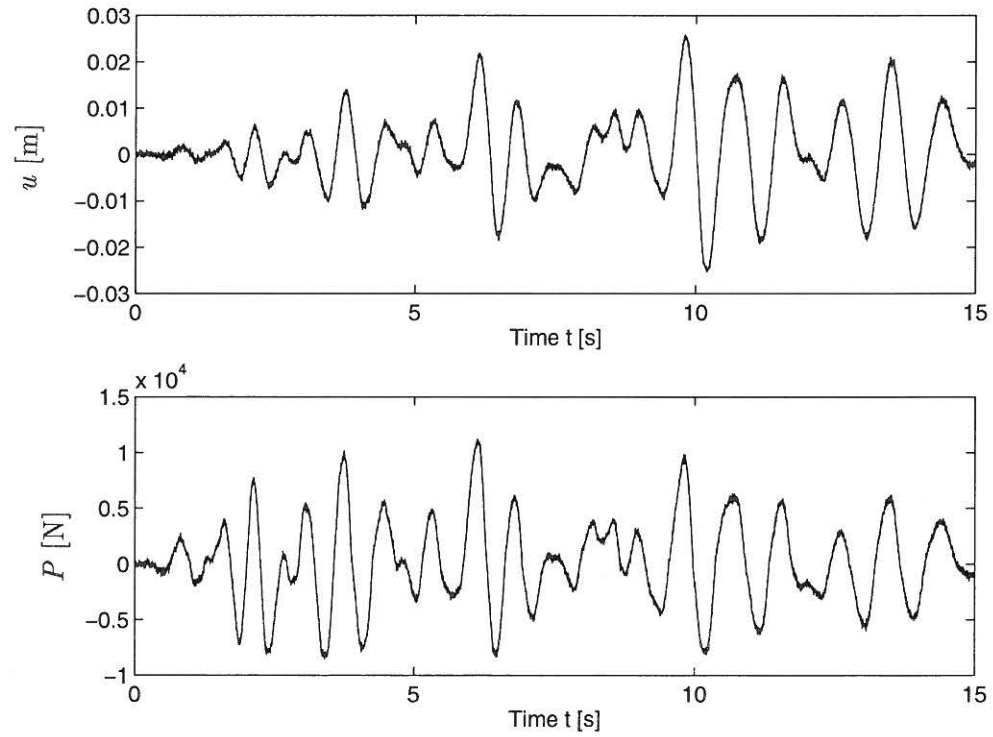

Figure 4.12: Noise filled restoring force and interstorey displacement time series.

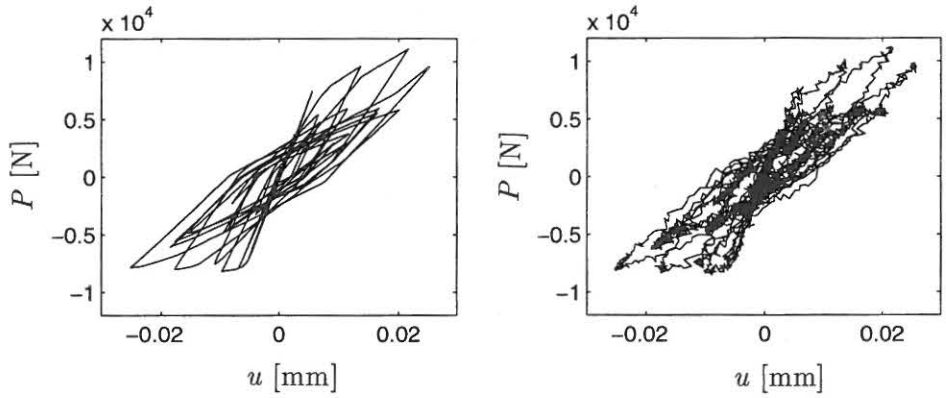

Figure 4.13: Force-deformation curves. a) Correct, b) Force-deformation curve obtained directly using noise filled time series.

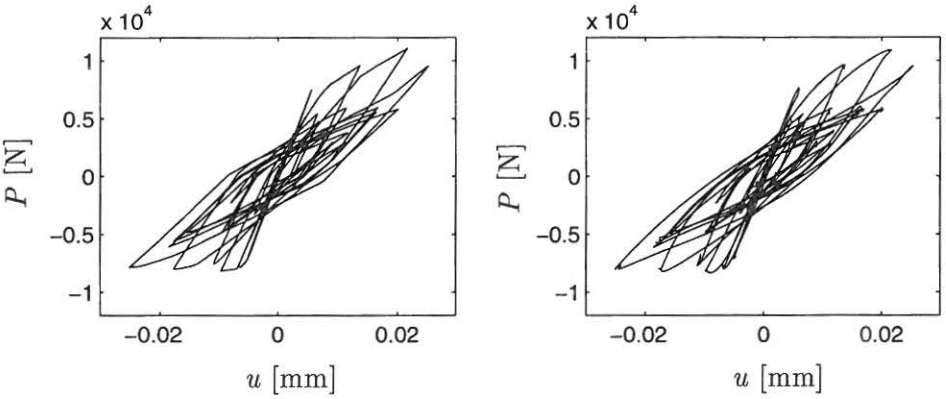

Figure 4.14: Force-deformation curves. a) Correct, b) Force-deformation curve obtained using the piecewise interpolated force and deformation curves.

Chapter 5

Conduction of static tests

5.1 Material testing

For both reinforcement and concrete and appropriate number of reference samples was stored for determination of material parameters. The purpose of this section is to explain the used techniques used for testing of these reference experiments.

5.1.1 Compression tests of concrete specimens

The 100 by 200 mm standard concrete reference specimens were tested in two stages. Initially the modulus of elasticity was evaluated by placing a deformation transducer on the specimen and apply a compression load with a maximum amplitude of 40 per cent of the expected compression capacity of the concrete. Next the deformation transducer was removed and the specimen was loaded all the way up to fracture of the concrete and the maximum compression strength of the concrete was determined.

5.1.2 Tension tests of reinforcement steel

The 500 mm steel specimens was tested in a standard tension apparature for reinforcement bars. During the tests corresponding values of deformations and force are measured and the modulus of elasticity and the yield strength can be determined.

5.2 "Cut up" of test frame

After the dynamic tests are performed on all test frames the frames are cut in to pieces consisting of half beams and columns. The "cut up" and the used labels for each test specimen are illustrated in figure 5.1.

5.3 Static tests on reference and damaged specimens

Each of the half beams and columns are after the dynamic tests statically tested and the bending stiffness are evaluated for all elements in the structure. At the same time the reference specimens are tested so the damage of each element in the structure can be evaluated. The experimental set-up for the static testing are shown in figure 5.2.

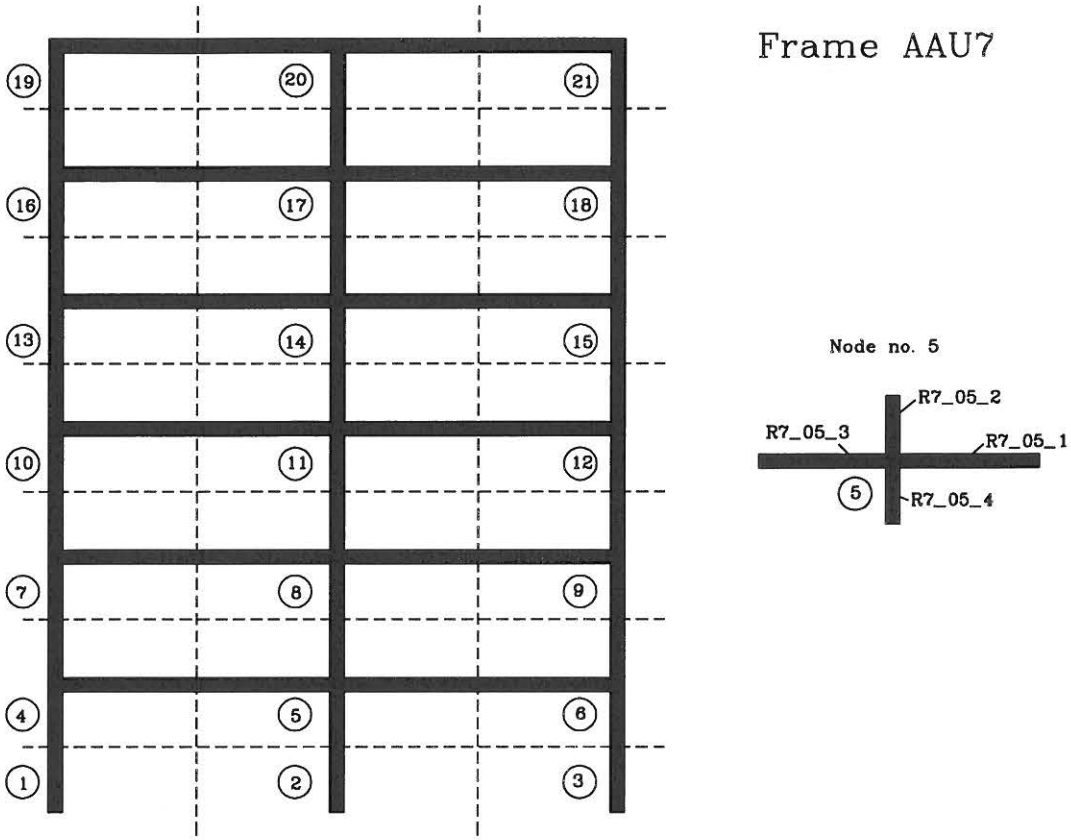

Figure 5.1: Cutting lines for seperation of frames into smaller specimens for statical testing. Example for frame no. 7.

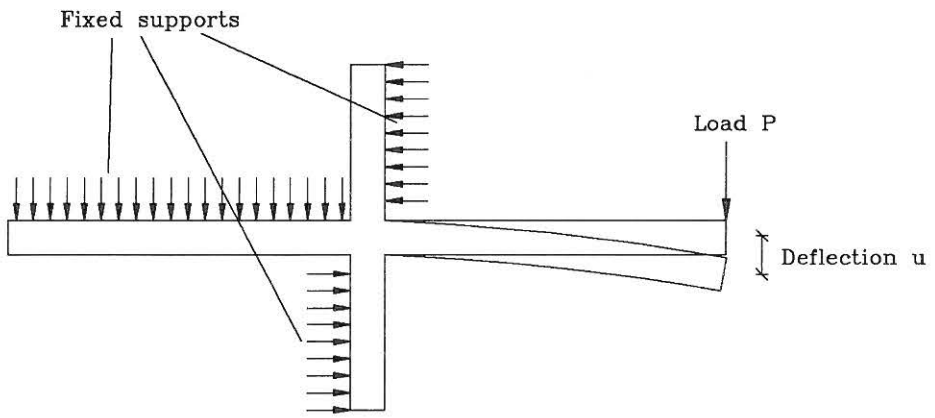

Figure 5.2: Schematical set-up of static testing of reference and damaged specimens.

Chapter 6

Non-destructive testing

In this chapter the results of the non-destructive testing of the frames in the virgin state and after each earthquake are presented. Each of the frames is before strong motions are applied subjected to various loadings in the linear range to provide data for modal identification of the virgin structure. Furthermore, free decay tests and weak motion testing are performed after each earthquake to provide "clean" data for identification of the damaged structure. The data from the weak motion testing is not presented in this report but are stored on the enclosed CD-ROM. The various filenames can be found in table 6.1.

Each frame are subject to the following:

- Free decays from 3 pull-outs in bending (see figure 6.1a).
- Free decays from 3 pull-outs in rotation (see figure 6.1b).
- Weak earthquake excitation with earthquake type a and intensity of 1% of the signal shown in figure 6.2.
- Weak earthquake excitation with earthquake type b and intensity of 1% of the signal shown in figure 6.2.
- Weak earthquake excitation with earthquake type c and intensity of 1% of the signal shown in figure 6.2.

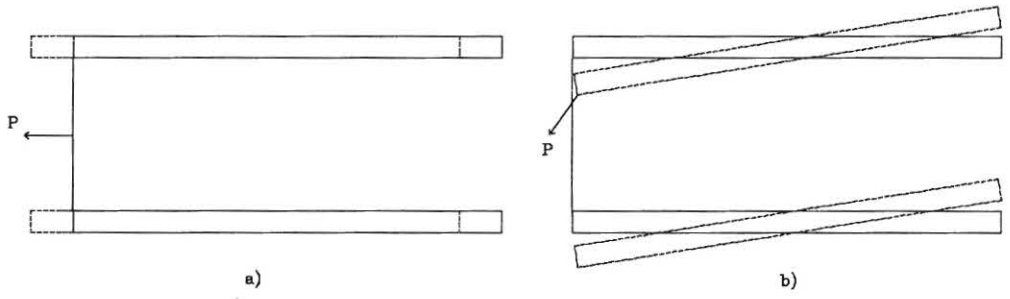

Figure 6.1: Pull-out of the frame in a) bending and b) rotation.

The purpose of applying the weak earthquake ground motions is to provide structural response time series generated using different types of ground motions. Main emphasis is put on providing data that allow identification of the structure and data where the ground motions are nonstationary in both amplitude and frequency content, to provide basis for investigation of the influence of the type of ground motions to the accuracy of the identification. All data presented here can be found in electronic form on the enclosed CD-ROM.

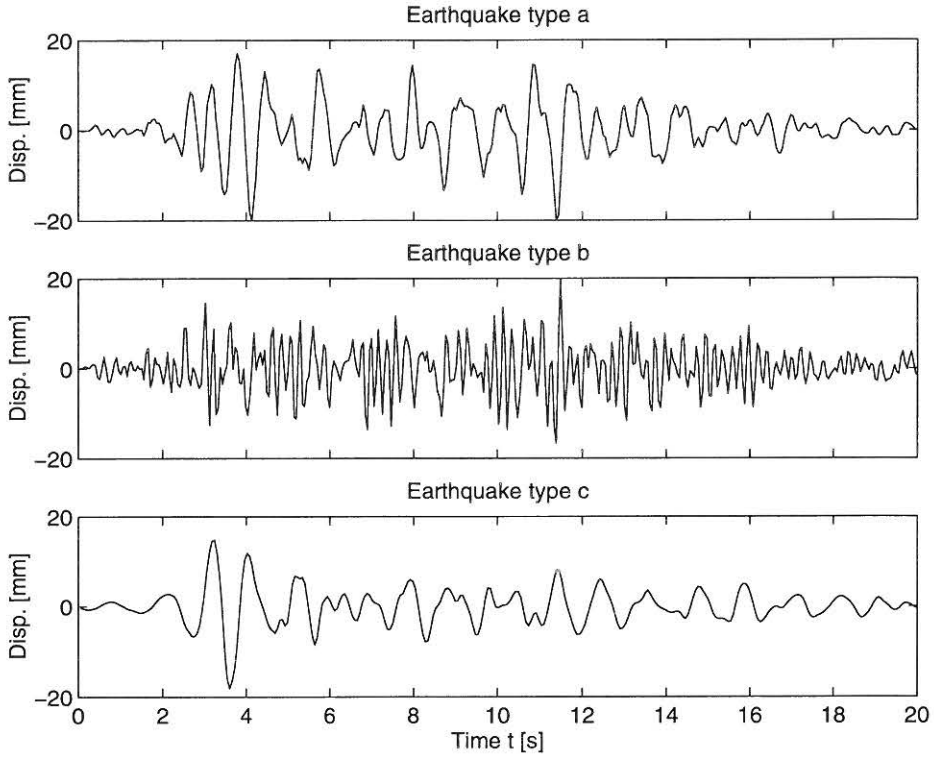

Figure 6.2: The three applied earthquake types scaled to maximum amplitude of 20 mm.

The name of the files for frame number one are shown in table 6.1

Name	Case
fd1_b01.dat	Free decay in the plane, No. 1.
fd1_b02.dat	Free decay in the plane, No. 2.
fd1_b03.dat	Free decay in the plane, No. 3.
fd1_r01.dat	Free decay in rotation, No. 1.
fd1_r02.dat	Free decay in rotation, No. 2.
fd1_r03.dat	Free decay in rotation, No. 3.
wm1_ta01.dat	Type a earthquake with intensity 1%.
wm1_tb01.dat	Type b earthquake with intensity 1%.
wm1_tc01.dat	Type c earthquake with intensity 1%.

Table 6.1: *File names for the data from non-destructive testing of frame AAU1 in the virgin state.*

Due to the previous mentioned changes in the experimental set-up the rotational pull-out tests were left out for frame AAU2 and AAU3. For frames number 2 and 3 the file names will only change on the third character which will be 2 and 3, respectively.

In the free decay tests the frames are subject to a pull-out in bending and one in rotation in order to give data for identification of the bending as well as the rotation modes.

6.1 Data Processing

All data presented in this chapter are detrended in order to remove any trends in the signals.

6.2 Non-destructive testing of frame AAU1

In this section some selected results of the non-destructive tests are shown for frame AAU1.

6.2.1 Free decay tests

In this section the free decay tests performed on the undamaged structure and the the damaged structure after each earthquake are shown. Due to a minor hydraulic accident the undamaged structure was exposed to a impulse loading where no measurements was performed. This impulse loading incurred minor damage into the structure giving a change in the frequencies. In figure 6.3 the free decay test performed before the accident is shown and in figure 6.4 the free decay test after the accident is shown.
The free decay test time series was analyzed using an AutoRegressive Vector model (ARV) and the modal parameters shown in table 6.2 was obtained.

State	f_1 [Hz]	f_2 [Hz]	ζ_1 [%]	ζ_2 [%]
Undamaged before impulse	1.95	6.57	2.9	1.7
Undamaged after impulse (series 1)	1.65	5.79	3.9	1.8
After EQ1	1.58	5.62	3.8	2.2
After EQ2	1.32	5.01	4.5	2.2

Table 6.2: *Estimated modal parameters for frame AAU1.*

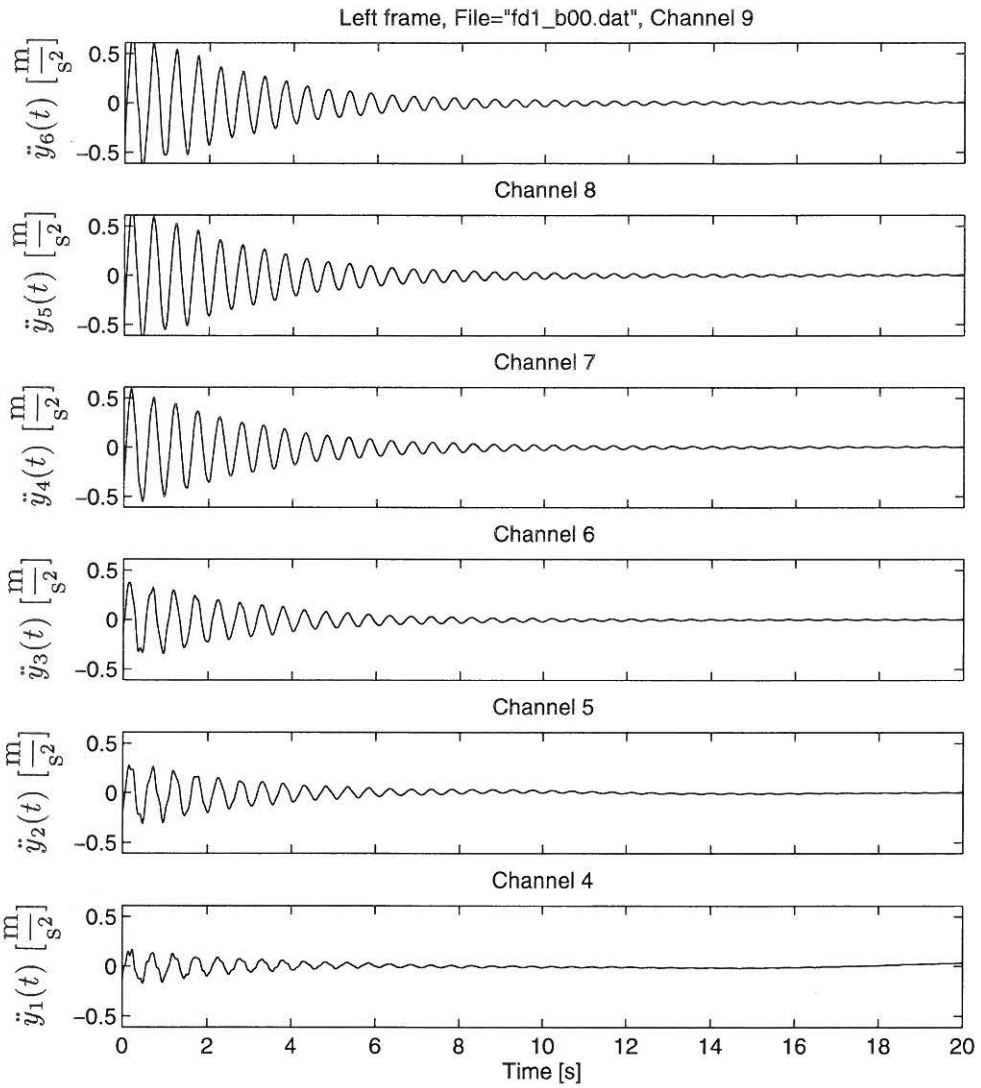

Figure 6.3: Measured accelerations from pull-out test of undamaged frame AAU1 before impulse loading.

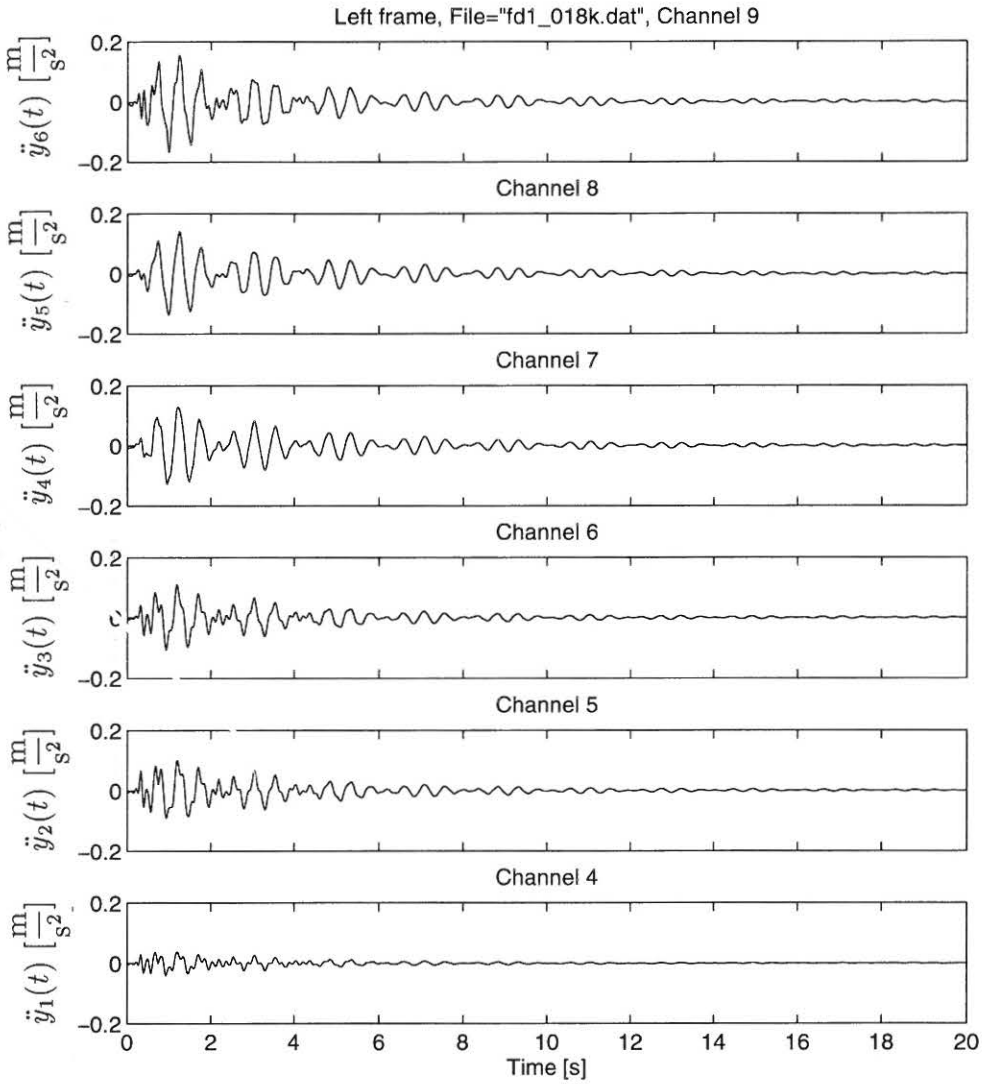

Figure 6.4: Measured accelerations from pull-out test of "undamaged" frame AAU1 after impulse loading.

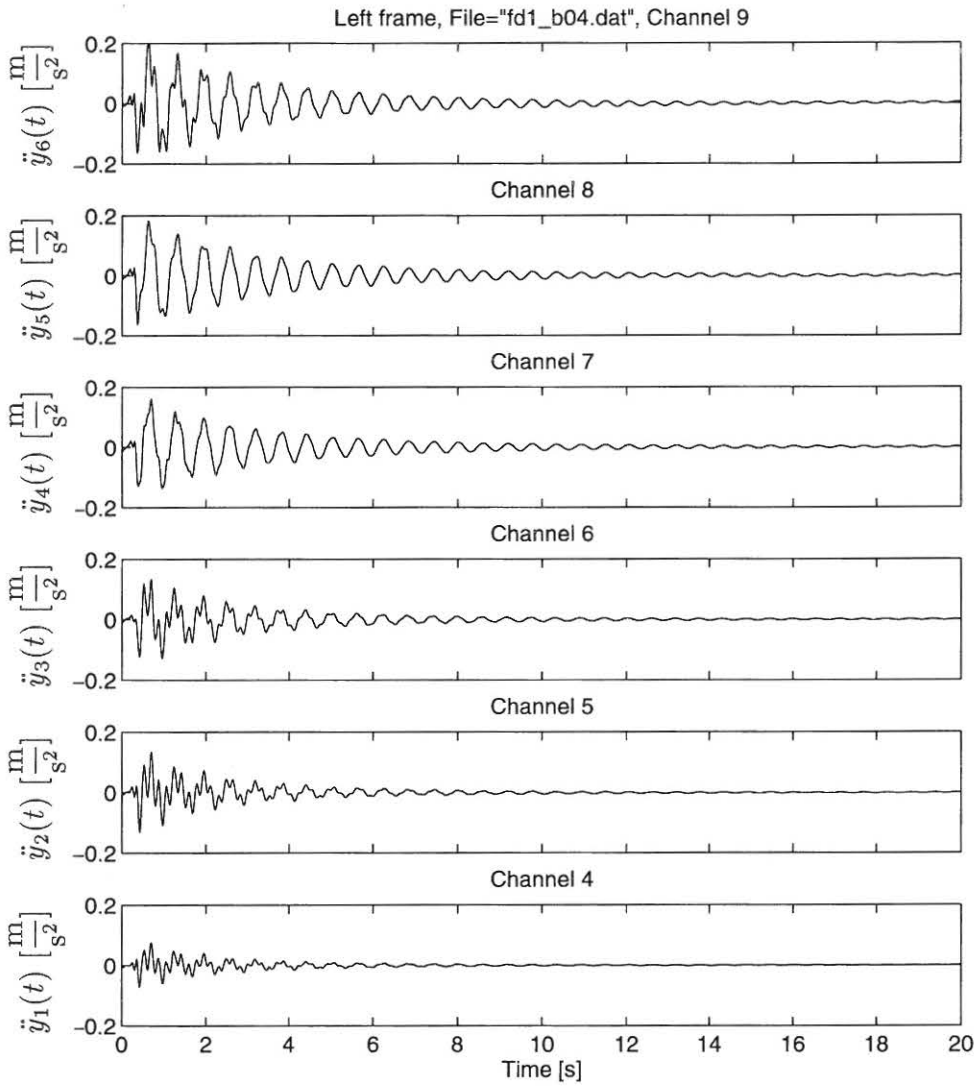

Figure 6.5: Measured accelerations from pull-out test of frame AAU1 after EQ1.

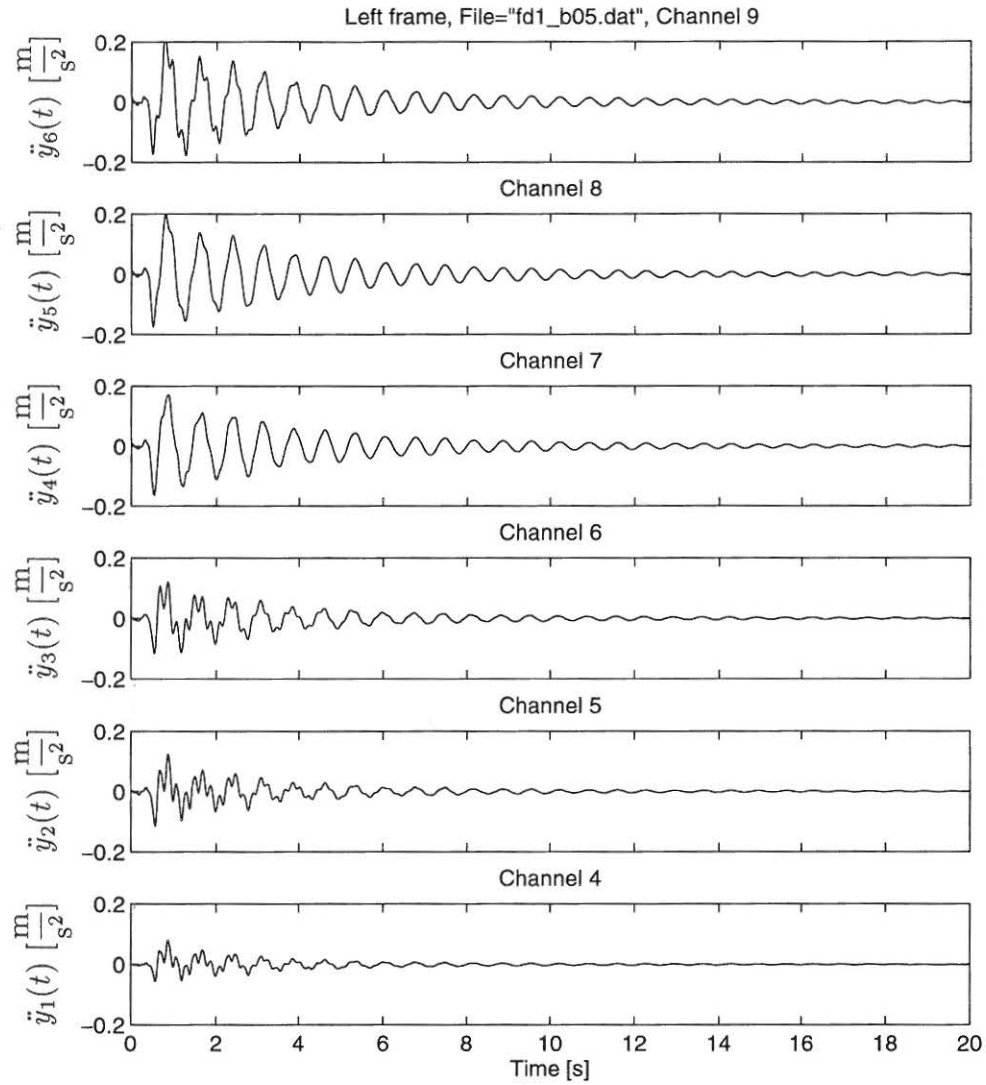

Figure 6.6: Measured accelerations from pull-out test of frame AAU1 after EQ2.

6.3 Non-destructive testing of frame AAU2

In this section some selected results of the non-destructive tests are shown for frame AAU2.

6.3.1 Free decay tests

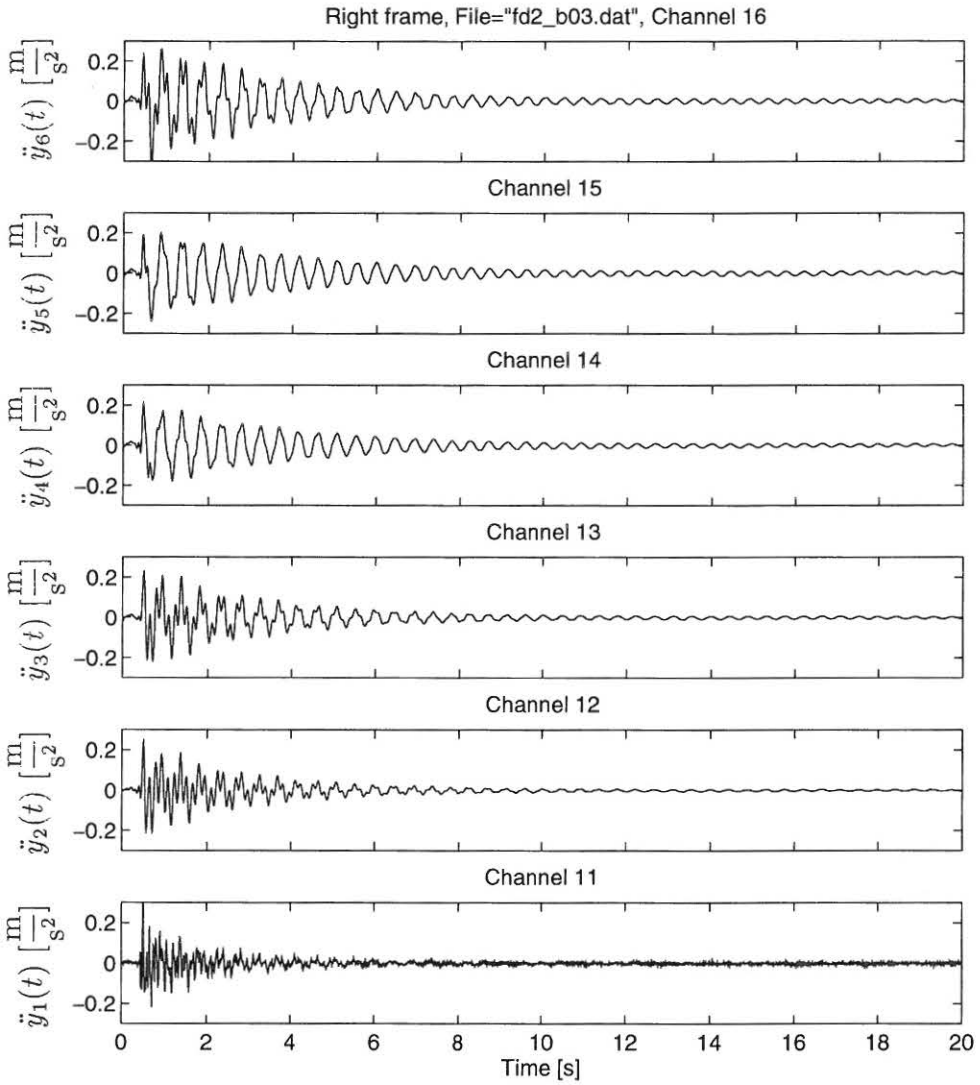

Figure 6.7: Measured accelerations from pull-out test of undamaged frame AAU2.

The free decay test time series was analyzed using an AutoRegressive Vector model (ARV) and the modal parameters shown in table 6.3 was obtained.

State	f_1 [Hz]	f_2 [Hz]	ζ_1 [%]	ζ_2 [%]
Undamaged	2.15	6.95	1.7	1.4
After EQ1	1.79	6.13	2.9	2.5
After EQ2	1.48	5.38	3.8	2.9

Table 6.3: *Estimated modal parameters for frame AAU2.*

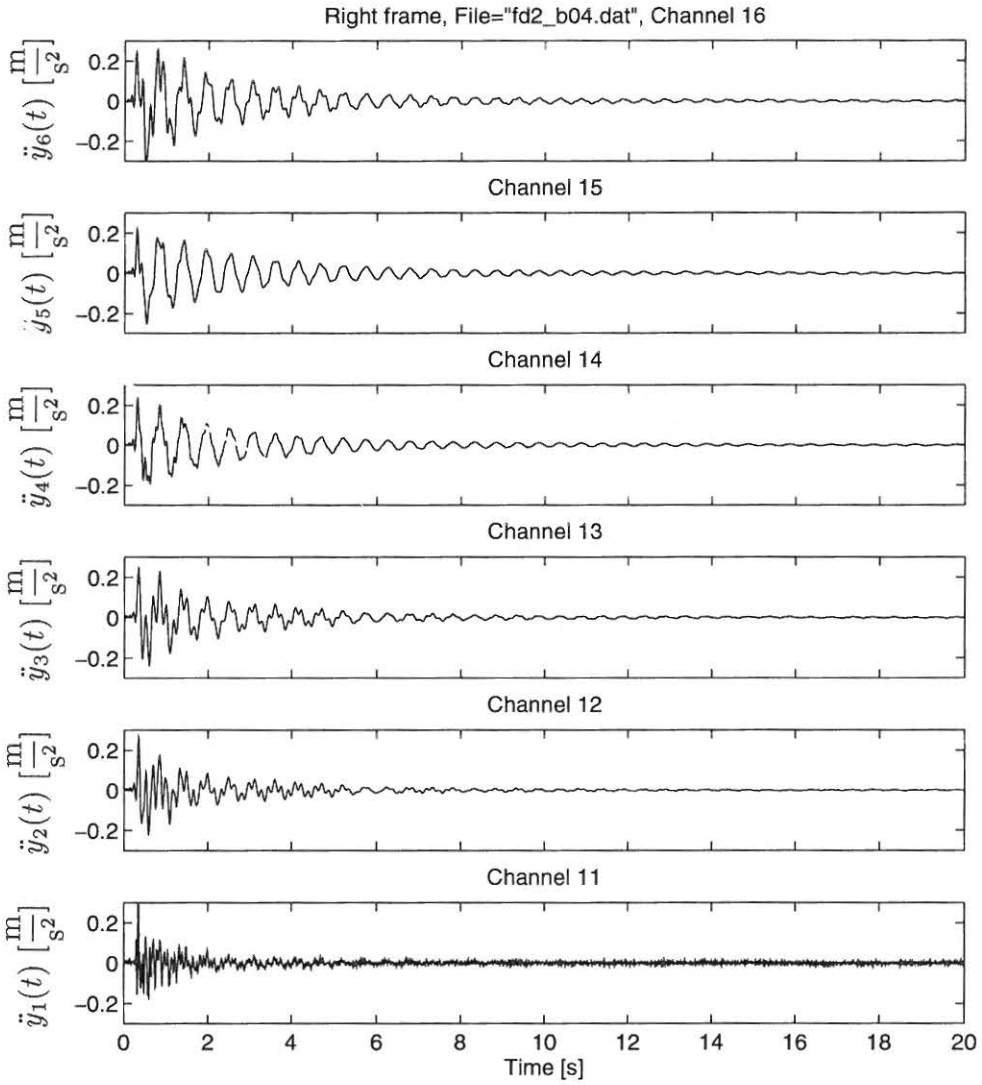

Figure 6.8: Measured accelerations from pull-out test of frame AAU2 after EQ1.

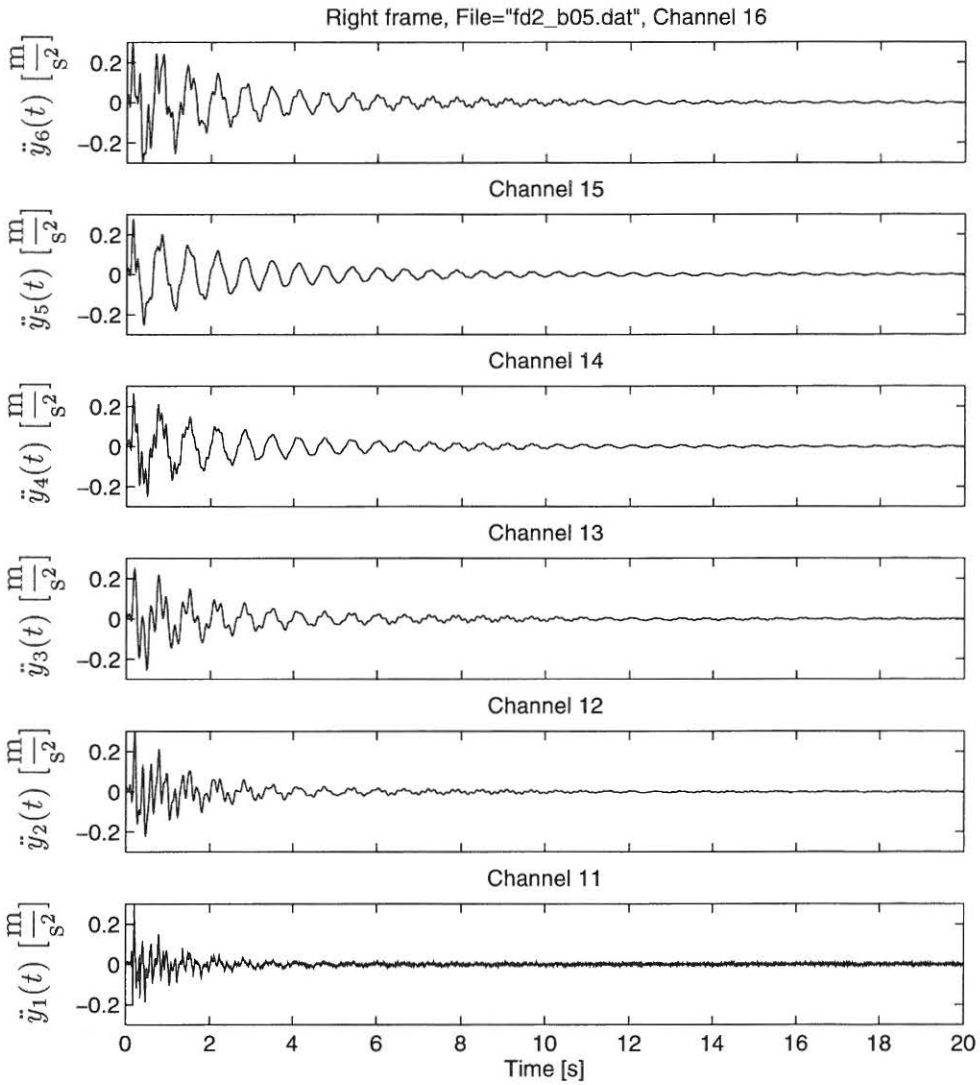

Figure 6.9: Measured accelerations from pull-out test of frame AAU2 after EQ2.

6.4 Non-destructive testing of frame AAU3

In this section some selected results of the non-destructive tests are shown for frame AAU3.

6.4.1 Free decay tests

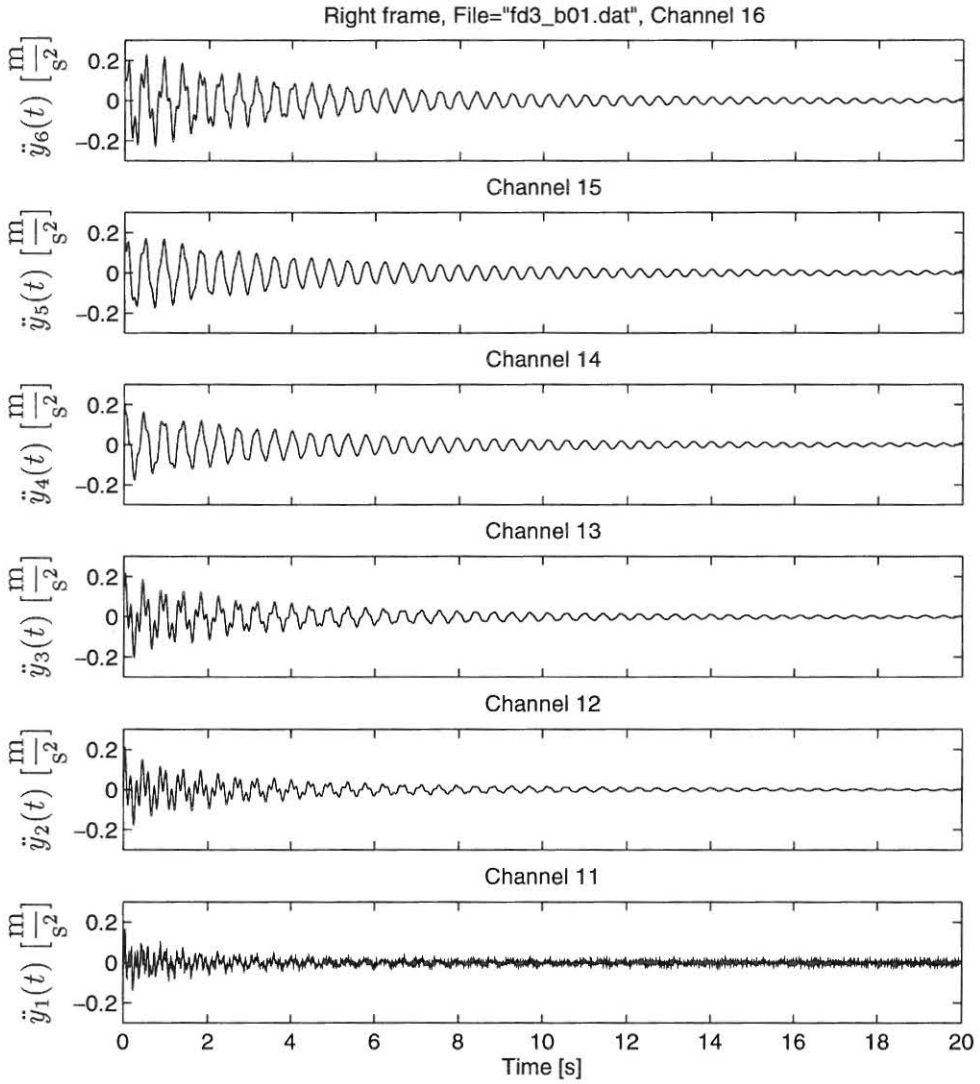

Figure 6.10: Measured accelerations from pull-out test of undamaged frame AAU3.

The free decay test time series was analyzed using an AutoRegressive Vector model (ARV) and the modal parameters shown in table 6.4 was obtained.

State	f_1 [Hz]	f_2 [Hz]	ζ_1 [%]	ζ_2 [%]
Undamaged	2.25	7.27	1.5	1.0
After EQ1	1.97	6.39	2.4	1.9
After EQ2	1.73	5.67	3.2	2.4
After EQ3	1.41	4.55	4.6	3.2

Table 6.4: *Estimated modal parameters for frame AAU3.*

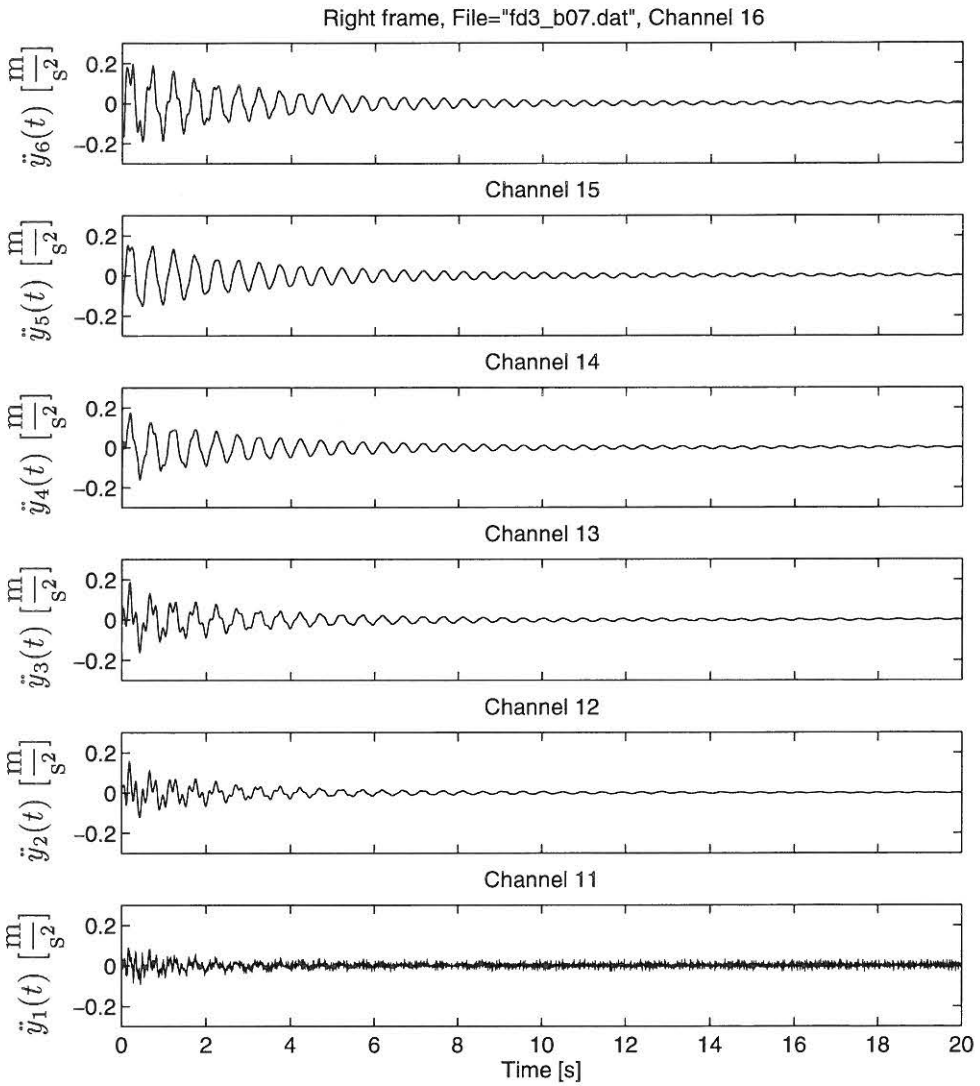

Figure 6.11: Measured accelerations from pull-out test of frame AAU3 after EQ1.

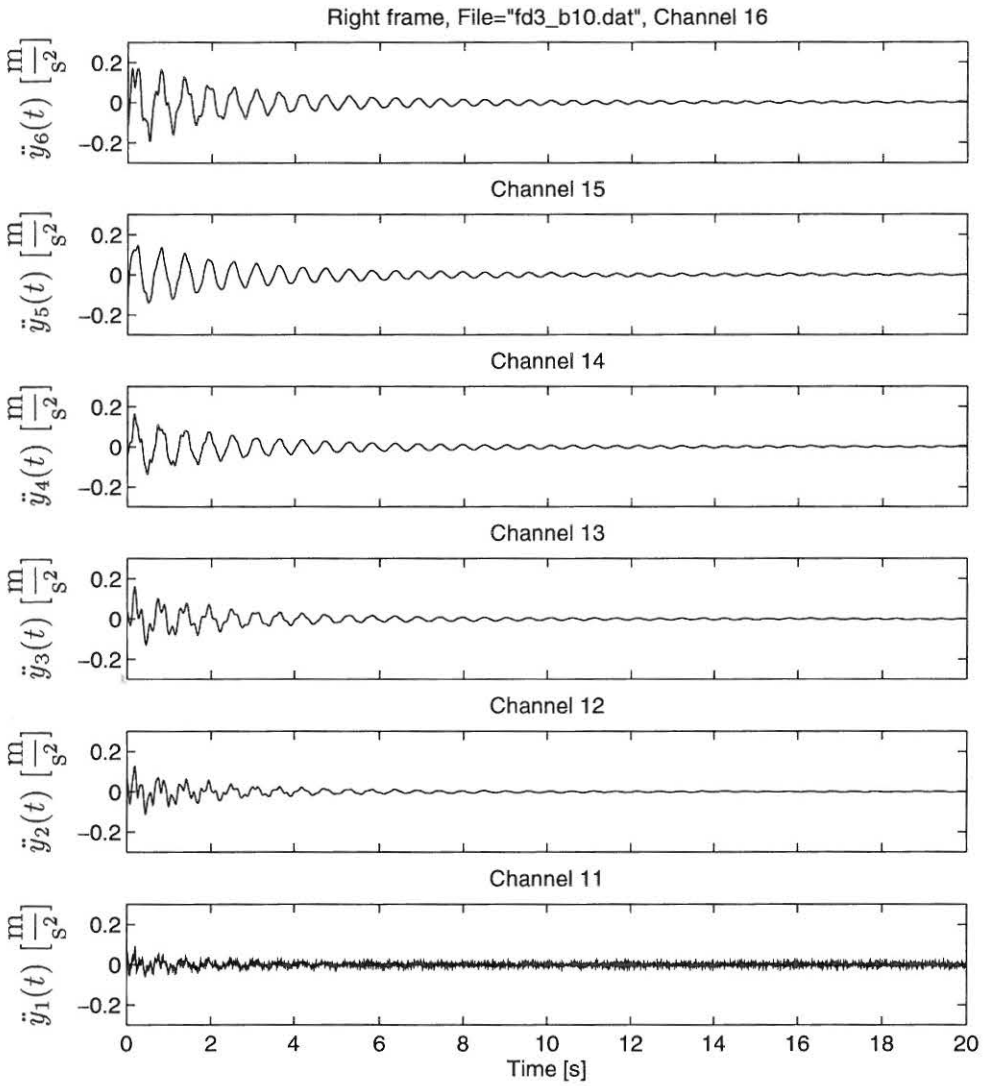

Figure 6.12: Measured accelerations from pull-out test of frame AAU3 after EQ2.

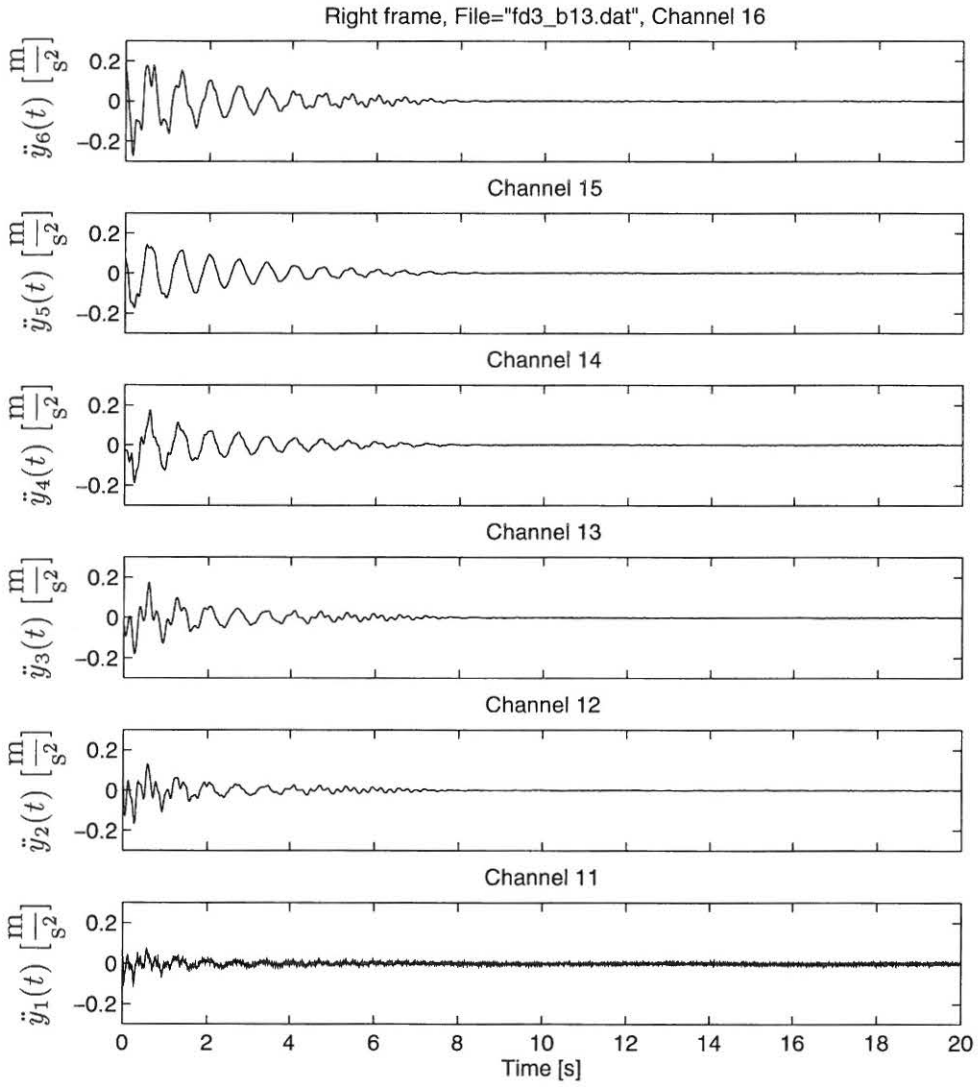

Figure 6.13: Measured accelerations from pull-out test of frame AAU3 after EQ3.

Chapter 7

Destructive testing

In this chapter data collected during and after strong motions have been applied to the structure are presented. The three frames AAU1, AAU2 and AAU3 are in the destructive testing exposed to three sequential earthquakes of increasing magnitude called EQ1a, EQ2a and EQ3a in the case where an earthquake of type a is applied, see figure 6.2.

After each run, i.e. EQ1a, EQ2a etc. non-destructive testing og the frame are performed in order to provide data for evaluation of the modal parameters of the damaged structure. The non-destructive tests are:

- Free decay test from pull-outs in bending (see figure 6.1a).
- Free decays test from pull-outs in rotation (see figure 6.1b).
- Weak earthquake excitation with the same earthquake type as used in the strong motion run.

The files with the data from the strong motion and the non-destructive testing are named as shown in table 7.1.

Name	Case
sm1_25a.dat	Strong motion earthquake EQ1 (type a) with intensity of 25 % of maximum
fd1_b04.dat	Free decay in the plane, No. 4. after EQ1
fd1_r04.dat	Free decay in rotation, No. 4. after EQ1
wm1_1a1.dat	Weak motion earthquake of type a with intensity 1%. After EQ1.
sm1_50a.dat	Strong motion earthquake EQ2 (type a) with intensity of 50 % of maximum
fd1_b05.dat	Free decay in the plane, No. 5. after EQ2
fd1_r05.dat	Free decay in rotation, No. 5. after EQ2
wm1_1a2.dat	Weak motion earthquake of type a with intensity 1%. After EQ2.
sm1_75a.dat	Strong motion earthquake EQ3 (type a) with intensity of 75 % of maximum
fd1_b06.dat	Free decay in the plane, No. 6. after EQ3
fd1_r06.dat	Free decay in rotation, No. 6. after EQ3
wm1_1a3.dat	Weak motion earthquake of type a with intensity 1%. After EQ3.

Table 7.1: *File names for the data from destructive and non-destructive testing. Frame AAU1.*

As for the files containing data from the non-destructive testing in the virgin state the names will only change on the third character to 2 and 3 for frame AAU2 and AAU3, respectively.

7.1 Results for frame AAU1

The structure AAU1 was exposed to three sequential earthquakes (type a) of increasing magnitude. In the figures 7.1-7.5 the data sampled from one of the frames in set-up AAU1 during the three runs are presented. Figures 7.1 and 7.2 shows storey accelerations, cylinder force and cylinder displacements during EQ1. In the same manner figures 7.3 and 7.4 show the data collected during EQ2 and figures 7.5 and 7.6 the data collected during EQ3.

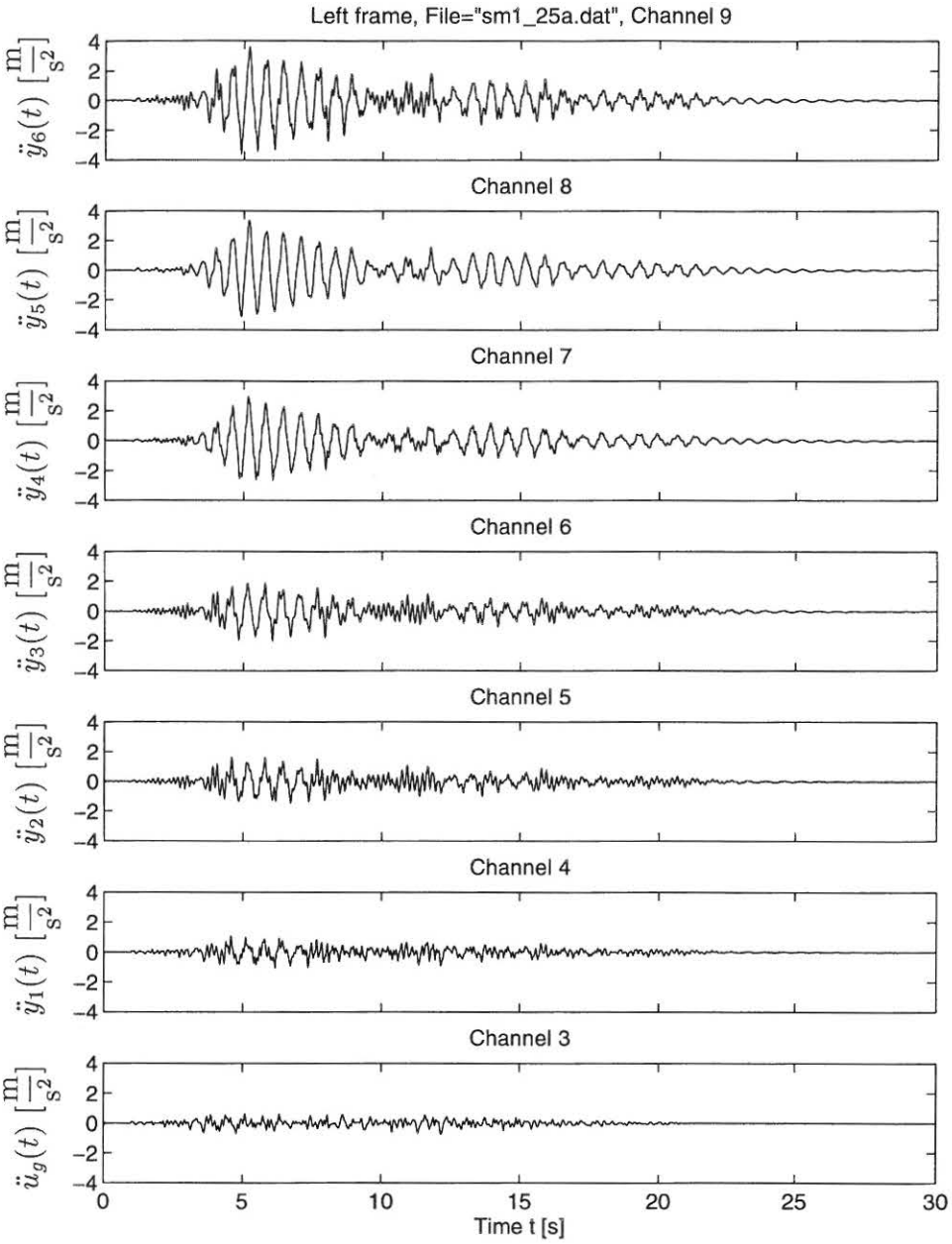

Figure 7.1: Measured accelerations during EQ1 for frame AAU1.

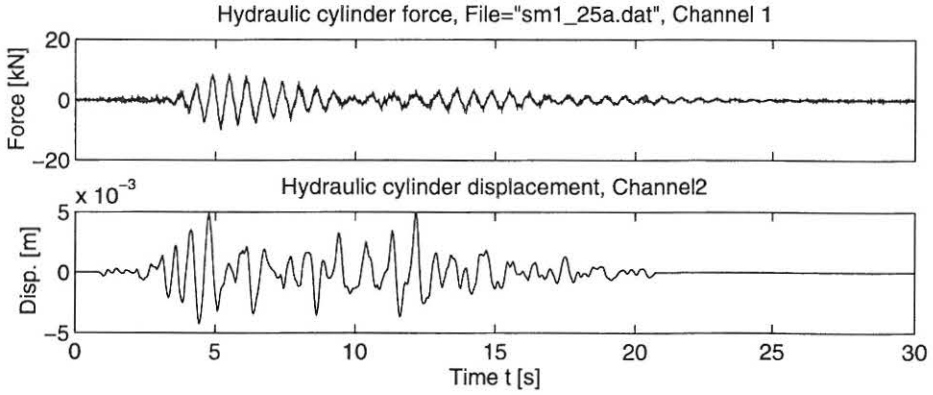

Figure 7.2: Measured shaking table displacement and cylinder force during EQ1 for frame AAU1.

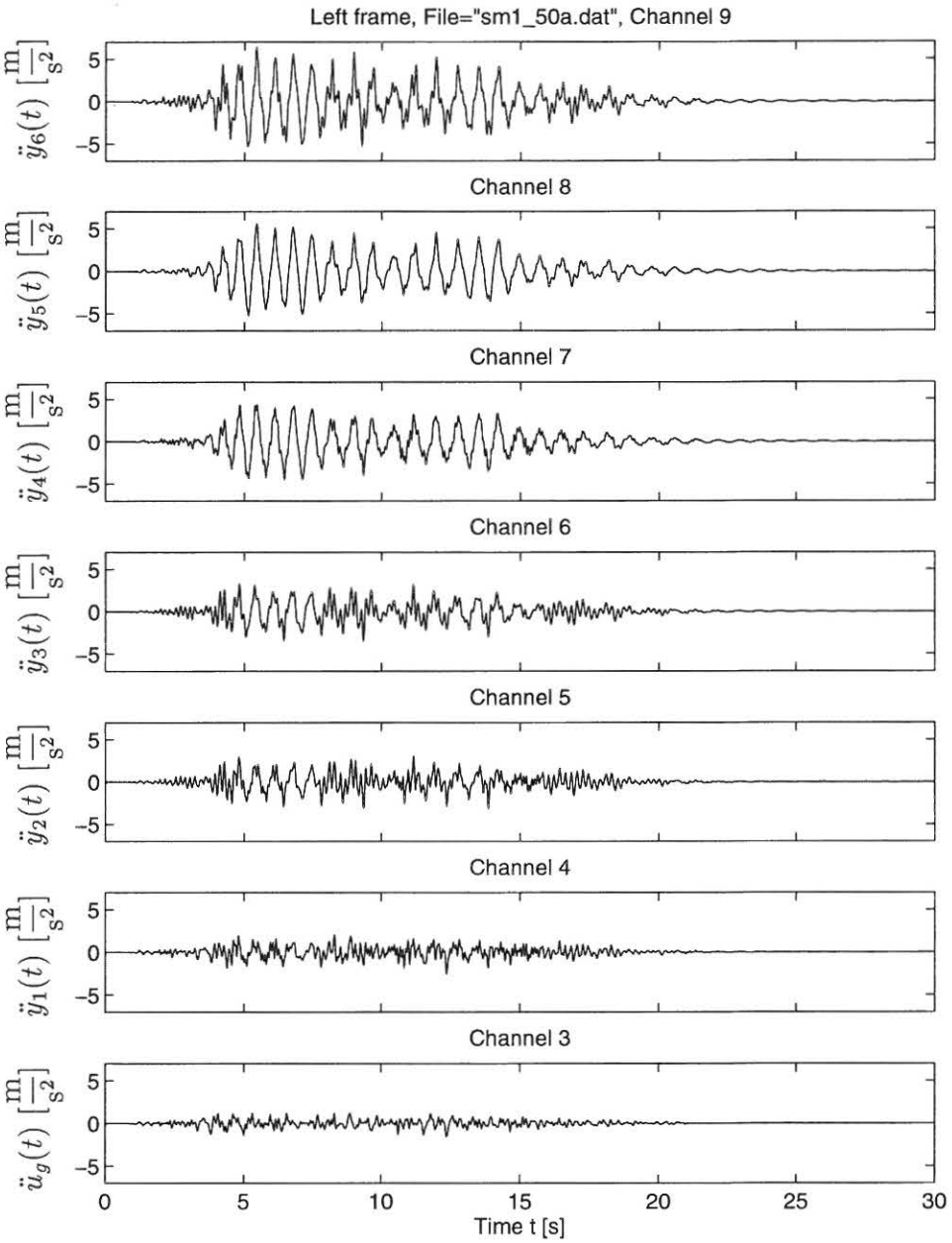

Figure 7.3: Measured accelerations during EQ2 for frame AAU1.

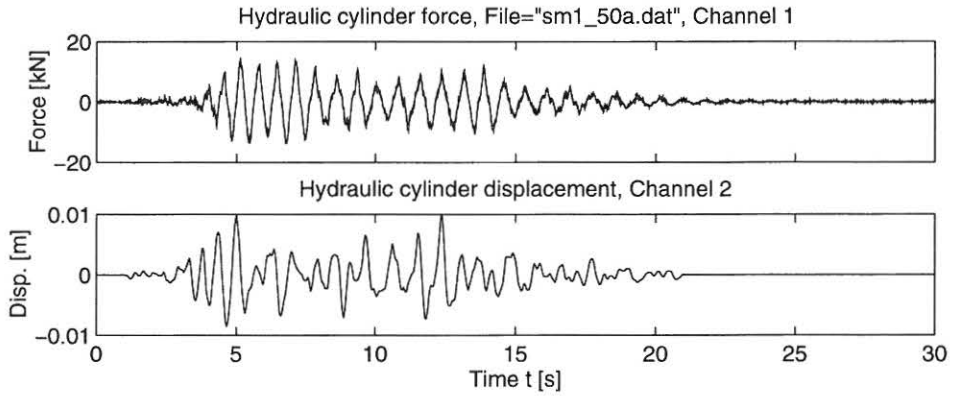

Figure 7.4: Measured shaking table displacement and cylinder force during EQ2 for frame AAU1.

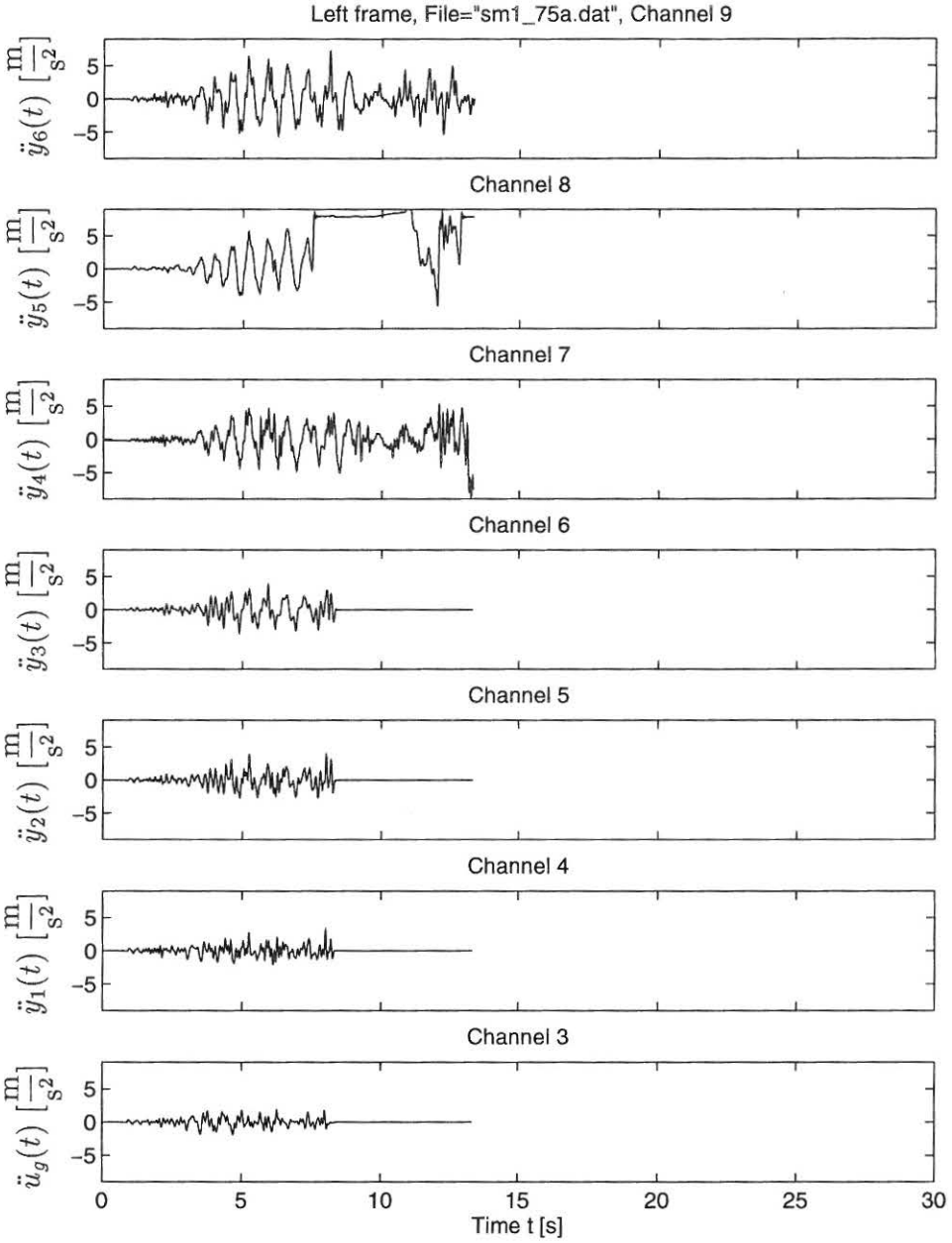

Figure 7.5: Measured accelerations during EQ3 for frame AAU1.

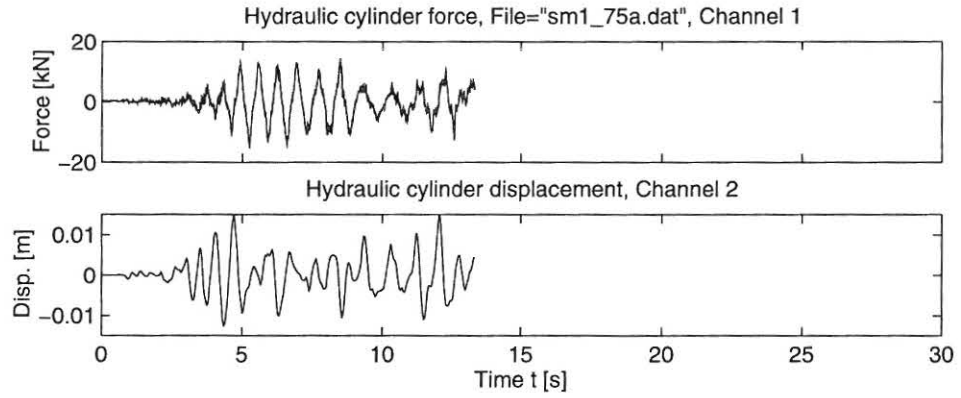

Figure 7.6: Measured shaking table displacement and cylinder force during EQ3 for frame AAU1.

7.1.1 Processed data

This section presents processed data where top-storey displacements have been found using the procedures described in section 4.3 and frequency developments. The frequency estimation is described in Kirkegaard et al. [16].

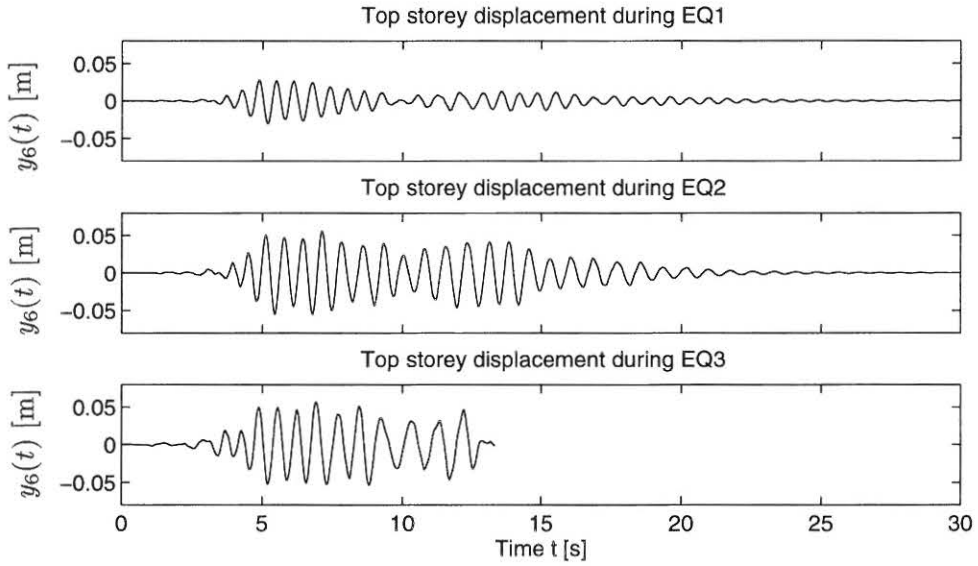

Figure 7.7: Top storey displacements during EQ1, EQ2 and EQ3.

During the integration process where displacements are obtained a butterworth 6th order high-pass digital filter with a cut-off frequency of 0.5 Hz and a butterworth 8th order low-pass digital filter with a cut-off frequency of 20 Hz have been used.

The estimated eigenfrequency development during the three earthquakes are shown in figures 7.8-7.10.

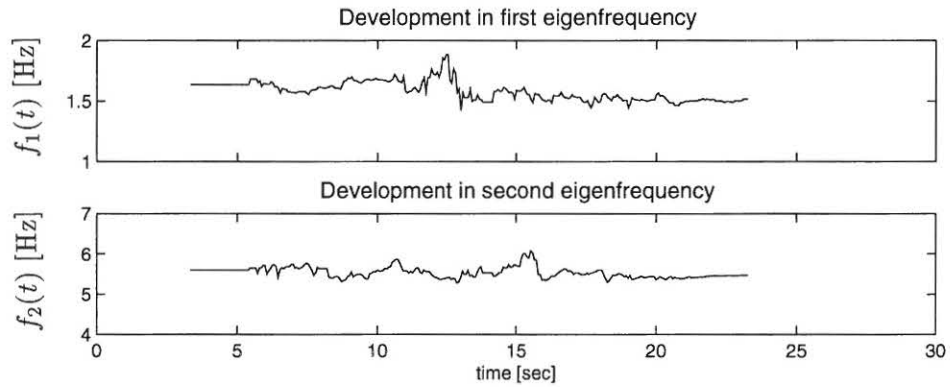

Figure 7.8: Development of eigenfrequencies in first and second mode during EQ1.

The maximum softenings during the three runs are shown in table 7.2.

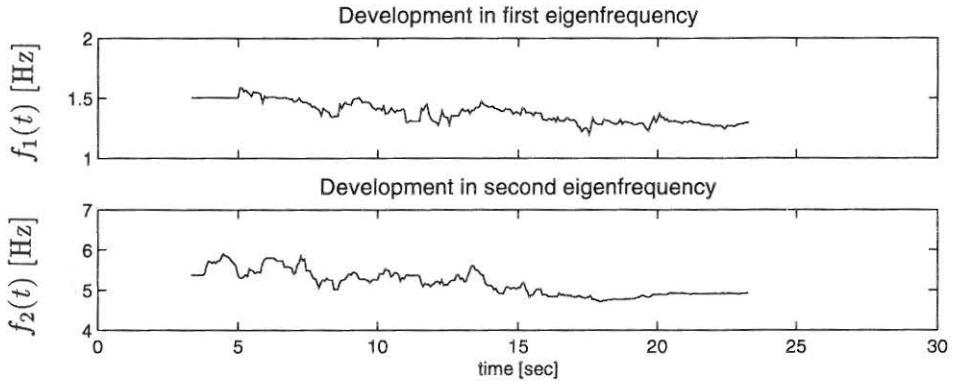

Figure 7.9: Development of eigenfrequencies in first and second mode during EQ2.

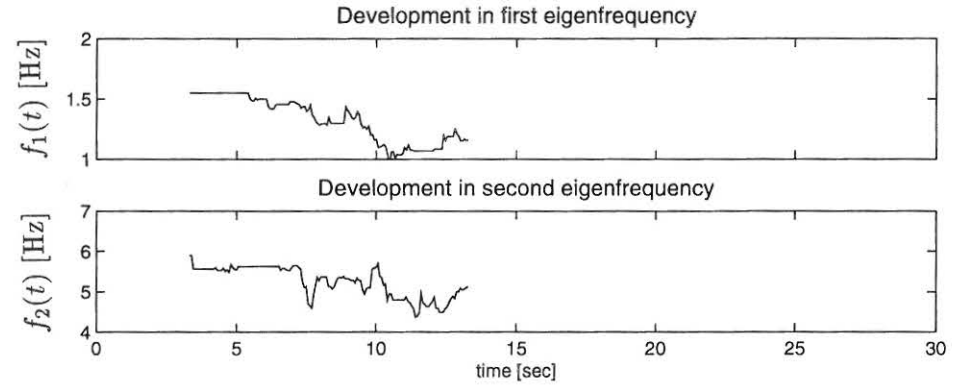

Figure 7.10: Development of eigenfrequencies in first and second mode during EQ3.

	$f_{\min,1}\ [Hz]$	$f_{\min,2}\ [Hz]$	$\delta_{M,1}$	$\delta_{M,2}$
EQ1	1.42	5.28	0.27	0.20
EQ2	1.19	4.71	0.38	0.28
EQ3	0.96	4.37	0.51	0.33

Table 7.2: *Estimated minimum frequencies and maximum softenings during the three earthquakes.*

7.2 Results for frame AAU2

Test structure AAU2 were exposed to two sequential earthquakes (type a) of increasing magnitude. The data sampled from one of the two frames are shown in the figures 7.11-7.14.

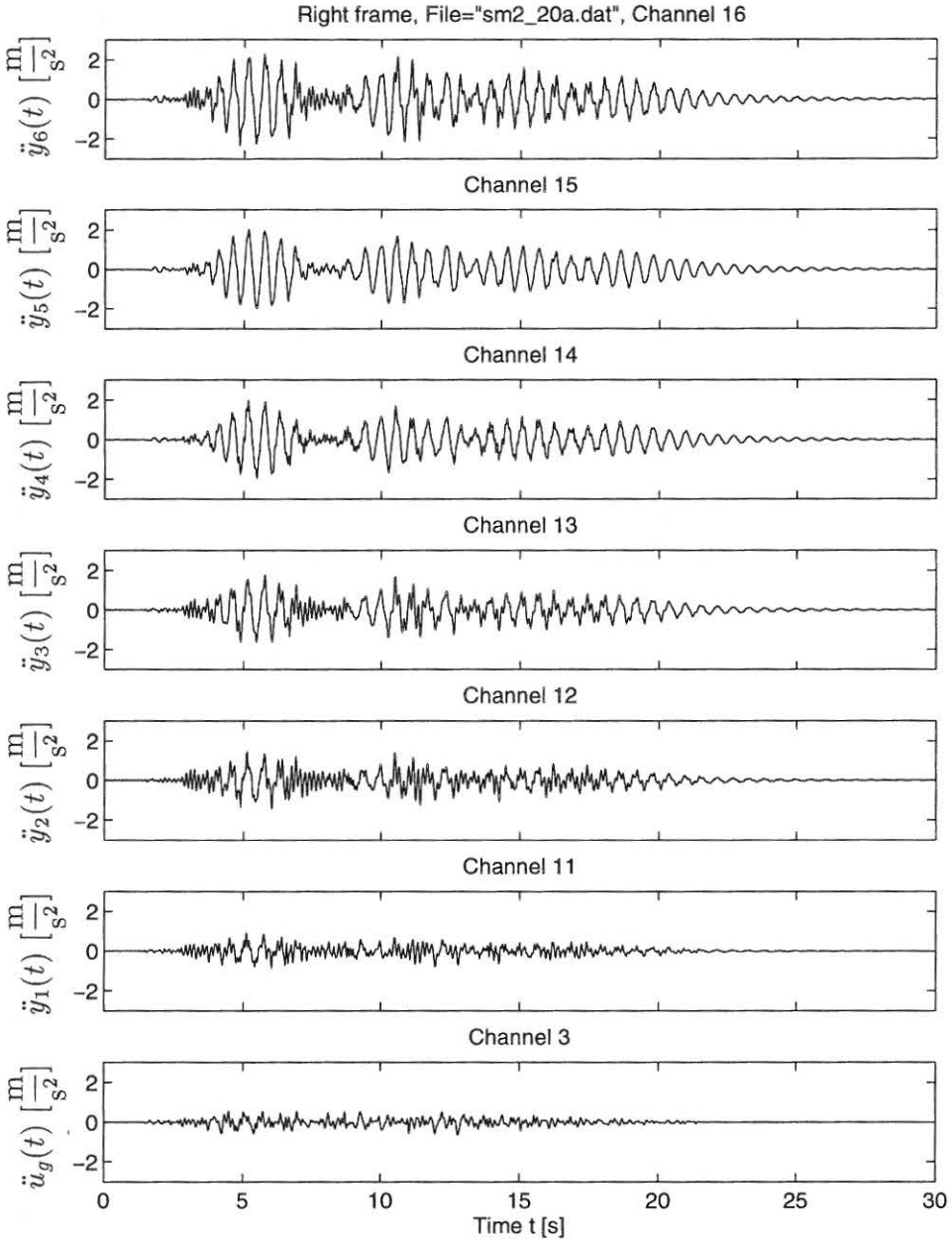

Figure 7.11: Measured accelerations during EQ1 for frame AAU2.

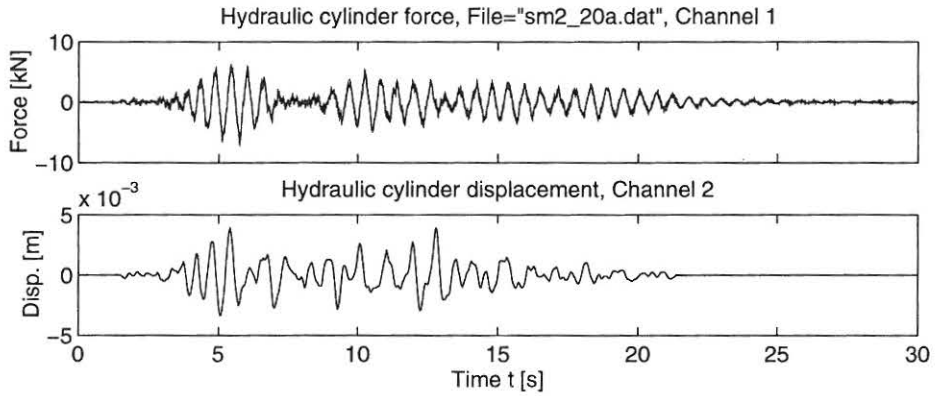

Figure 7.12: Measured shaking table displacement and cylinder force during EQ1 for frame AAU2.

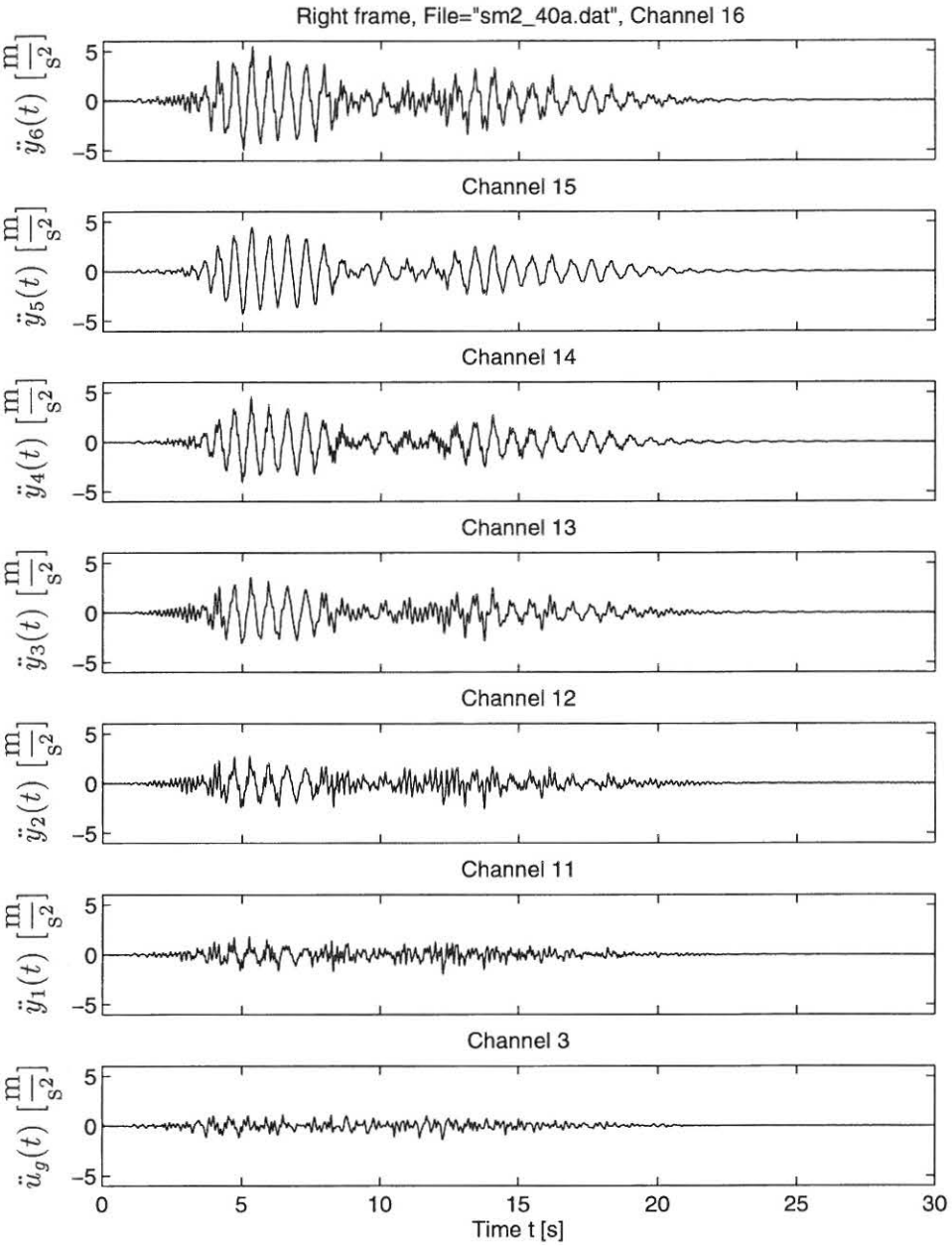

Figure 7.13: Measured accelerations during EQ2 for frame AAU2.

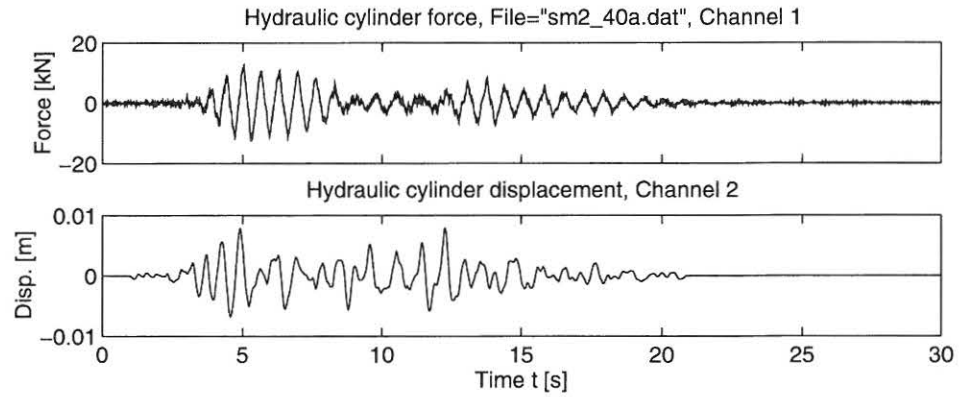

Figure 7.14: Measured shaking table displacement and cylinder force during EQ2 for frame AAU2.

7.2.1 Processed data

This section presents processed data where top-storey displacements, frequency developments and force-deformation curves have been found using the procedures described in section 4.3.

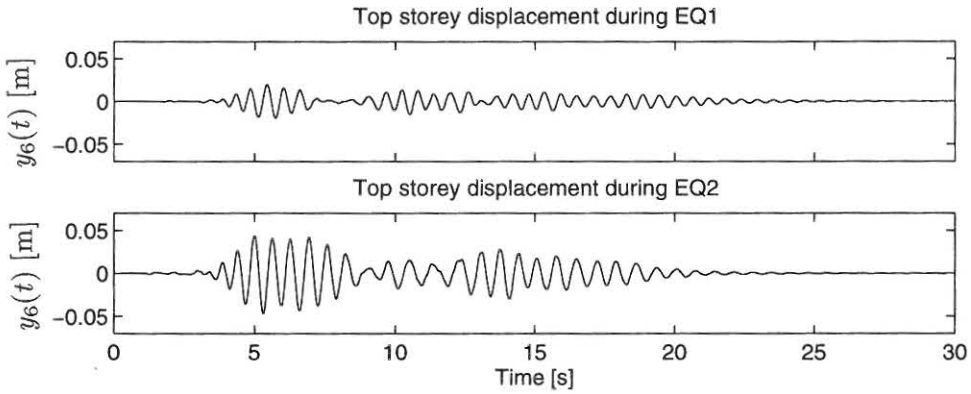

Figure 7.15: Top storey displacements during EQ1 and EQ2.

During the integration process where displacements are obtained a butterworth 6th order high-pass digital filter with a cut-off frequency of 0.5 Hz and a butterworth 8th order low-pass digital filter with a cut-off frequency of 20 Hz have been used.

The estimated development in eigenfrequencies during the two runs are shown in figures 7.16-7.17.

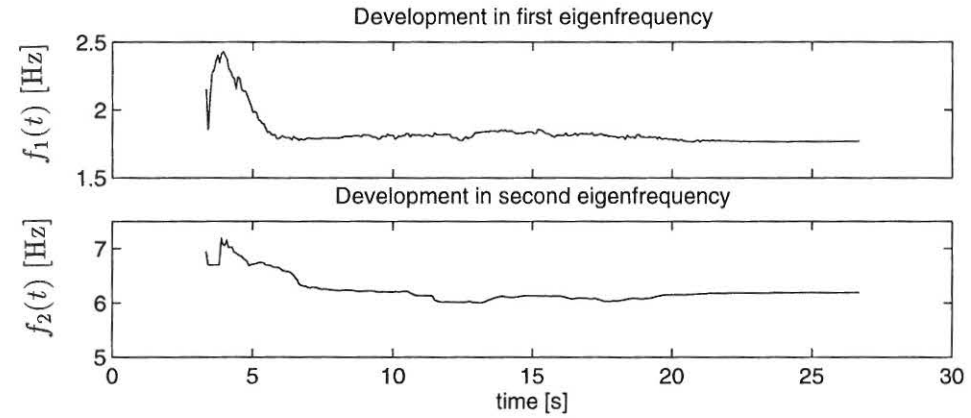

Figure 7.16: Development of softening in first and second mode during EQ1.

	$f_{\min,1}$ $[Hz]$	$f_{\min,2}$ $[Hz]$	$\delta_{M,1}$	$\delta_{M,2}$
EQ1	1.76	6.00	0.18	0.14
EQ2	1.46	5.28	0.32	0.24

Table 7.3: *Estimated minimum frequencies and maximum softenings during the three earthquakes.*

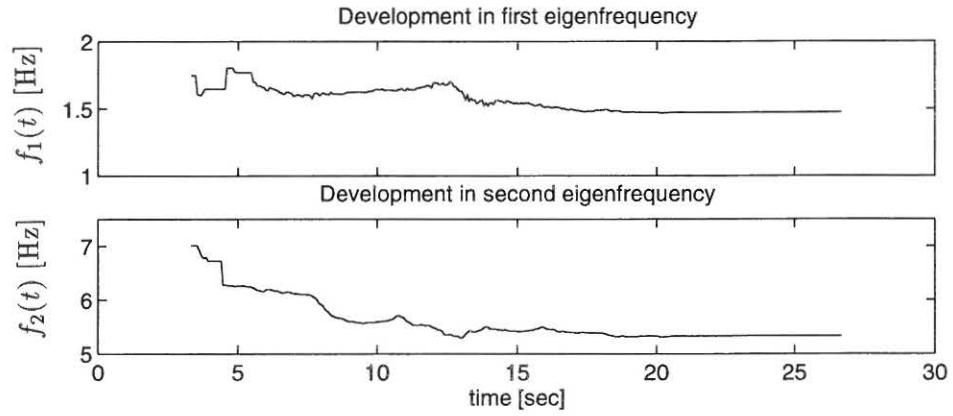

Figure 7.17: Development of softening in first and second mode during EQ2.

Figure 7.18 show the force-deformation curves obtained for each storey during EQ1 and figure 7.19 show the force-deformation curves obtained for the storeys during EQ2.

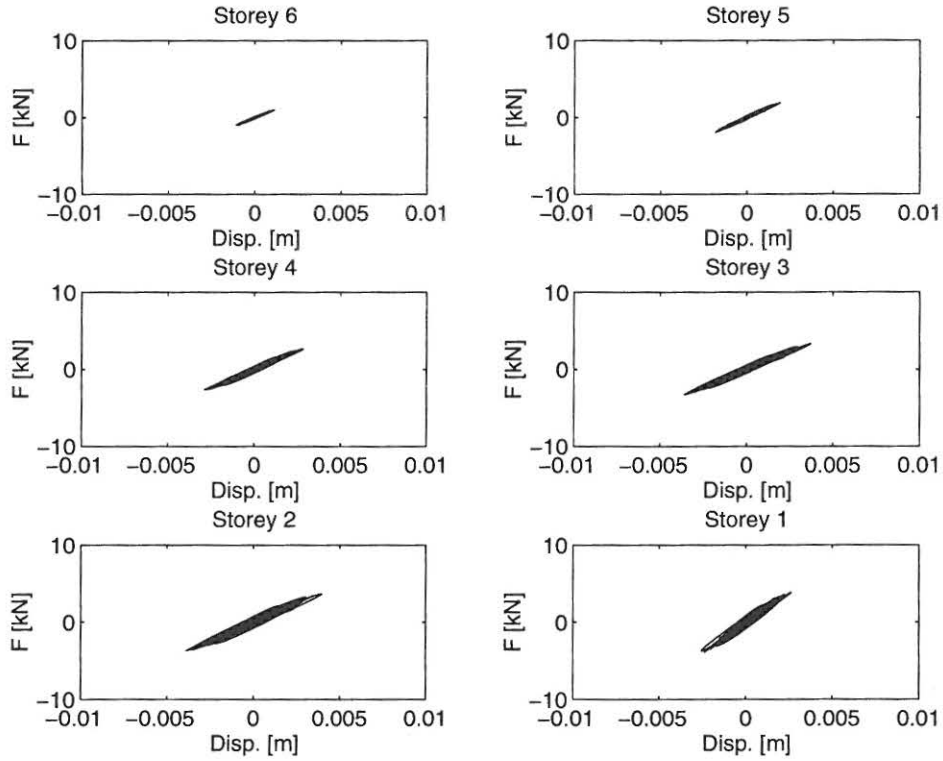

Figure 7.18: Force-deformation curves during EQ1 for frame AAU2.

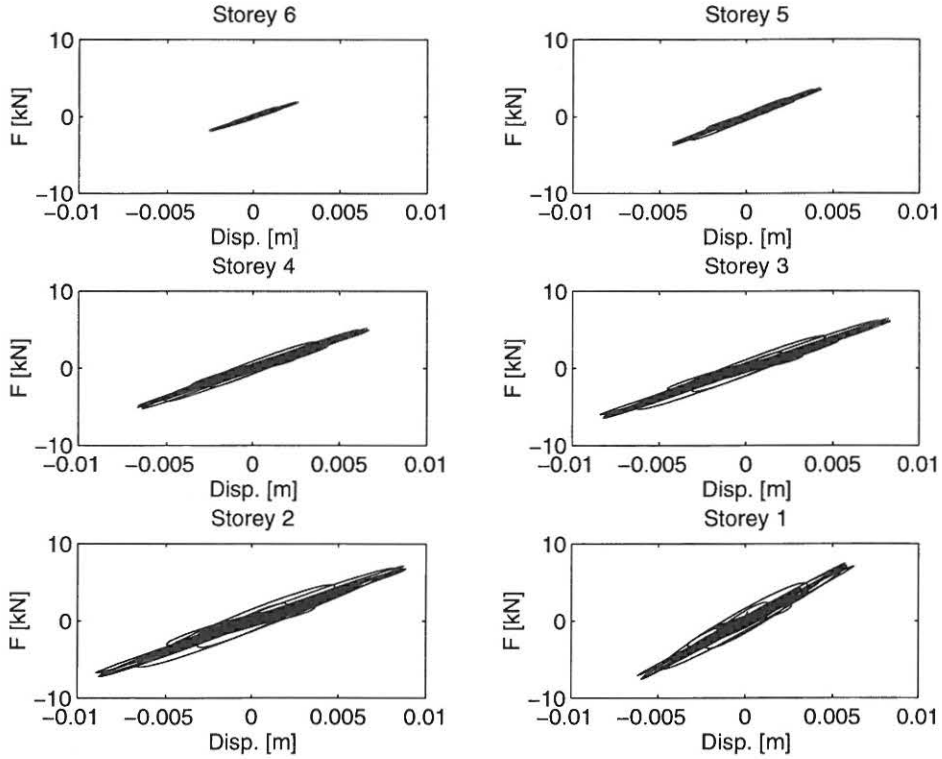

Figure 7.19: Force-deformation curves during EQ2 for frame AAU2.

7.3 Results for frame AAU3

Test structure AAU3 was exposed to three sequential strong motion sequences of type b. The recorded data during the three sequences are shown in the figures 7.20-7.25.

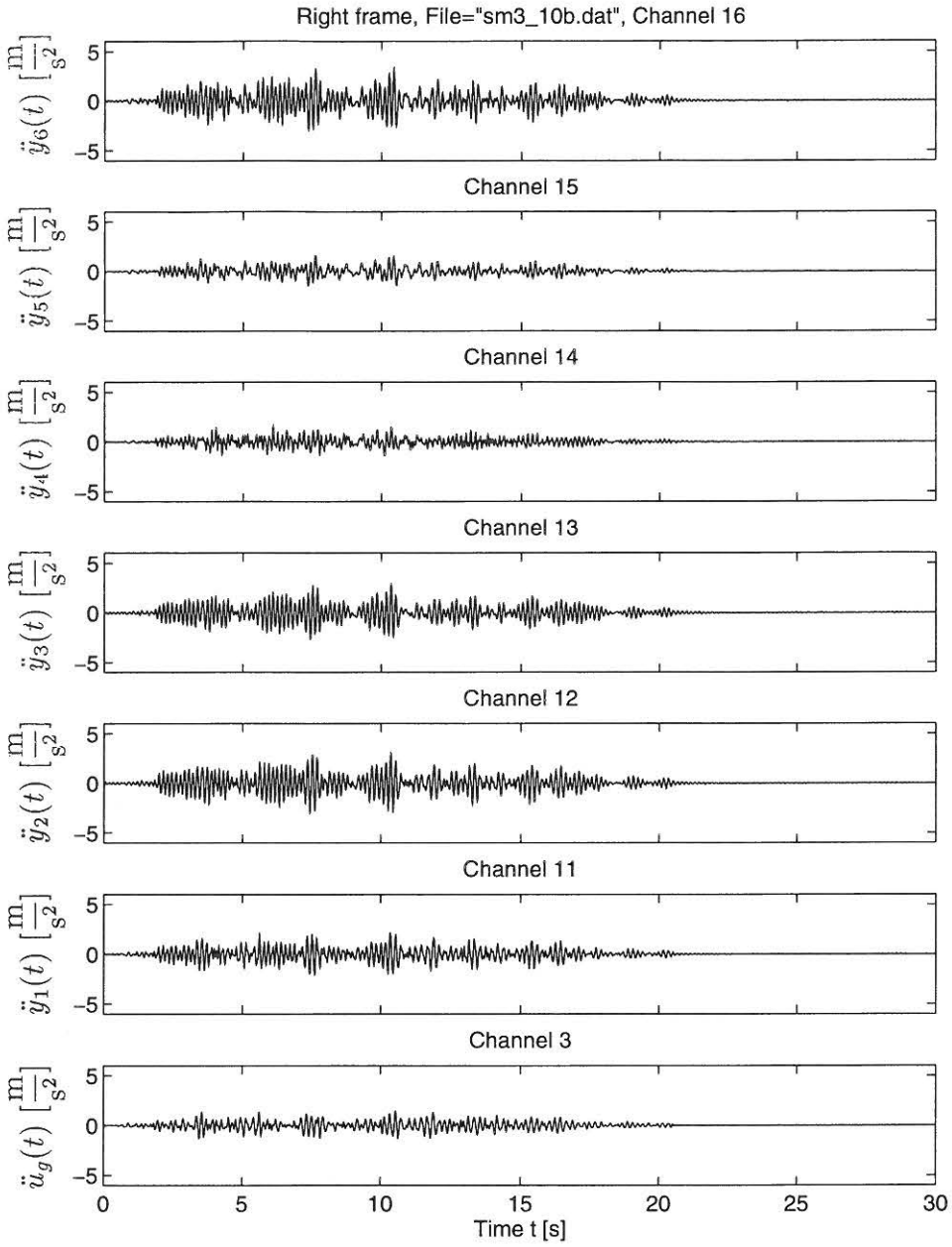

Figure 7.20: Measured accelerations during EQ1 for frame AAU3.

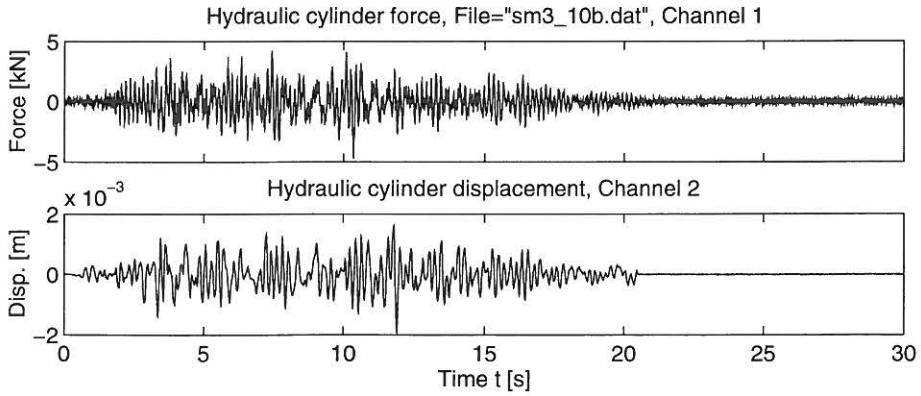

Figure 7.21: Measured shaking table displacement and cylinder force during EQ1 for frame AAU3.

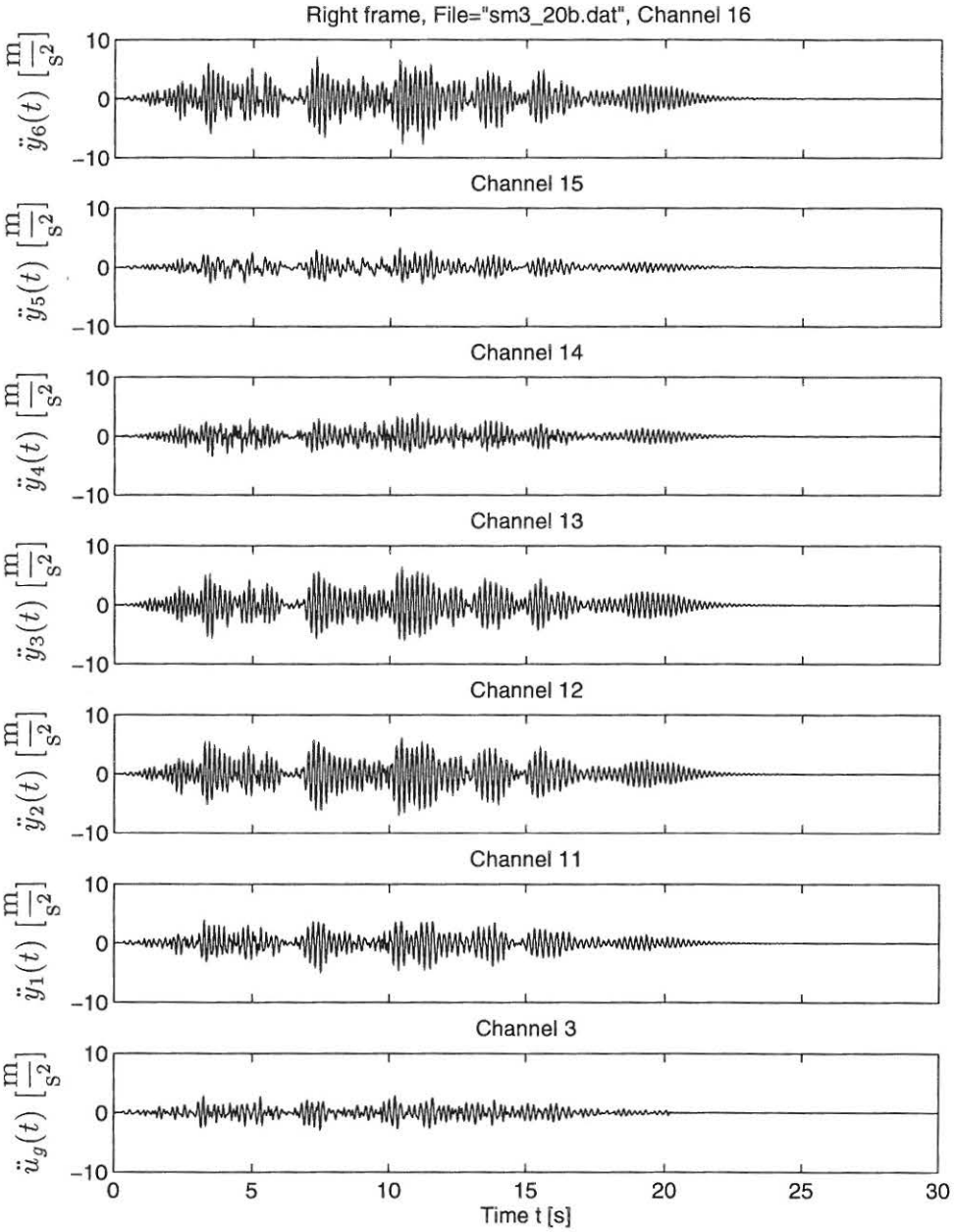

Figure 7.22: Measured accelerations during EQ2 for frame AAU3.

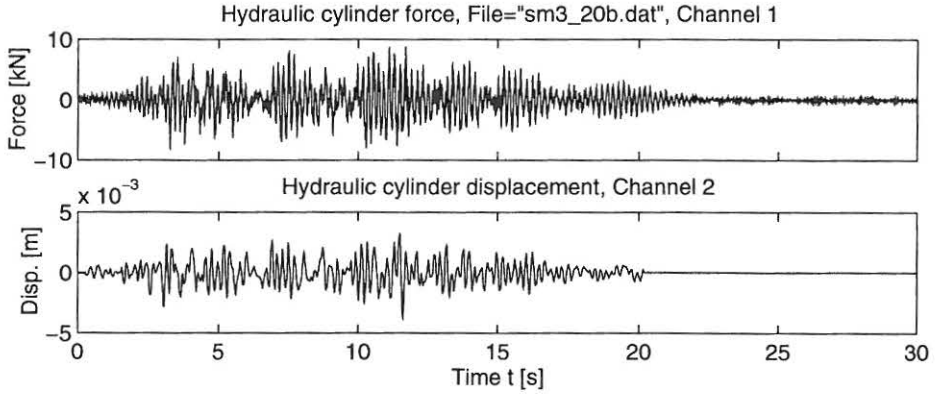

Figure 7.23: Measured shaking table displacement and cylinder force during EQ2 for frame AAU3.

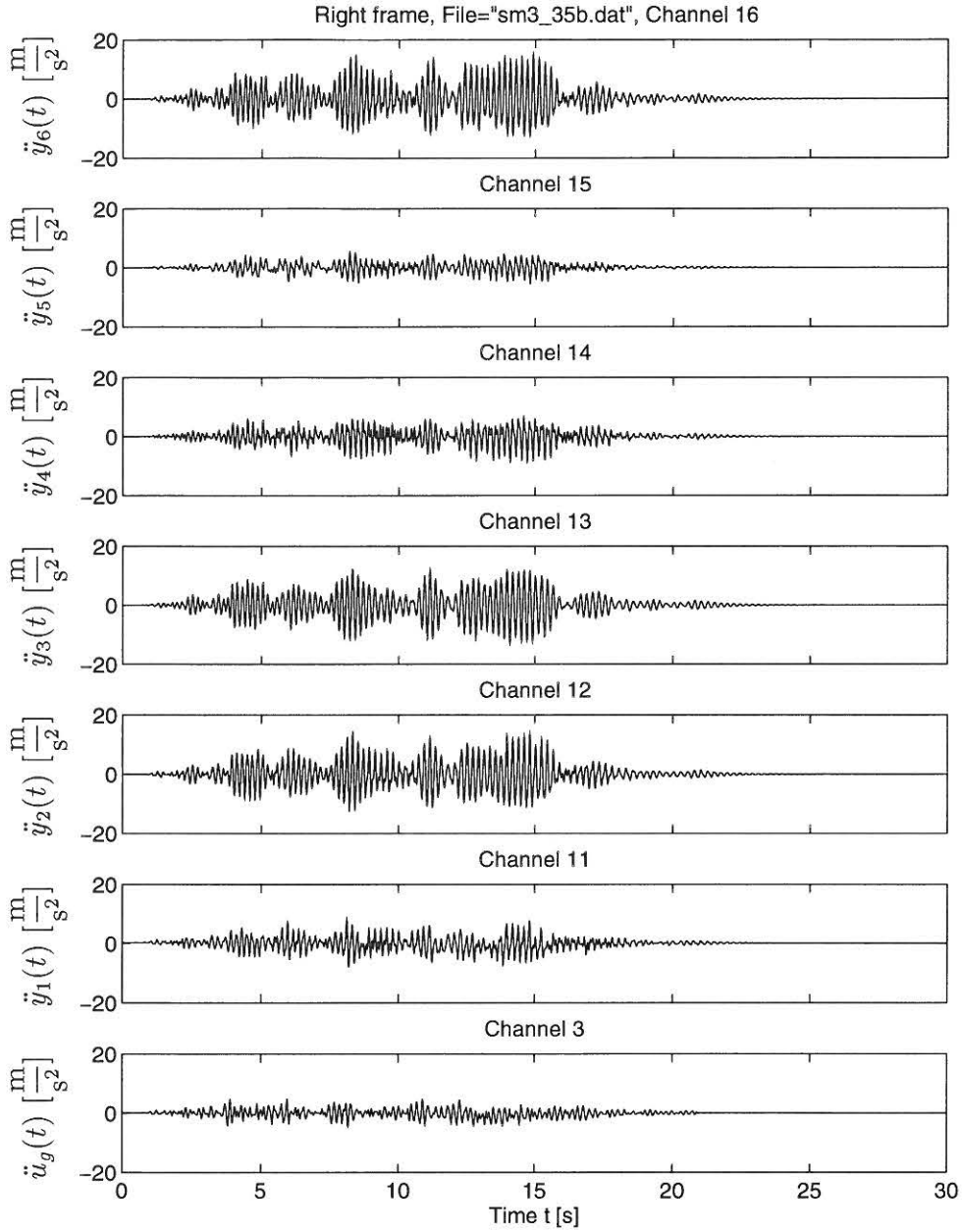

Figure 7.24: Measured accelerations during EQ3 for frame AAU3.

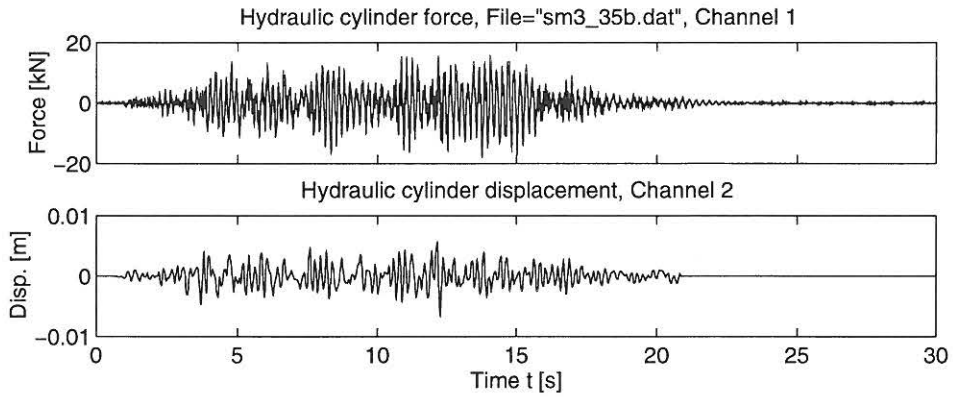

Figure 7.25: Measured shaking table displacement and cylinder force during EQ3 for frame AAU3.

7.3.1 Processed data

This section presents processed data from AAU3 where top-storey displacements, frequency developments and force-deformation curves have been found using the procedures described in section 4.3.

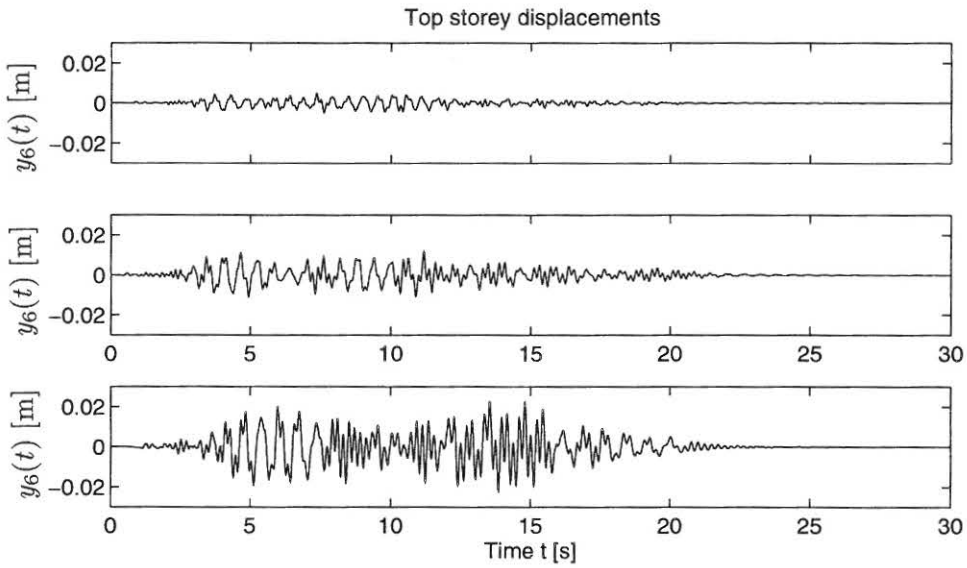

Figure 7.26: Top storey displacements during EQ1, EQ2 and EQ3.

During the integration process where displacements are obtained a butterworth 6th order high-pass digital filter with a cut-off frequency of 0.5 Hz and a butterworth 8th order low-pass digital filter with a cut-off frequency of 20 Hz have been used.

The development in the two lowest eigenfrequencies during the three sequences are shown in figures 7.27-7.29, respectively.

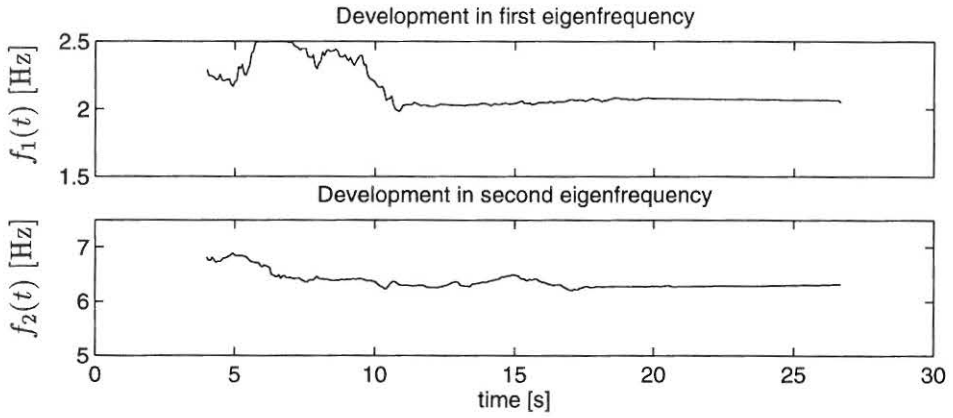

Figure 7.27: Development of softening in first and second mode during EQ1.

In table 7.4 the minimum values of the eigenfrequencies are listed along with the corresponding maximum softenings.

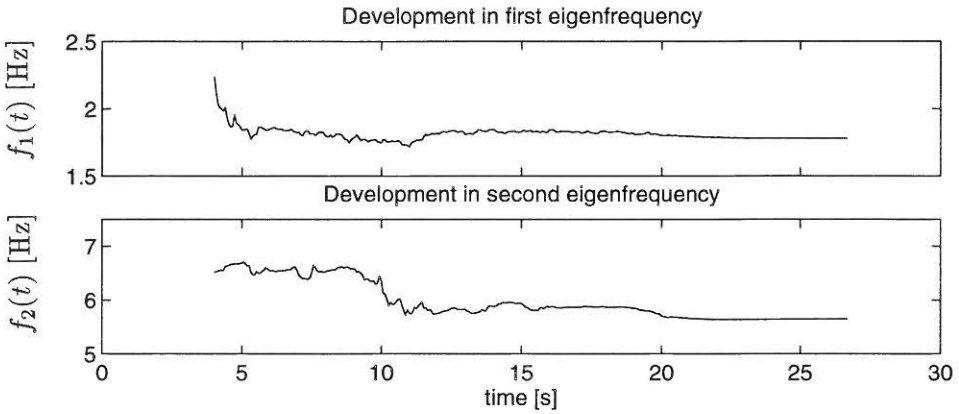

Figure 7.28: Development of softening in first and second mode during EQ2.

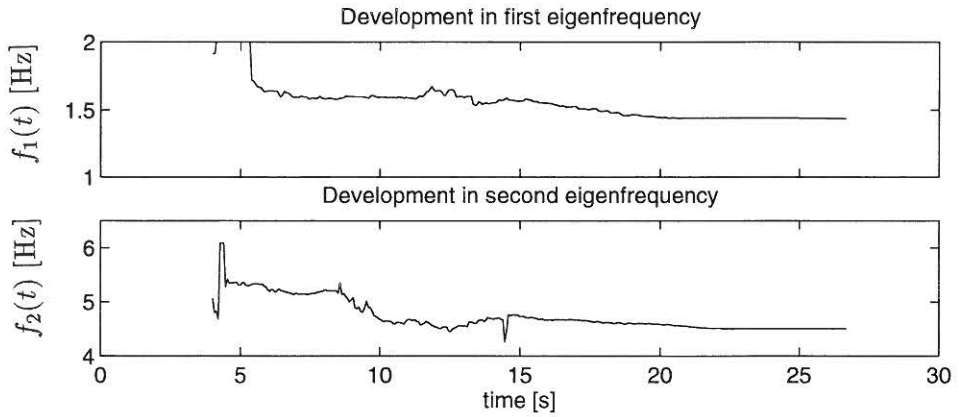

Figure 7.29: Development of softening in first and second mode during EQ3.

	$f_{\min,1}\ [Hz]$	$f_{\min,2}\ [Hz]$	$\delta_{M,1}$	$\delta_{M,2}$
EQ1	1.97	6.39	0.12	0.15
EQ2	1.73	5.67	0.24	0.22
EQ3	1.41	4.55	0.37	0.41

Table 7.4: *Estimated minimum frequencies and maximum softenings during the three earthquakes.*

Chapter 8

Results of reference tests and static bending tests

In this chapter the results of the reference tests of the used materials and the static bending tests of parts from undamaged as well as damaged frames are presented.

8.1 Compression tests of reference concrete specimens

For each frame three circular concrete specimens as illustrated in figure 2.5 were casted and was at the same day as the strong motion dynamic tests loaded until failure in a standard compression test. The purpose of these tests is to determine the compression strength f_c and the initial modulus of elasticity E_0.

The results of the tests for all concrete specimens are shown in table 8.1.

8.2 Tension tests of reference steel specimens

As in the case of the concrete, reference specimens of the used steel for reinforcement of the frames were stored. Since all the steel used for longitudinal reinforcement is from the same collections of steel only a total of three samples were collected. Ther purpose of testing the reference specimens is to determine the modulus of elasticity E_s, the yield strength f_{sy} and the ultimate strength f_{su}.

8.2.1 Longitudinal reinforcement steel

All steel used for longitudinal reinforcement are KS410 with a diameter of 6 mm. Three samples were collected and the results of the tension tests are shown in table 8.2.
In figure 8.1 the force-deformation curves for the steel samples are shown.

8.3 Static bending tests of beams and columns

The purpose of performing static bending tests of the different beams and columns of the frames is to obtain a measure of the damage state of the members of the structures. Due to symmetry only the outer columns and beams in one side of the frame and the center columns are tested.

Specimen	f_c [MPa]	E_0 [MPa]
AAU1a-1	20.2	-
AAU1a-2	20.9	-
AAU1a-3	20.5	16900
AAU1b-1	19.6	-
AAU1b-2	21.0	-
AAU1b-3	19.7	19200
AAU2a-1	22.6	-
AAU2a-2	21.7	-
AAU2a-3	22.2	20000
AAU2b-1	22.7	-
AAU2b-2	23.0	-
AAU2b-3	22.9	21600
AAU3a-1	21.6	-
AAU3a-2	21.7	-
AAU3a-3	22.3	20200
AAU3b-1	22.6	-
AAU3b-2	22.0	-
AAU3b-3	20.7	18200
AAU4-1	22.8	-
AAU4-2	27.1	-
AAU4-3	24.9	20800

Table 8.1: *Determined characteristics of the concrete for the frames.*

Specimen	f_{sy} [MPa]	f_{su} [MPa]	E_s [$\frac{10^5 \mathrm{N}}{\mathrm{m}^2}$]
1	535	642	2.003
2	535	644	1.842
3	542	650	2.013

Table 8.2: *Determined characteristics of the longitudinal reinforcement.*

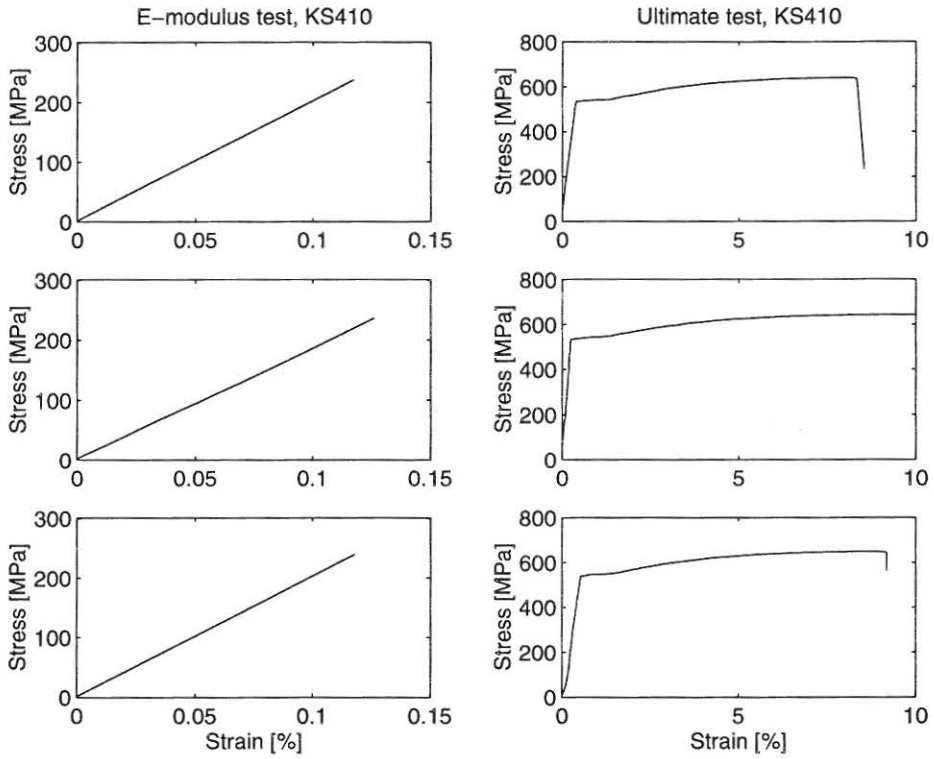

Figure 8.1: Force deformation curves for the steel specimens.

8.3.1 Results of Static bending tests

In this section the results of the static bending tests are presented. From figure 5.1 it is seen that in general five types of test specimens are available after the frame are cut into pieces. These five types are illustrated in figure 8.2. An adequate number of each of these five types of test specimens are tested from the undamaged frame, and the obtained force-deformation curves serves as references.

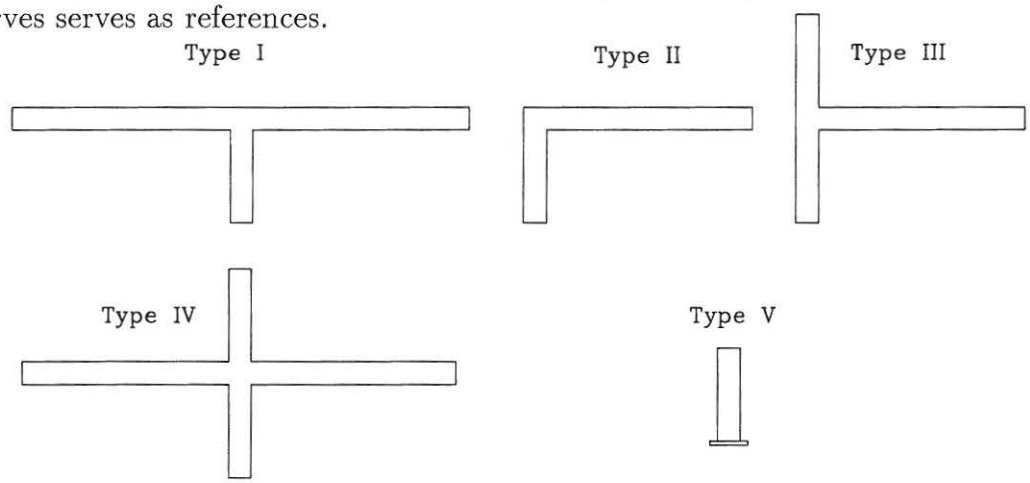

Figure 8.2: The five types of test specimens.

Undamaged reference frame

Force-deformation curves obtained for the beams and columns of the four different types of test specimens are shown in figure 8.3.

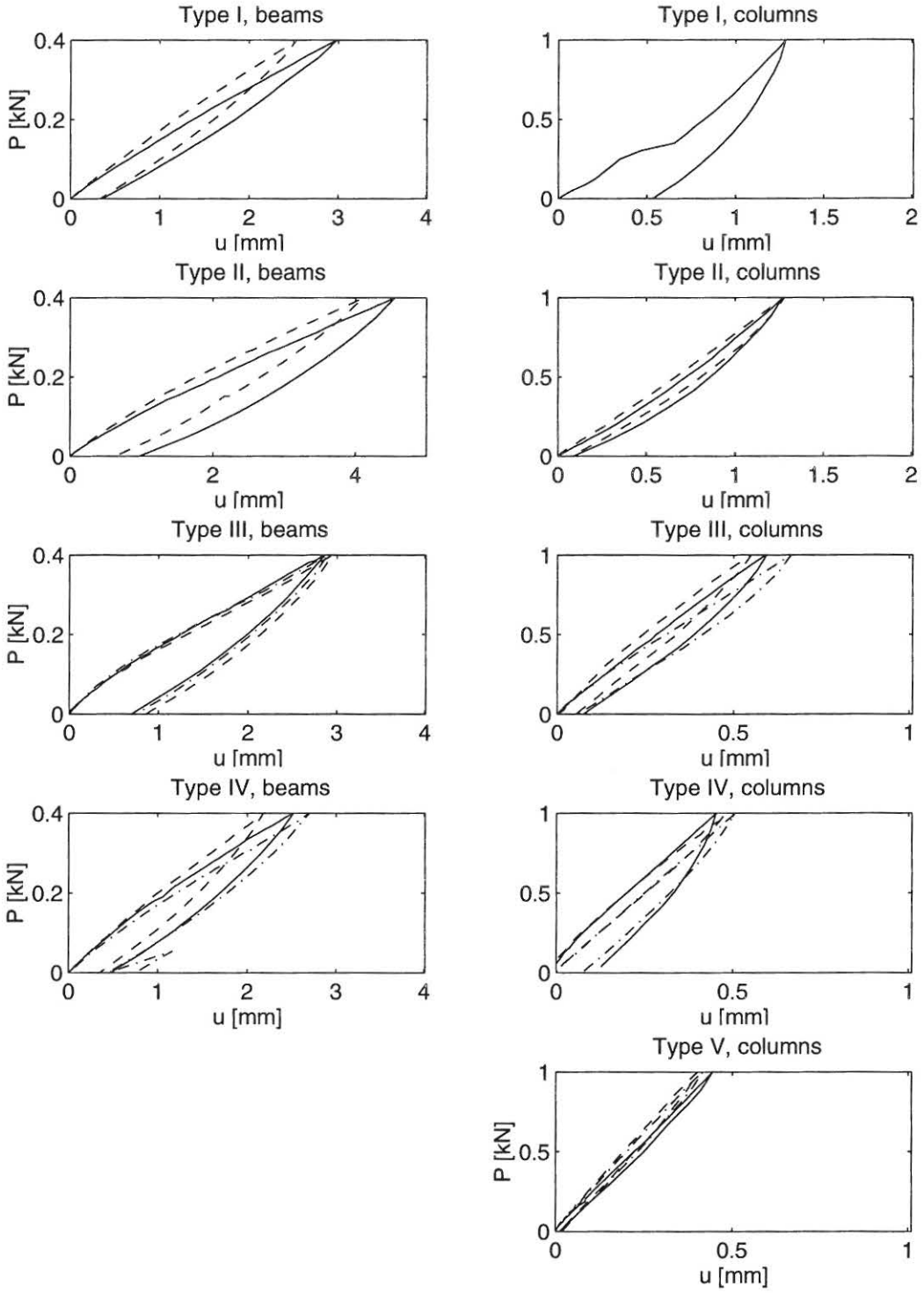

Figure 8.3: Force deformation curves obtained for the columns and beams in the five different types of test specimens.

Frame AAU2

The force-deformation curve obtained for each of the half-beams and half-columns in frame AAU2 are shown in figures 8.4-8.6.

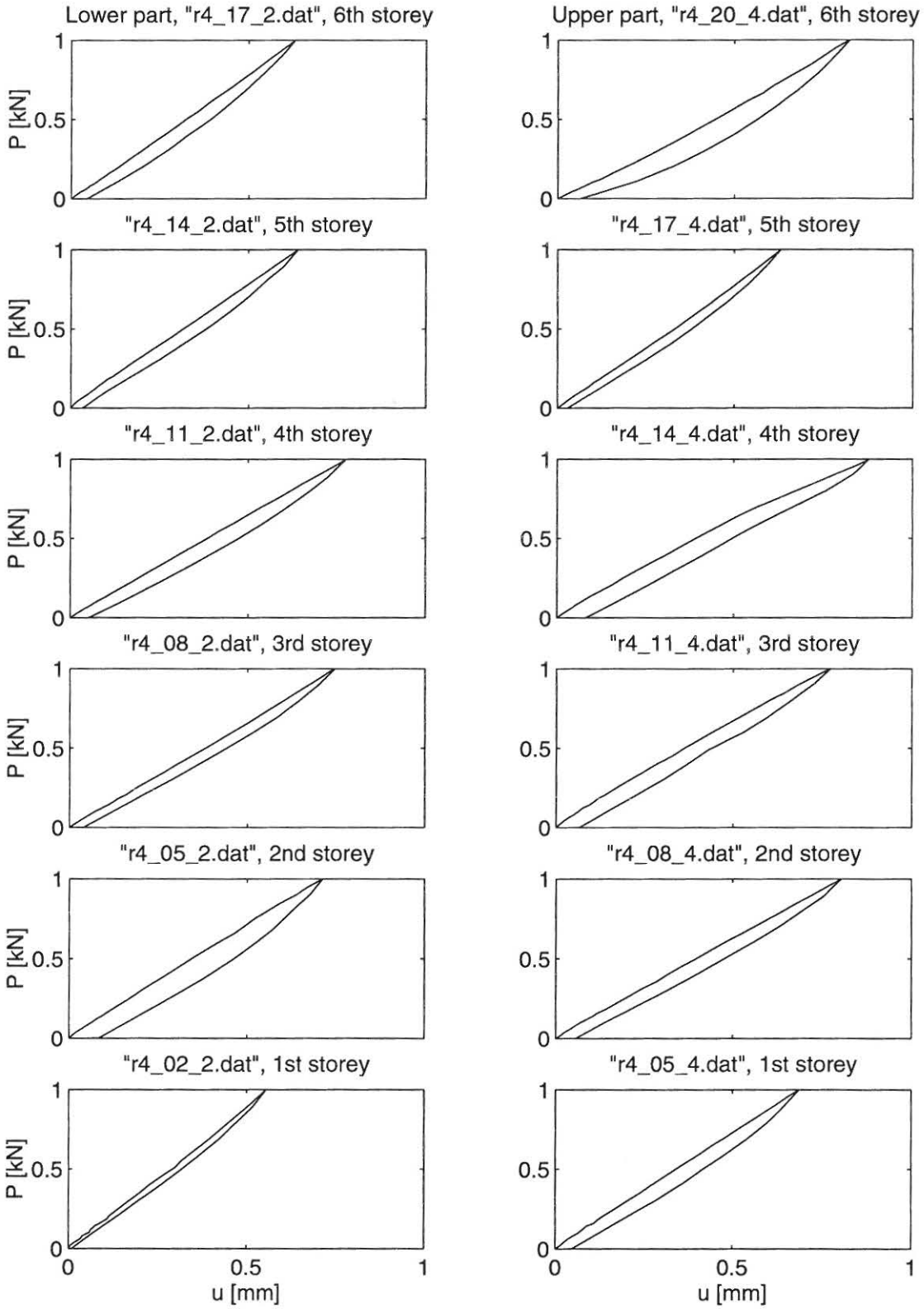

Figure 8.4: Force-deformation curves for the center columns obtained from the static tests. Frame AAU2.

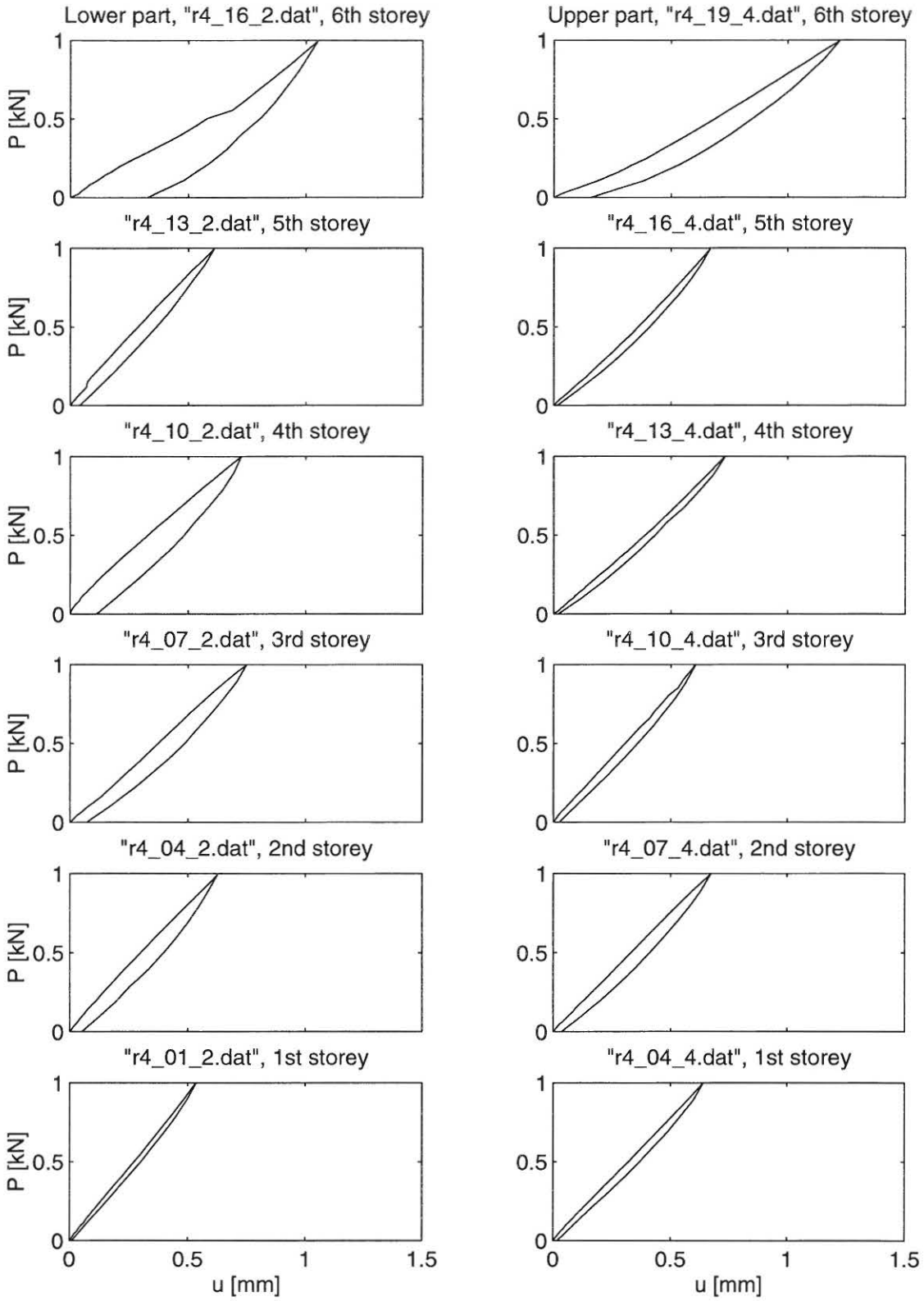

Figure 8.5: Force-deformation curves for the outer columns obtained from the static tests. Frame AAU2.

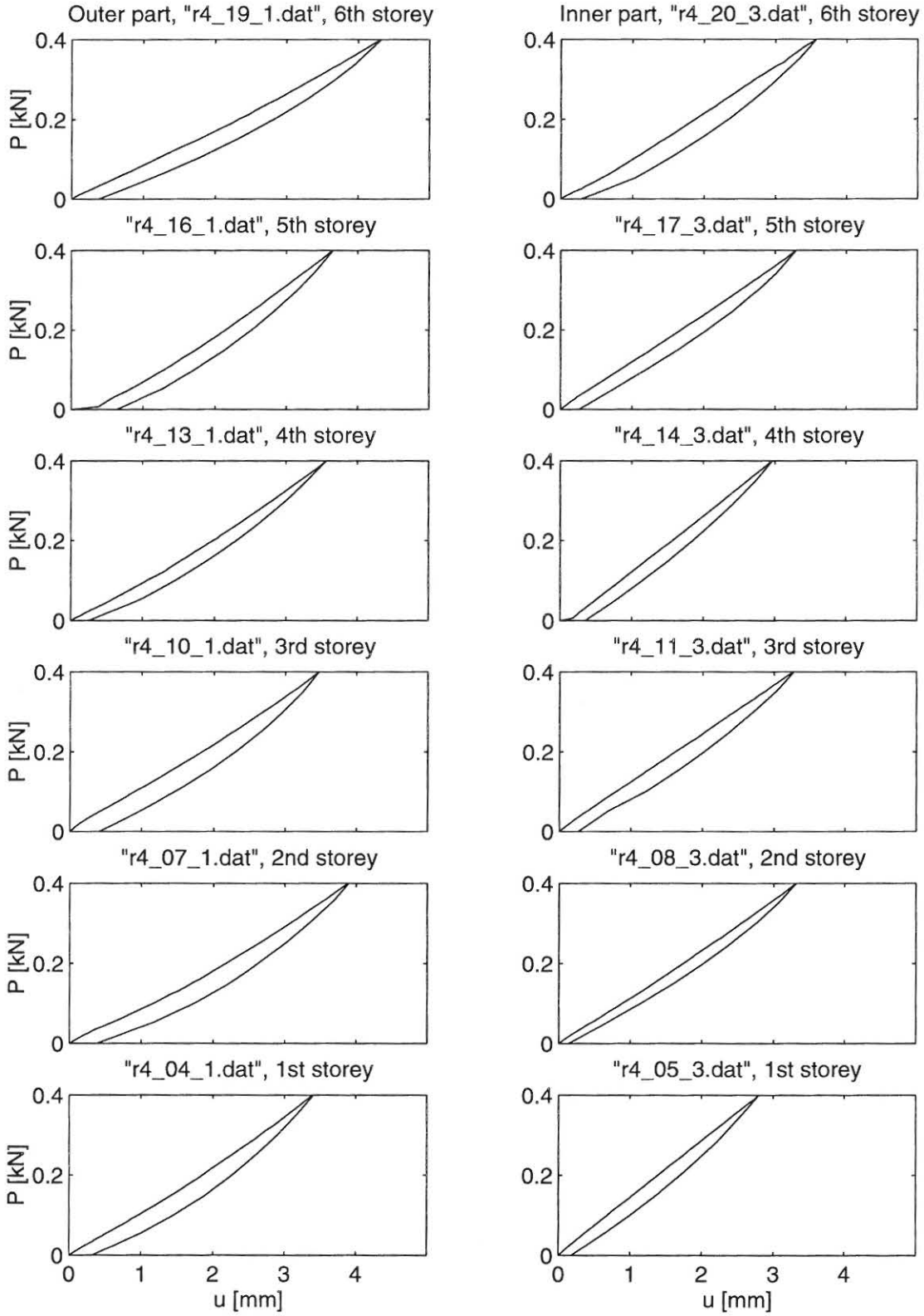

Figure 8.6: Force-deformation curves for the beams obtained from the static tests. Frame AAU2.

Frame AAU3

The force-deformation curve obtained for each of the half-beams and half-columns in frame AAU3 are shown in figures 8.7-8.9.

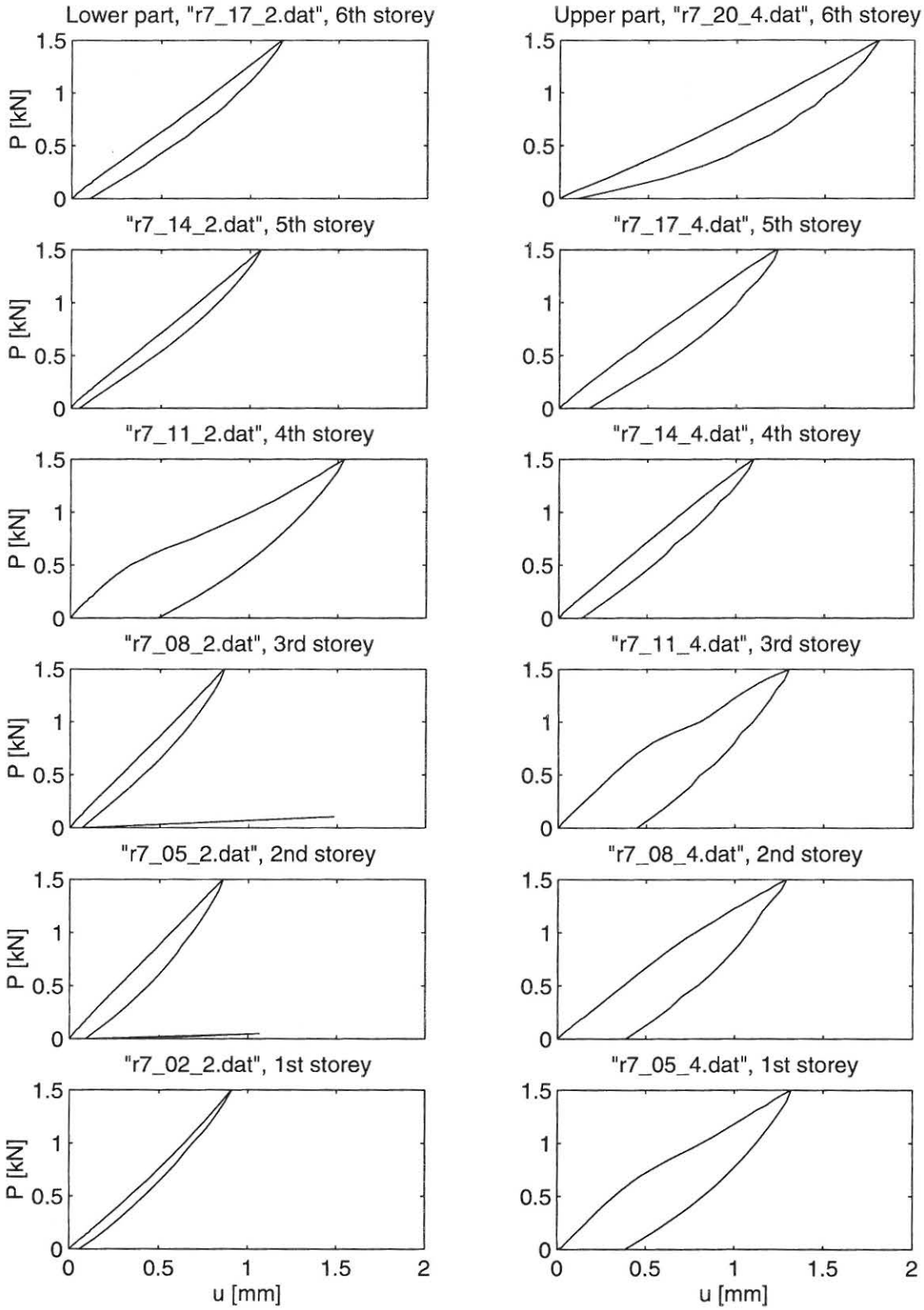

Figure 8.7: Force-deformation curves for the center columns obtained from the static tests. Frame AAU3.

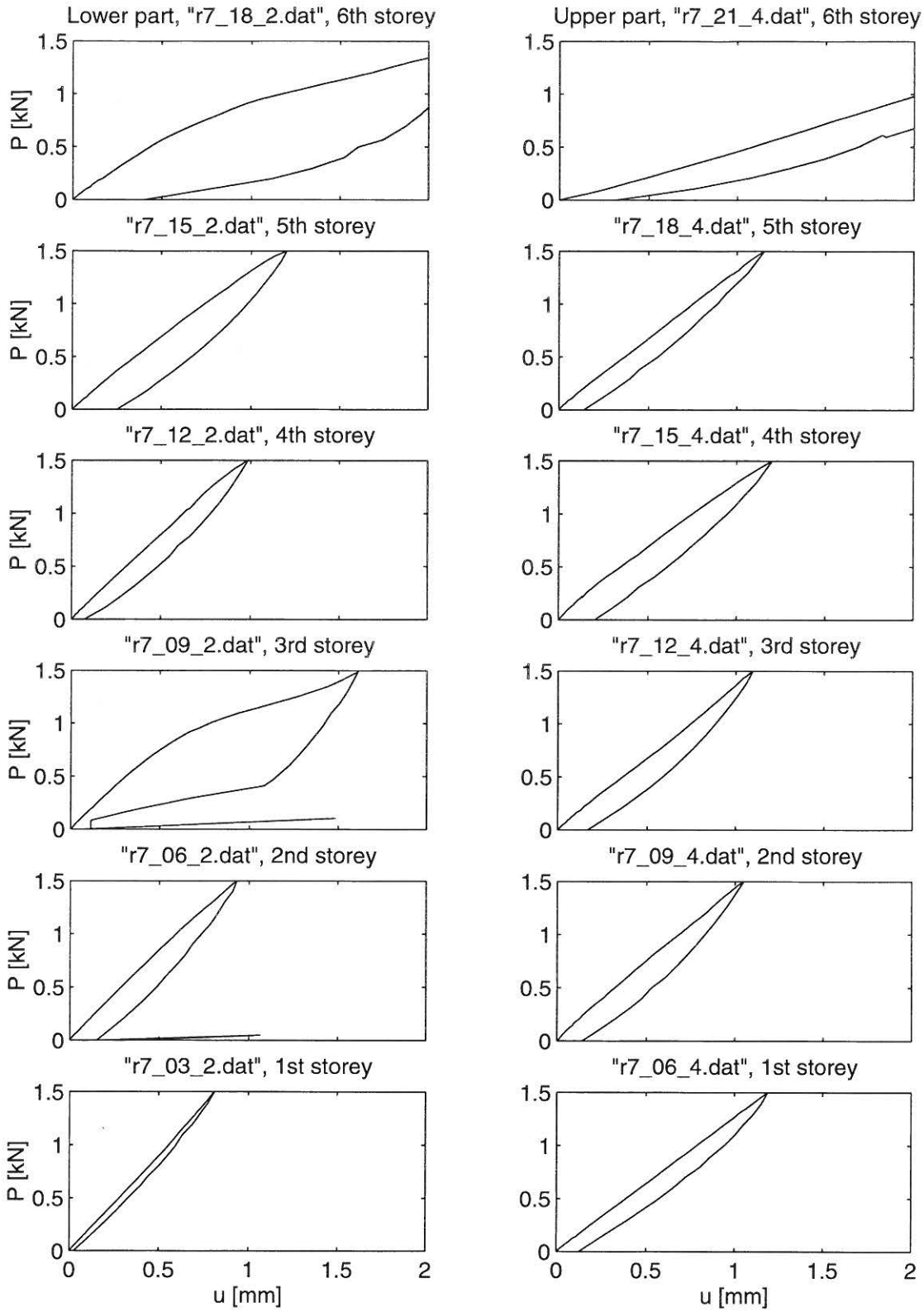

Figure 8.8: Force-deformation curves for the outer columns obtained from the static tests. Frame AAU3.

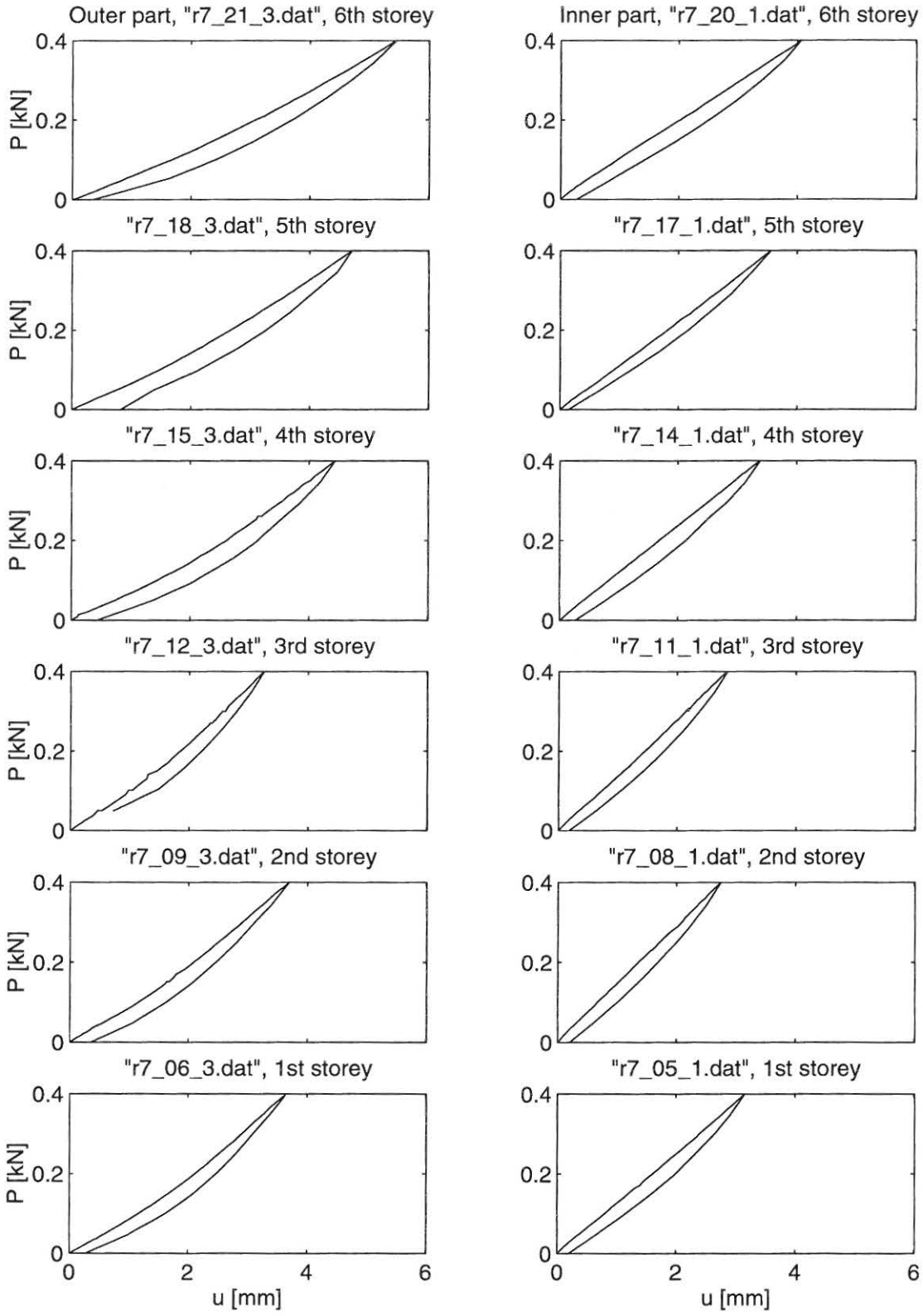

Figure 8.9: Force-deformation curves for the beams obtained from the static tests. Frame AAU3.

Chapter 9

Results of visual inspection after each run

In this section the results of the visual inspection of the frames are presented. The inspection is performed by scanning the structure with a magnification glas and each time a crack is observed it is marked by a pencil and photos are taken.

9.1 Definition of used classifications

After each series of ground motions the structure is throughout visually examined and the damage state of each storey of the building is classified into one of the following 6 classifications: Undamaged (U), Cracked (CR), Lightly Damaged (LD), Damaged (D), Severly Damaged (SD) or Collapse (CO). Each of the 6 classifications are defined in table 9.1.

Category	Definition
Undamaged UD	No external sign of changed integrity of any of the columns or beams in the storey
Cracked CR	Lightly cracking observed in several members but no permanent deformation
Lightly Dam. LD	Severe cracking observed with minor permanent deformations
Damaged D	Severe cracking and locally large permanent deformations observed.
Severely Dam. SD	Large permanent deformations observed and spalling of concrete at some members
Collapse CO	Very large permanent deformations observed and severe spalling of concrete at several members

Table 9.1: *Definition of the 6 damage classifications used.*

9.2 Frame AAU1

The frame AAU1 was exposed to three sequential earthquake like ground motion of type a, see figure 6.2 and the visual damage assessment was performed after each of these. The results of

the visual damage assessment are shown in table 9.2

Storey	EQ1	EQ2	EQ3
1	UD	CR	SD
2	CR	LD	CO
3	CR	LD	CO
4	UD	CR	LD
5	UD	CR	CR
6	UD	CR	CR

Table 9.2: *Damage classifications after the three earthquake events for frame AAU1.*

As indicated in table 9.2 only a few cracks was found in the structure after the first earthquake. The cracks was concentrated at the connections between columns and beams in the second and third storey. At the remaining storeys small cracks was found. After the second earthquake extensive crack growth was observed in the lower part of the frame and localized crushing of concrete at node 2 and 5 was observed. During the third earthquake damage developed dramatically in the second and third storey and after approximately 10 seconds of excitation these two storeys collapsed. Photos of the collapsed structure are shown in figures A.11-A.12.

9.3 Frame AAU2

The frame AAU2 was exposed to two sequential earthquake like ground motion of type a, see figure 6.2, and the visual damage assessment was performed after each of these. The results of the visual damage assessment are shown in table 9.3. Furthermore, photos of all nodes taken after the last strong motion event are stored on the enclosed CD-ROM. Cracks that were present in the undamaged virgin structure are marked with pencil-grey, after the first strong motion event with a red lines and after the second strong motion event with blue lines. A review of the photos are given in black and white in figure A.16.

Storey	EQ1	EQ2
1	CR	LD
2	CR	D
3	CR	LD
4	UD	CR
5	UD	CR
6	CR	CR

Table 9.3: *Damage classifications after the two earthquake events for frame AAU2.*

Before strong motion testing the structure was examined and shear cracks were found in the beams at the first, third and sixth storey.

After the first earthquake only a limited amount of micro crack were observed at the three lower storey and the top storey. The crack were largest and most dense in the nodes at the first and second storey. At the remaining storeys only small cracks was found. After the second earthquake extensive crack growth was observed in the lower part of the frame and localized crushing of concrete at node 2 and 5 was observed. Also in the beams at the top storeys shear cracks became longer.

9.4 Frame AAU3

The frame AAU3 was exposed to three sequential earthquake like ground motion of type b, see figure 6.2 and the visual damage assessment was performed after each of these. The results of the visual damage assessment are shown in table 9.4. Furthermore, photos of all nodes taken after the last strong motion event are stored on the enclosed CD-ROM. Cracks that were present in the undamaged virgin structure are marked with pencil-grey, after the first strong motion event with a red lines, after the second strong motion event with green lines and after the third with blue lines. A review of the photos are given in black and white in figure A.17.

Storey	EQ1	EQ2	EQ3
1	CR	LD	D
2	CR	D	LD
3	CR	LD	LD
4	CR	LD	D
5	CR	LD	D
6	CR	CR	CR

Table 9.4: *Damage classifications after the three earthquake events for frame AAU3.*

Before strong motion testing the structure was examined and shear cracks were found in the beams at the first and sixth storey.

After the first earthquake only micro crack were observed at the three lower storey and the top storey. The crack were largest and most dense in the nodes at the third, fourth and fifth storey. At the remaining storeys generally only small cracks were found. After the second earthquake extensive crack growth was observed at the nodes in the fourth and fifth storey. Furthermore, several shear cuts (horizontal cracks) were observed in the columns at the third, fourth and fifth storey. After the third earthquake crack growth were observed in all storeys and furthermore crushing of concrete were seen at the center node in the first, fourth and fifth storey.

Chapter 10

Summary

In this report the results from a series of shaking table tests performed on 6-storey model test RC-frames tested at the Structural Laboratory at Aalborg University, Denmark are presented. In the study a total of 3 experimental set-ups were tested. The structures are instrumented with accelerometers at all storeys and at the shaking table. Before strong motion sequences are applied to the structures free decay tests are performed at different excitation levels to provide data for modal identification of the undamaged structure. Two or three sequences of strong motions of increasing magnitude were applied to each of the structures and acceleration time series at all storey were collected. In between the strong motion events and after the last one free decays as well as static tests were performed as for the undamaged structure. After each strong motion event all cracks were marked with pens of different colours and after the termination of the dynamic tests pictures were taken off all nodes, where the cracks were located. When the test structures was taken down one of the frames in the set-up was cut into smaller specimens and each beam and column was statically tested in order to evaluate the reduced bending stiffness. These stiffnesses were compared to stiffnessess obtained from a reference frame.

Bibliography

[1] Banon, H., Biggs, J. M. and Irvine, H. M., *Seismic Damage in Reinforced Concrete Frames.* Journal of the Structural Division, Proc., ASCE, Vol. 107, No. ST9, Sept. 1981, pp 1713-1729.

[2] Banon, H., and Veneziano, D., *Seismic Safety of Reinforced Concrete Members and Structures.* Earthquake Engineering and Structural Dynamics, Vol. 10, 1982, pp 179-193.

[3] Banon, H. *Prediction of Seismic Damage in Reinforced Concrete Frames.* Publication R80-16, Department of Civil Engineering, MIT, Cambridge Mass., May 1980.

[4] Beck, J.L. and Jennings, P.C., *Structural Identification using Linear Models and Earthquake Records.* Earthquake Engineering and Structural Dynamics, Vol. 8, 1980, pp. 145-160.

[5] Bracci, J.M. and Reinhorn, A.M., *Shaking Table Testing of a 1:3 scale RC Frame Model.* Proceedings of Structural Dynamics - EURODYN'96, Ed. Augusti, Borri and Spinelli, Torino, Italy, 1996, pp. 893-897.

[6] Casas, J.R. *Structural Damage Identification from Dynamic-Test Data.* ASCE J. Struc. Eng. Vol. 120, No. 8, Aug. 1994, pp. 2437-2450.

[7] Cecen, H., *Response of Ten Story, Reinforced Model Frames to Simulated Earthquakes.* Thesis presented to the University of Illinois, Urbana, I11., in partial fulfilment of the requirements for the degree of Doctor of Philosophy, 1979.

[8] DiPasquale, E. and Çakmak, A. Ş. *Detection of Seismic Structural Damage using Parameter-Based Global Damage Indices.* Probalistic Engineering Mechanics, Vol. 5, No. 2, pp. 60-65, 1990.

[9] DiPasquale, E. and Çakmak, A. Ş. *Damage Assesment from Earthquake Records.* Structures and Stochastic Methods, Elsevier, Amsterdam, pp. 123-138.

[10] DiPasquale, E. and Çakmak, A. Ş. *Seismic Damage Assessment using Linear Models.* Soil Dynamics and Earthquake Engineering, Vol. 9, No. 4, pp. 194-215, 1990.

[11] DiPasquale, E., Ju, J.-W., Askar, A. and Çakmak, A. Ş. *Relation Between Global Damage Indices and Local Stiffness Degradation.* Journal of Structural Engineering, Vol. 116, No. 5, pp. 1440-1456, 1990.

[12] Hassotis, S and Jeong, G.D. *Assessment of Structural Damage from Natural Frequency Measurements.* Computers and Structures, Vol. 49, No. 4, pp. 679-691, 1993.

[13] Hoshiya, M. and Saito, E. *Structural Identification by Extended Kalman Filter.* Journal of Engineering Mechanics, Vol. 110, No. 12, Dec. 1984.

[14] Kirkegaard, P.H. and Rytter, A. *Use of a Neural Network for Damage Detection in a Steel Member.* Presented at the third Int. Conf. in the Application of Artificial Intelligence to Civil Engineering Structures, Civil-Comp93, Edinburgh, August 17-19, 1993.

[15] Kirkegaard, P.H., Skjærbæk, P.S. and Andersen, P., *Identification of Time-Varying Civil Engineering Structures using Multivariate Recursive Time Domain Models.* Proceedings of the 21st international Symposium on Noise and Vibrations, ISMA21, Leuven, Belgium, September 18-20, 1996.

[16] Kirkegaard, P.H., Skjærbæk, P.S. and Nielsen, S.R.K., *Identification Report: Earthquake Tests on Scale 1:5 Reinforced Concrete Frames.* Internal Laboratory Report, Fracture and Dynamics, Paper no. 85, Aalborg University, Denmark, 1997.

[17] Koh, C.G., See, L.M. and Balendra, T. *Estimation of Structural Parameters in Time Domain: A Substructure Approach.* Earthquake Engineering and Structural Dynamics, Vol. 20, No. 8, pp. 787-801, Aug. 1991.

[18] Koh, C.G., See, L.M. and Balendra, T. *Damage Detection of Buildings: Numerical and Experimental studies.* ASCE J. Str.Eng., Vol. 121, No. 8, pp. 1155-1160, Aug. 1995.

[19] Kratzig, W.B. *Seismic Damage Simulation: A Low-cycle fatigue Process.* Proceedings of Structural Dynamics - EURODYN'96, Ed. Augusti, Borri and Spinelli, Torino, Italy, 1996, pp. 15-22.

[20] Köylüoğlu, H. U., Nielsen, S. R. K., Çakmak, A.Ş. and Kirkegaard, P. H. *Prediction of Global and Localized Damage and Future Reliability for RC Structures subject to Earthquakes.* Structural Reliability Theory, paper 128, Aalborg University 1994 (submitted to Soil Dynamics and Earthquake Engineering).

[21] Lin, J.-S. and Zhang, Y. *Nonlinear Structural Identification using Extended Kalman Filter.* Computers and Structures, Vol. 52, No. 4, pp. 757-764, 1994

[22] Micaletti, R.C., Çakmak, A. Ş., Nielsen, S.R.K. and Kirkegaard, P. H. *Construction of Time-Dependent Spectra using Wavelet Analysis for Determination of the Maximum Softening Index.* Structural Reliability Theory, paper 147, Aalborg University 1995 (To be submitted to ISMA 21, Noise and Vibration Engineering Conference, September 18-20, 1996, Belgium).

[23] Mullen, C., Micaletti, R.C. and Çakmak, A.Ş. *A Simple Method for Estimating the Maximum Softening Damage Index.* Proc. of the 7th int. Conf. on Soil Dynamics and Structural Engineering 24-26 May 1995, Chania, Crete, Greece, pp. 371-378.

[24] Mørk, K.J., *Stochastic Analysis of Reinforced Concrete Frames under Seismic Excitation.* Soil Dynamics and Earthquake Engineering, Vol. 11, No. 3, 1992.

[25] Mørk, K.J. and Nielsen, S.R.K., *Program for Stochastic Analysis of Plane Reinforced Concrete Frames under Seismic Excitation.* Structural Reliability Theory Paper No. 91, University of Aalborg, 1991.

[26] Nielsen, S.R.K., Köylüoğlu, H.U. and Çakmak, A.Ş., *One and Two-Dimensional Maximum Softening Damage Indicators for Reinforced Concrete Structures Under Seismic Excitation.* Soil Dynamics and Earthquake Engineering, 11, pp. 435-443, 1992.

[27] Nielsen, S.R.K. and Çakmak, A.Ş., *Evaluation of Maximum Softening Damage Indicator for Reinforced Concrete Under Seismic Excitation.* Proceedings of the First International Conference on Computional Stochastic Mechanics. Ed. Spanos and Brebbia, pp. 169-184, 1992. SS

[28] Nielsen, S.R.K., Skjærbæk, P.S., Köylüoğlu, H.U. and Çakmak, A.Ş., *Prediction of Global Damage and Reliability based upon Sequential Identification and Updating of RC-Structures subject to Earthquakes.* Proc. of 7th int. Conf. on Soil Dynamics and Earthquake Engineering 24-26 May 1995, Chania, Crete, Greece, pp. 361-369.

[29] Olafson, S., Remseth, S. and Sigbjornson, R., *Simulation of Probabilistic Non-Linear Response Spectra.* Proceedings of Structural Dynamics - EURODYN'96, Ed. Augusti, Borri and Spinelli, Torino, Italy, 1996, pp. 97-104.

[30] Pandey, A.K. and Biswas, M., *Damage Detection in Structures using Changes in Flexibility.* Journal of Sound and Vibration 169(1), pp. 3-17, 1994.

[31] Park, Y.J. and Ang, A. H.-S., *Mechanistic Seismic Damage Model for Reinforced Concrete.* ASCE J. Struc. Eng., 111(4) April 1985, pp.722-739.

[32] Park, Y.J., Ang, A. H.-S., and Wen, Y.K., *Seismic Damage Analysis of Reinforced Concrete Buildings.* ASCE J. Struc. Eng., 111 (4) April 1985, pp. 740-757.

[33] Park, Y.J., Ang, A. H.-S., and Wen, Y.K., *Damage Limiting Aseismic Design of Buildings.* Earthquake Spectra, Vol. 3 No. 1, Feb. 1987, pp. 1-26.

[34] Park, Y.S., Park, H.S., and Lee, S.S., *Weighted-Error-Matrix Application to Detect Stiffness Damage by Dynamic-Characteristic Measurement.* Journal of Modal Analysis, July. 1988, pp. 101-107.

[35] Penny, J.E.T., Wilson, D.A.L., and Friswell, M.I., *Damage Location in Structures using Vibration Data.* Aston University, Birmingham, UK, 1993.

[36] Reinhorn, A.M., Seidel, M.J., Kunnath, S.K. and Park, Y.J., *Damage Assessment of Reinforced Concrete Structures in Eastern United States.* NCEER-88-0016 technical report, June 1988.

[37] Rodriguez-Gomez, S., *Evaluation of Seismic Damage Indices for Reinforced Concrete Structures.* M.Sc. Thesis, Princeton University, Oct. 1990.

[38] Ruiz, P. and Penzien, J., *Probabilistic Study of Behaviour of Structures during Earthquakes.* Report No. EERC 69-3, University of California, Berkeley, California, USA.

[39] Rytter, A. *Vibration Based Inspection of Civil Engineering Structures.* Ph.D. Thesis, Aalborg University, 1993.

[40] Seible, F., Hegenmier, G.A., Igarashi, A. and Kingsley, G.R., *Simulated Seismic-Load Tests on Full-Scale Five-Story Masonry Building.* ASCE J. Struc. Eng., Vol. 120, No. 3, March 1994, pp. 903-923.

[41] Shah, P.C. and Udwadia, F.E., *A Methodology for Optimal Sensor Locations for Identification of Dynamic Systems.* Journal of Applied Mechanics, Vol. 45, March 1978, pp. 188-196.

[42] Skjærbæk, P.S., Nielsen, S.R.K. and Çakmak, A.S., *Damage Localization of Severely Damaged RC-structures based on Measured Eigenperiods from a Single Response.* Proceedings of the 4th International Conference on Localized Damage 96, June 3-5 1996, Fukuoka, Japan, pp. 815-822.

[43] Skjærbæk, P.S., Nielsen, S.R.K. and Çakmak, A.S., *Assessment of Damage in Seismically Excited RC-structures from a Single Measured Response* Proceedings of the 14th IMAC, Dearborn, Michigan, USA, February 12-15, 1996, pp. 133-139.

[44] Skjærbæk, P.S., Çakmak, A.S. and Nielsen, S.R.K., *Identification of Damage in RC-Structures from Earthquake Records - Optimal Location of Sensors* Fracture and Dynamics, Paper 77. Journal of Soil Dynamics and Earthquake Engineering, No. , 1996, pp. ??-??.

[45] Skjærbæk, P.S., Nielsen, S.R.K. and Çakmak, A.Ş, *Damage Localization and Quantification of an Earthquake Excited Model Test Frame* Pending, To be submitted to Journal of Earthquake Engineering and Structural Dynamics, ultimo 1996.

[46] Skjærbæk, P.S., Nielsen, S.R.K., Kirkegaard, P.H. and Çakmak, A.Ş, *Experimental Study of Global Damage Indicators compared to Observed/Measured Damage for a 2-bay, 6-storey Model Test Frame* Pending, To be submitted to Journal of Structural Engineering, ASCE, ultimo 1996.

[47] Skjærbæk, P.S., Kirkegaard, P.H. and Nielsen, S.R.K., *Modal Identification of a Time-Invariant 6-storey Model Test Frame from Weak Motion Shaking Table Tests using Uni- and Multivariate Models.* Pending, To be submitted to the 15th International Modal Analysis Conference, February 3-6 1997, Orlando, Florida, USA, deadline October 7th, 1996.

[48] Skjærbæk, P.S., Kirkegaard, P.H. and Nielsen, S.R.K., *Modal Identification of a Time-varying 6-storey Model Test Frame from Strong Motion Shaking Table Tests using Uni- and Multivariate Models.* Pending, To be submitted to the 15th International Modal Analysis Conference, February 3-6 1997, Orlando, Florida, USA, deadline October 7th, 1996.

[49] Skjærbæk, P.S., Kirkegaard, P.H. and Nielsen, S.R.K., *Simulation of Near-Source Ground Motions using ARMA Models and Neural Networks.* Pending, To be submitted to the 15th International Modal Analysis Conference, February 3-6 1997, Orlando, Florida, USA, deadline October 7th, 1996.

[50] Skjærbæk, P.S., Kirkegaard, P.H. and Nielsen, S.R.K., *Experimental Case Study of Local Damage Indicators for a 2-bay, 6-Storey RC-Frame Subject to Earthquake.* Pending, To be submitted to the 15th International Modal Analysis Conference, February 3-6 1997, Orlando, Florida, USA, deadline October 7th, 1996.

[51] Snæbjornsson, J.T., Hjort-Hansen, E. and Sigbjornsson, R., *Variability of Natural Frequency and Damping ratio of a Concrete Building - Case Study in System identification.* Proceedings of Structural Dynamics - EURODYN'96, Ed. Augusti, Borri and Spinelli, Torino, Italy, 1996, pp. 949-956.

[52] Stephens, J.E. and Yao, J.P.T., *Damage Assesment Using Response Measurements.* ASCE J. Struc. Eng. 113 (4) April 1987, pp. 787-801.

[53] Stephens, J.E., *A Damage Function Using Structural Response Measurements.* Structural Safety Studies, ASCE, May 1985, pp. 22-39. SS

[54] Stephens, J.E., *Structural Damage Assesment Using Response Measurements.* Ph.D.-thesis, Purdue University, 1985.

[55] Stubbs, N. and Osegueda, R., *Damage Detection in Periodic Structures.* Damage Mechanics and Continuum Mechanics, ASCE, October 1985.

[56] Sues, R.H., Mau, S.T. and Wen, Y.K., *System identification of Degrading Restoring Forces.* Journal of Engineering Mechanics, ASCE, Vol. 114, No. 5, pp. 833-845, 1988. SS

[57] Tajimi, H., *Semi-Empirical Formula for the Seismic Characteristics of the Ground.* Proceedings of the 2nd World Conference on Earthquake Engineering, Vol. II, 781-798, Tokyo and Kyoto, 1960.

[58] Torkamani, M.A.M. and Ahmadi, A.K., *Stiffness Identification of a Tall Building during Construction Period using Ambient Tests.* Earthquake Engineering and Structural Dynamics, Vol. 16, 1988. pp. 1177-1188.

[59] McVerry, G. H., *Structural Identification in the Frequncy Domain from Earthquake Records.* Earthquake Engineering and Structural Dynamics, Vol. 8, 1980. pp. 161-180.

[60] Vestroni F., Cerri, M.N. and Antonacci, E., *Damage Detection in Vibrating Structures.* Proceedings of Structural Dynamics - EURODYN'96, Ed. Augusti, Borri and Spinelli, Torino, Italy, 1996, pp. 41-50.

[61] Wang, D. and Haldar, A., *Element-level System Identification with unknown input.* Journal of Engineering Mechanics, Vol. 120, No. 1, January 1994, pp. 159-176.

[62] Wang, D. and Haldar, A., *Stiffness and Damping Identification for Tall Buildings with Unknown Excitation.* Proc. of ICASP7, Application of Statistics and Probability, Lemaire, Favre and Mebarki, 1995, pp. 963-969.

Appendix A

Photos

In this appendix photos taken during the process of construction and testing of the frames.

A.1 The construction process

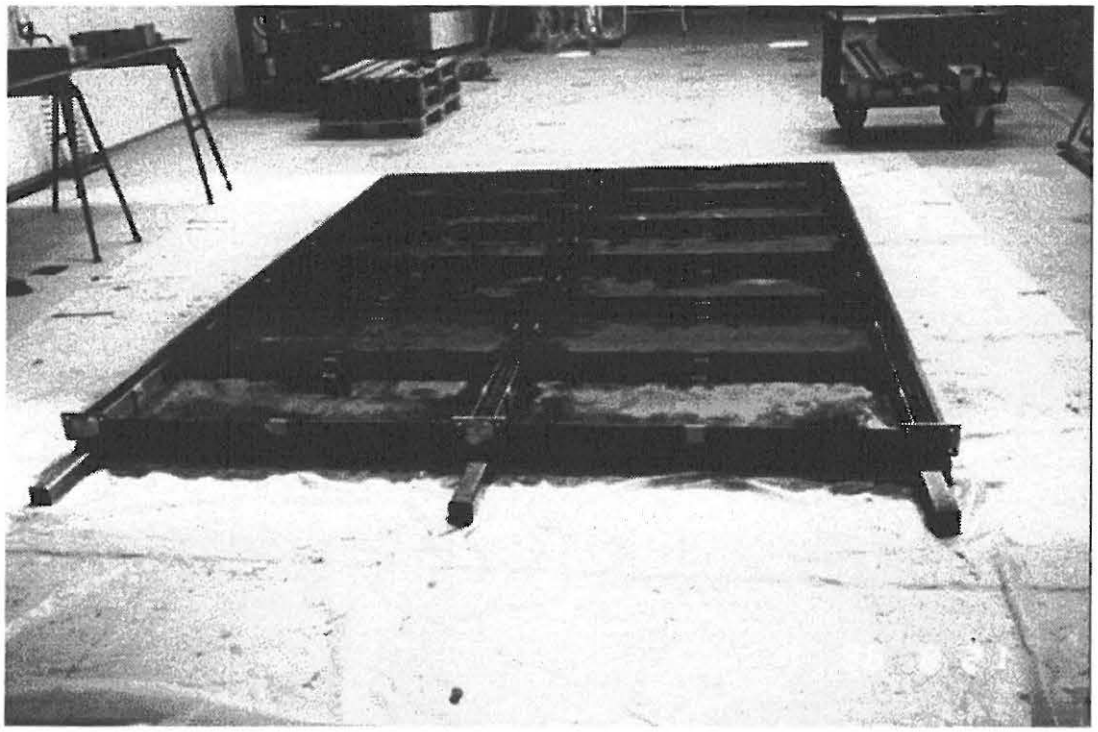

Figure A.1: The form used for construction of the frames.

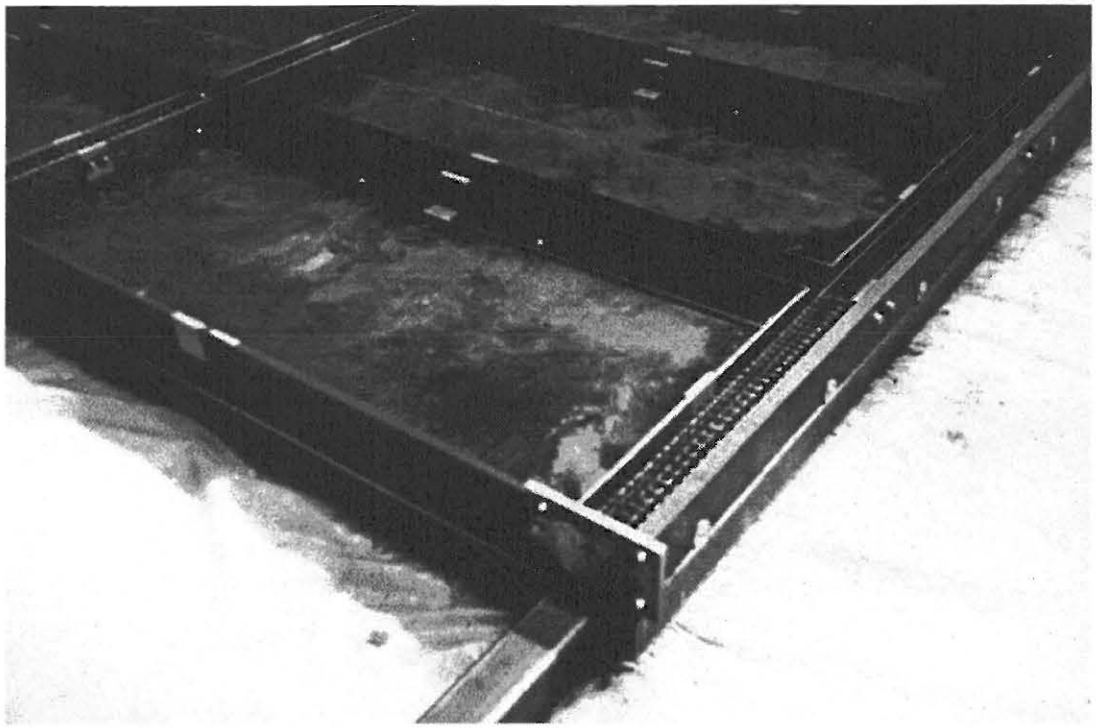

Figure A.2: Detail of reinforcement.

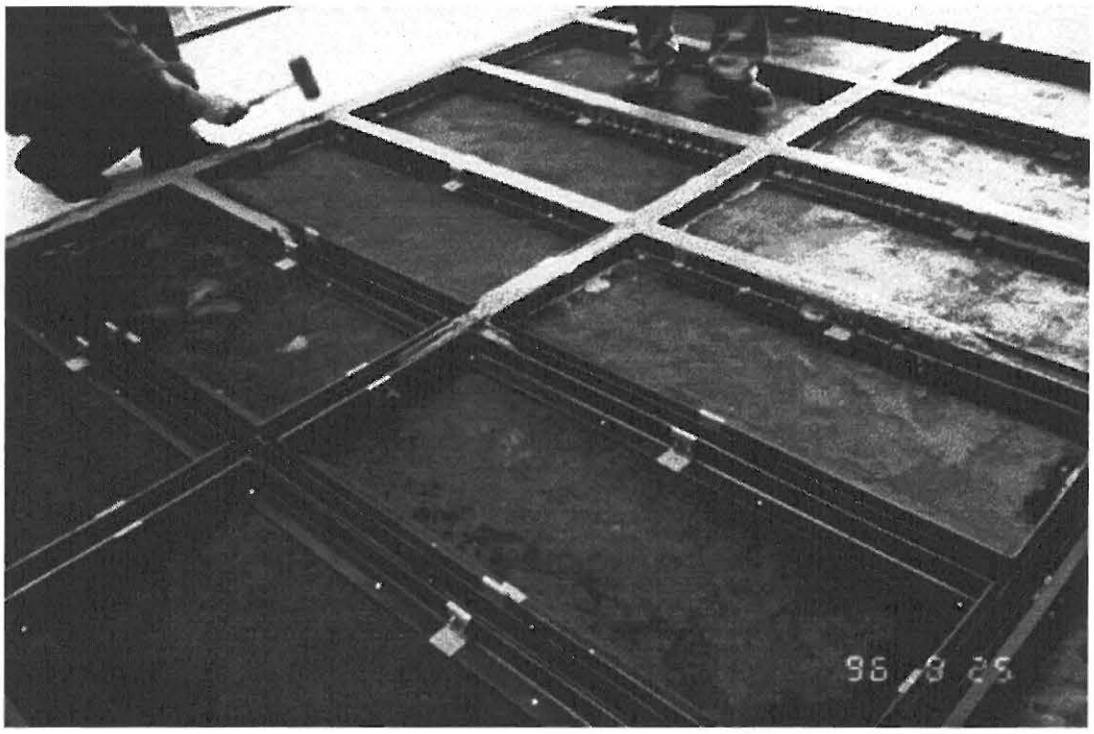

Figure A.3: Pouring and vibration of concrete.

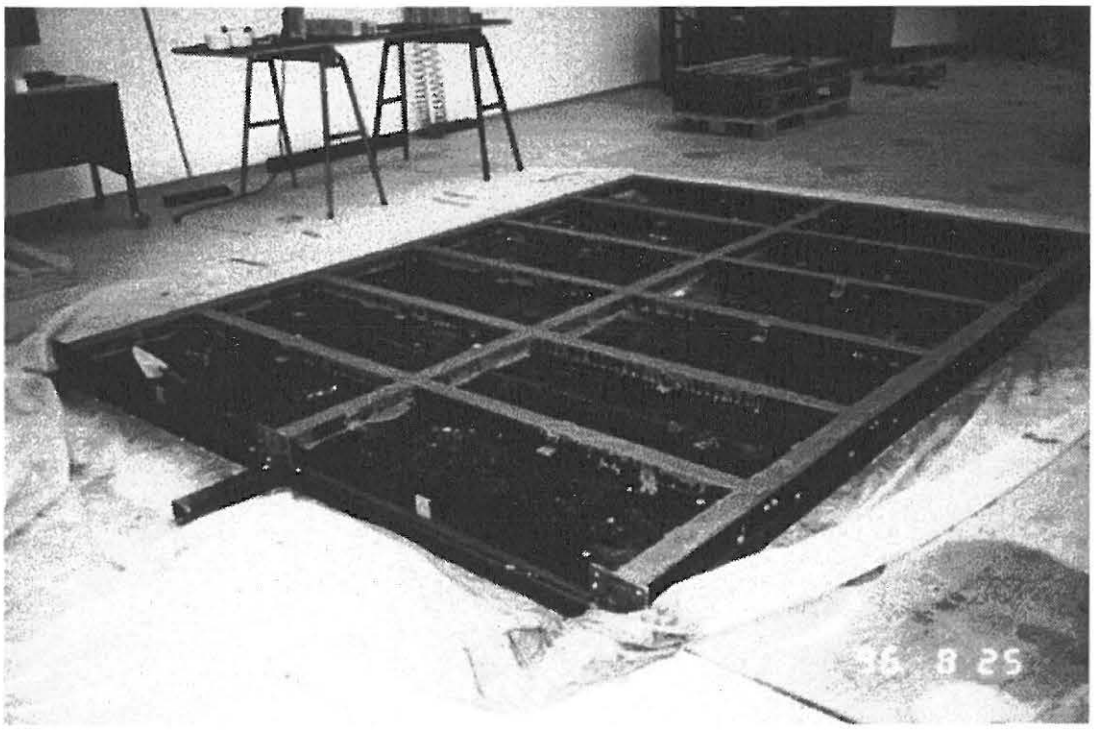

Figure A.4: The frame and form after pouring and vibrating of concrete.

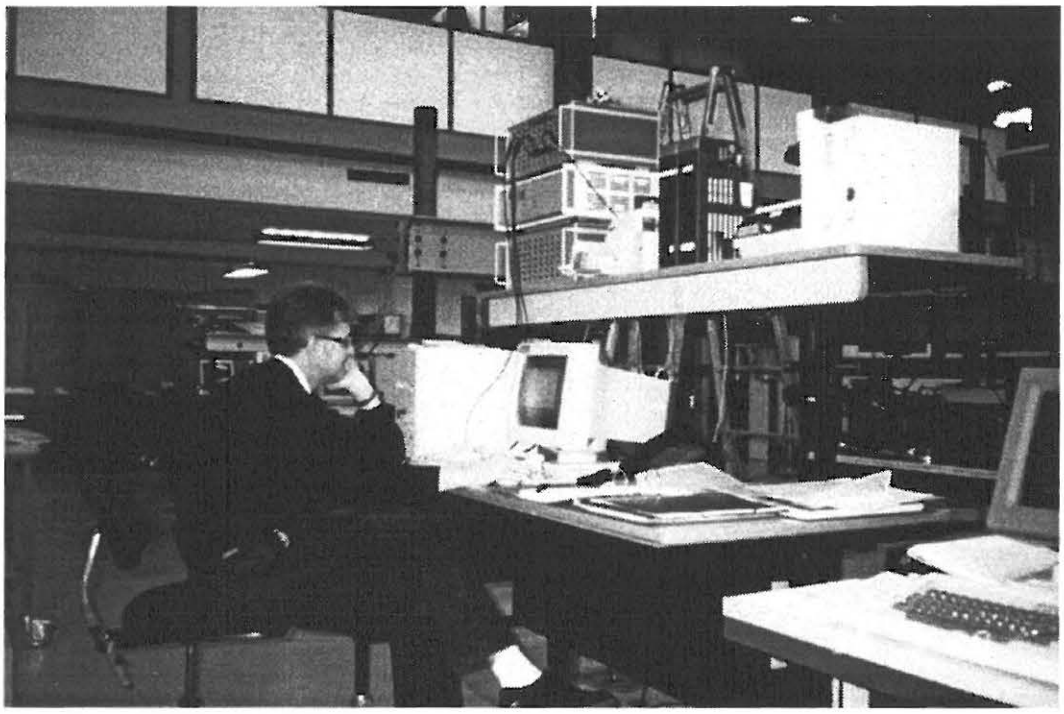

Figure A.5: Data aquisition system.

Figure A.6: Undamaged structure before testing. AAU1.

A.2 Destructive testing and damage evaluation

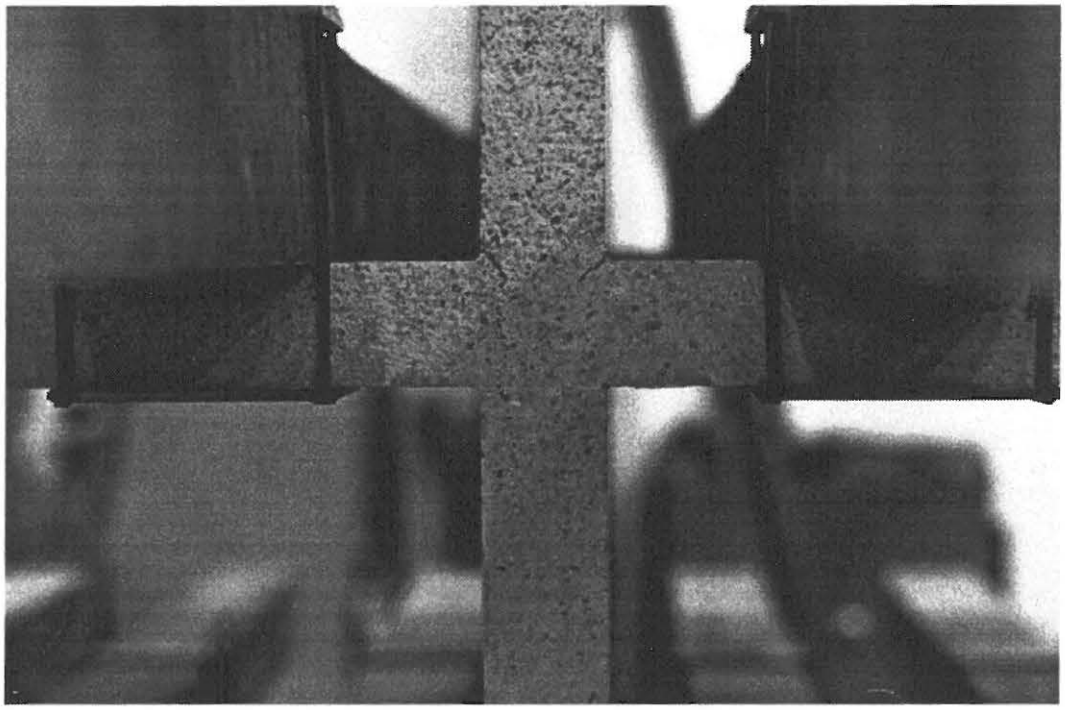

Figure A.7: Cracks in node 5 after EQ1. AAU1.

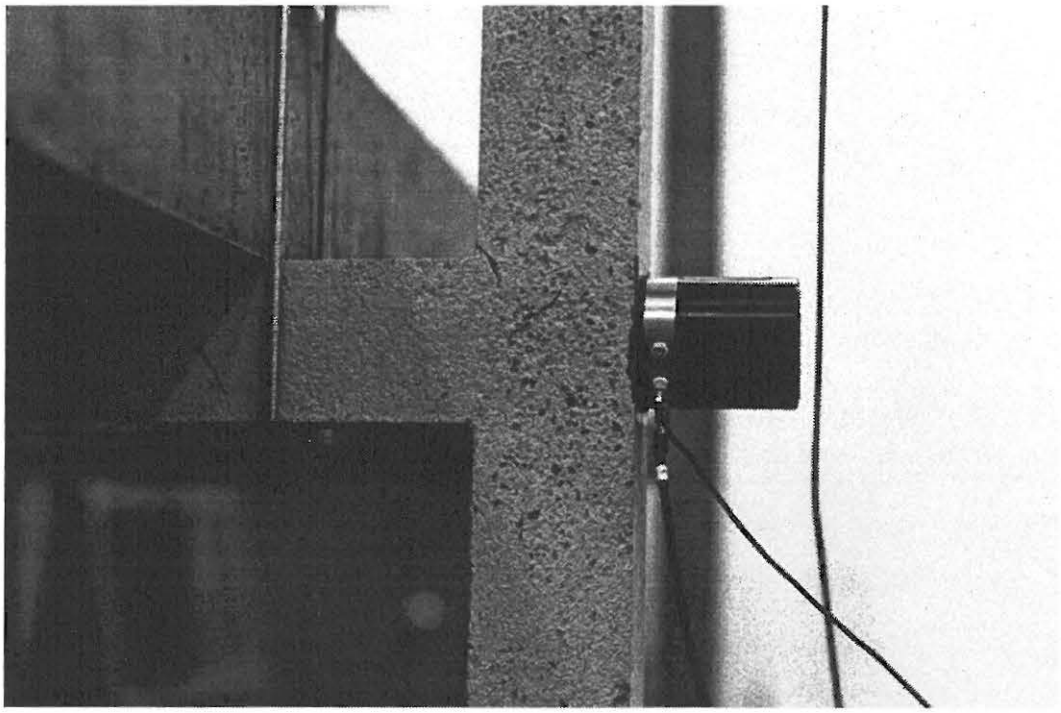

Figure A.8: Cracks in node 6 after EQ1. AAU1.

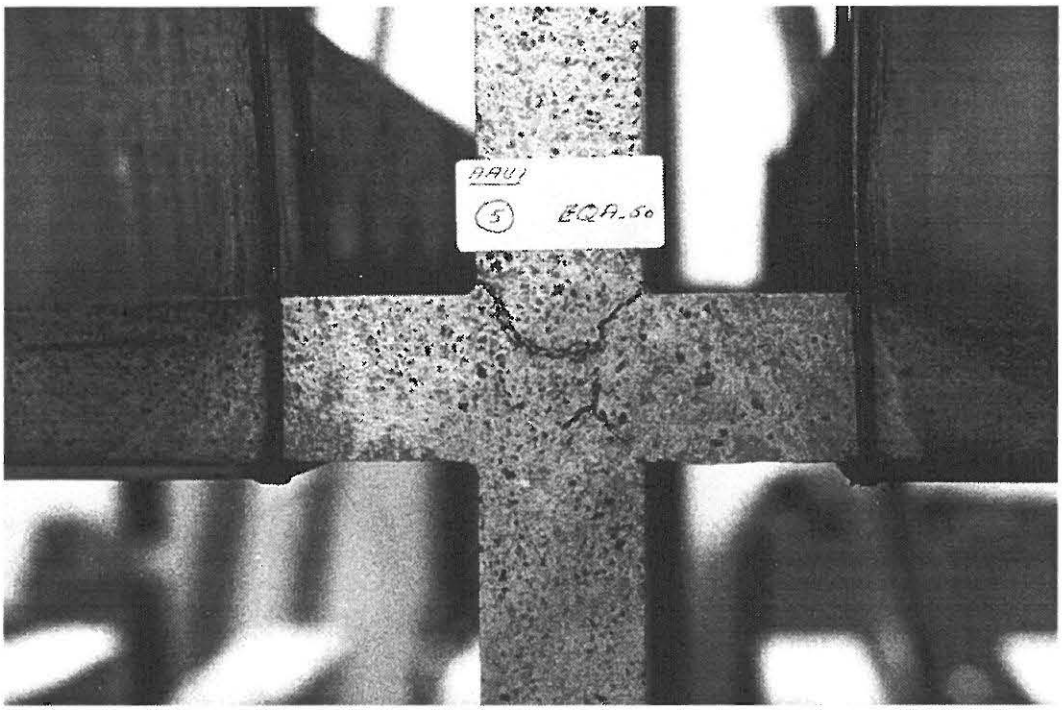

Figure A.9: Cracks in node 5 after EQ2. AAU1.

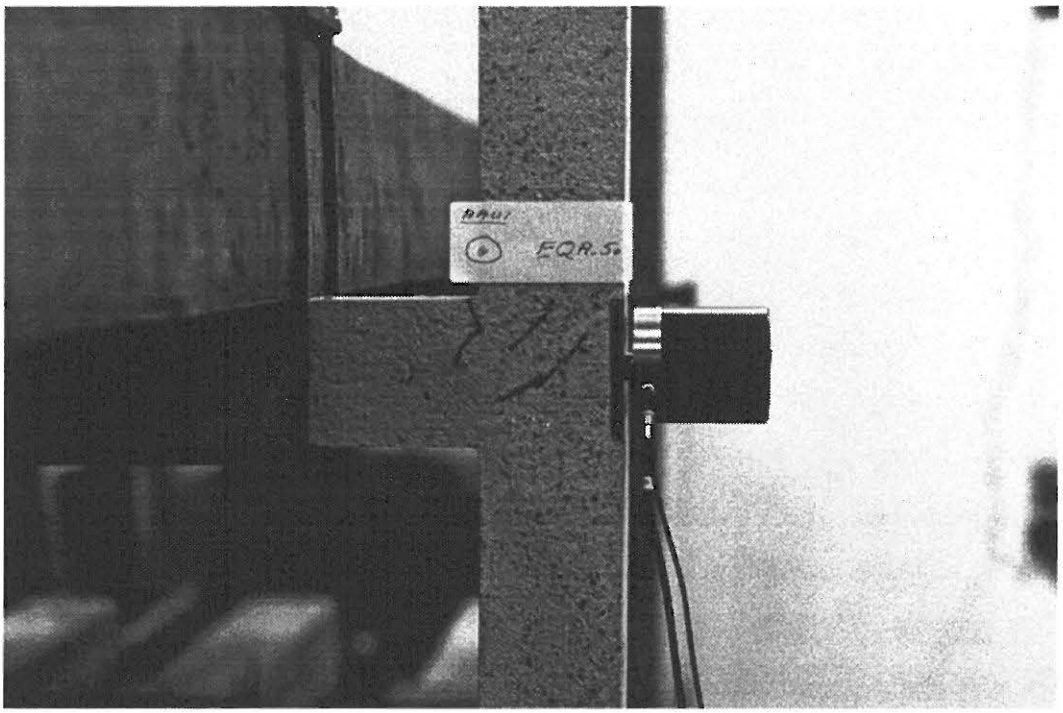

Figure A.10: Cracks in node 6 after EQ2. AAU1.

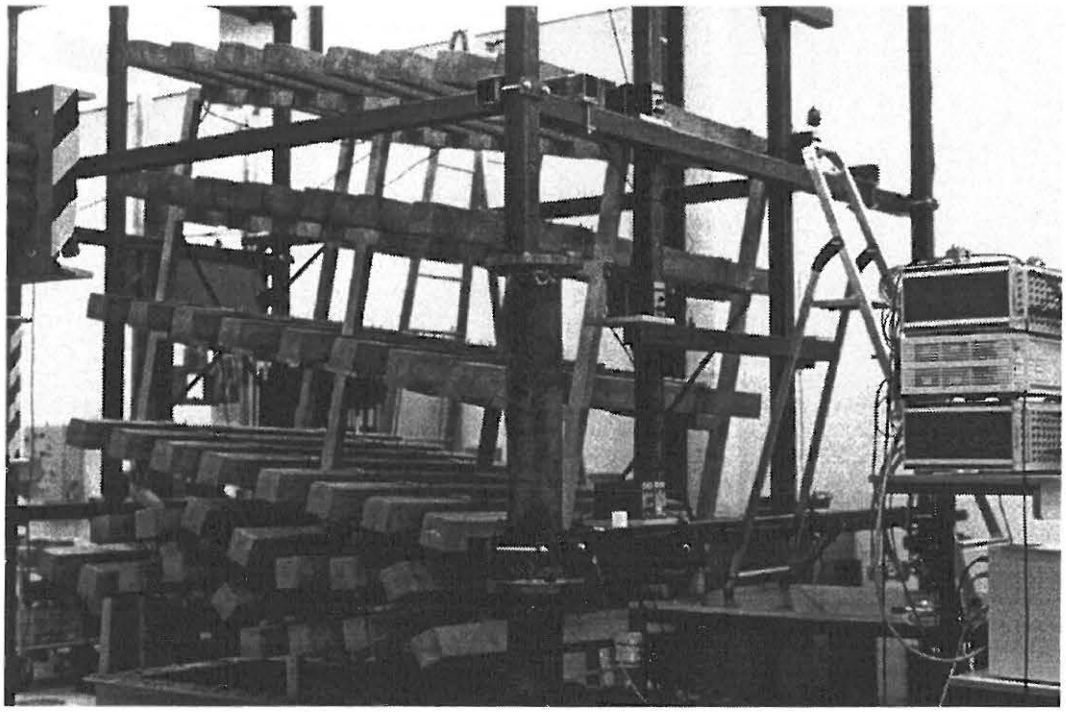

Figure A.11: Collapsed structure after EQ3. AAU1.

Figure A.12: Collapsed structure after EQ3. AAU1.

A.3 Static Testing

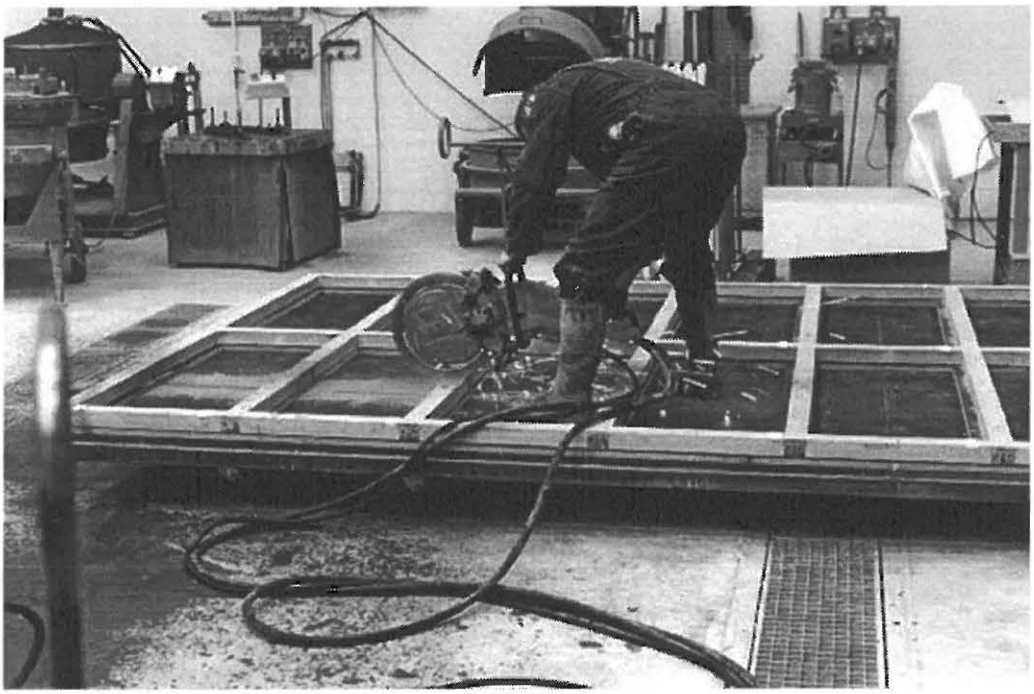

Figure A.13: Photo of the cutting.

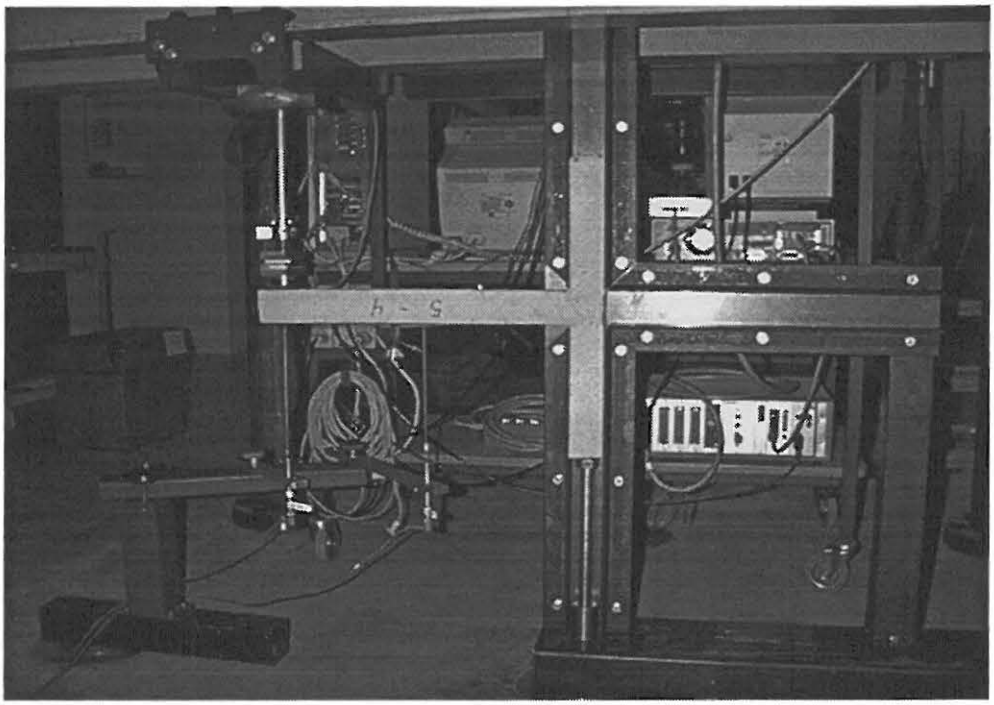

Figure A.14: Photo of the static test setup.

Figure A.15: Photo of the data acqusition system used for the static tests.

A.4 Visual inspection of AAU2 and AAU3

Figure A.16: Photos of all nodes in AAU2 after the last earthquake.

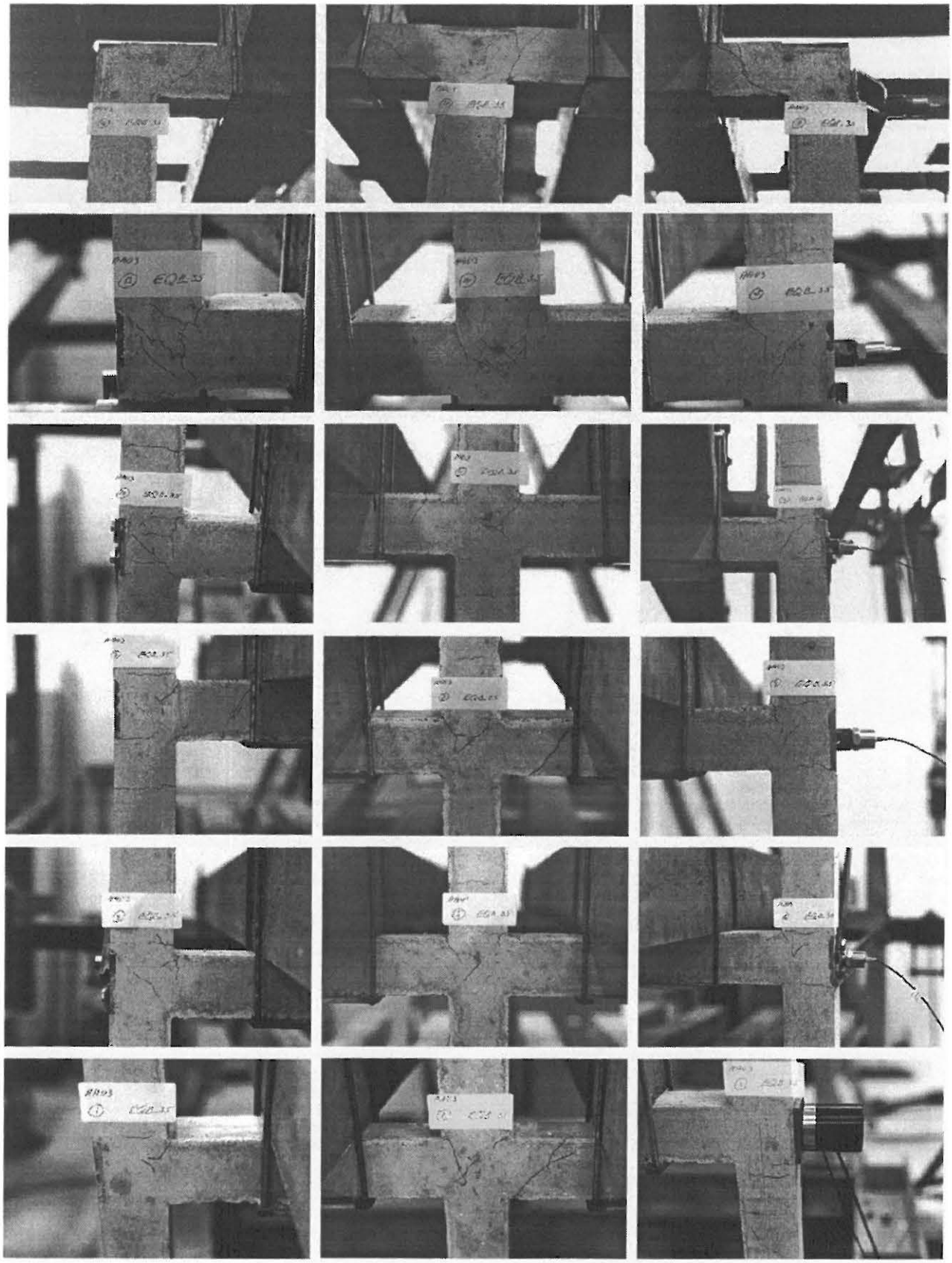

Figure A.17: Photos of all nodes in AAU3 after the last earthquake.

Appendix B

File Data Sheets

In this appendix the data sheets of all files are listed with all calibration factors, date of tests etc.

Data sheet no. 1.

Frame:	AAU1
Date:	111096
Sampling rate:	150 Hz
Number of points:	3000

Valid for the files:	
	fd1_b00.dat

Ch.	Amp.	LFL	UFL	Comments
1	10V/63kN	-	-	
2	10V/20mm	-	-	
3	$1V/ms^{-2}$	0.2 Hz	1 kHz	BK8306
4	$1V/ms^{-2}$	0.2 Hz	1 kHz	BK8306
5	$1V/ms^{-2}$	0.2 Hz	1 kHz	BK8306
6	$1V/ms^{-2}$	0.2 Hz	1 kHz	BK4370
7	$1V/ms^{-2}$	0.2 Hz	1 kHz	BK4370
8	$1V/ms^{-2}$	0.2 Hz	1 kHz	BK4370
9	$1V/ms^{-2}$	0.2 Hz	1 kHz	BK4370
10	1V/mm	1 Hz	1 kHz	BK4370
11	1V/mm	1 Hz	1kHz	BK4370
12	$0.956V/ms^{-2}$	-	-	K8304B2
13	$1V/ms^{-2}$	0.2 Hz	1 kHz	BK4371
14	$1V/ms^{-2}$	0.2 Hz	1 kHz	BK4371
15	$0.963V/ms^{-2}$	-	-	K8304B2
16	$1.027V/ms^{-2}$	-	-	K8304B2

Table B.1: *Data sheet 1.*

Data sheet no. 2.

Frame:	AAU1
Date:	251096
Sampling rate:	150 Hz
Number of points:	5000

Valid for the files:	
	fd1_b01.dat
	fd1_b02.dat
	fd1_b03.dat
	fd1_r01.dat
	fd1_r02.dat
	fd1_r03.dat
	fd1_r04.dat
	fd1_b04.dat
	fd1_r05.dat
	fd1_b05.dat

Ch.	Amp.	LFL	UFL	Comments
1	10V/63kN	-	-	
2	10V/20mm	-	-	
3	$1V/ms^{-2}$	0.2 Hz	1 kHz	BK8306
4	$1V/ms^{-2}$	0.2 Hz	1 kHz	BK8306
5	$1V/ms^{-2}$	0.2 Hz	1 kHz	BK8306
6	$1V/ms^{-2}$	0.2 Hz	1 kHz	BK4370
7	$1V/ms^{-2}$	0.2 Hz	1 kHz	BK4370
8	$1V/ms^{-2}$	0.2 Hz	1 kHz	BK4370
9	$1V/ms^{-2}$	0.2 Hz	1 kHz	BK4370
10	1V/mm	1 Hz	1 kHz	BK4370
11	1V/mm	1 Hz	1kHz	BK4370
12	$0.956V/ms^{-2}$	-	-	K8304B2
13	$1V/ms^{-2}$	0.2 Hz	1 kHz	BK4371
14	$1V/ms^{-2}$	0.2 Hz	1 kHz	BK4371
15	$0.963V/ms^{-2}$	-	-	K8304B2
16	$1.027V/ms^{-2}$	-	-	K8304B2

Table B.2: *Data sheet 2.*

Data sheet no. 3.

Frame:	AAU1
Date:	251096
Sampling rate:	150 Hz
Number of points:	6000

Valid for the files:	
	wm1_ta01.dat
	wm1_tb01.dat
	wm1_tc01.dat
	wm1_1a1.dat
	wm1_1a2.dat

Ch.	Amp.	LFL	UFL	Comments
1	10V/63kN	-	-	
2	10V/20mm	-	-	
3	$1V/ms^{-2}$	0.2 Hz	1 kHz	BK8306
4	$1V/ms^{-2}$	0.2 Hz	1 kHz	BK8306
5	$1V/ms^{-2}$	0.2 Hz	1 kHz	BK8306
6	$1V/ms^{-2}$	0.2 Hz	1 kHz	BK4370
7	$1V/ms^{-2}$	0.2 Hz	1 kHz	BK4370
8	$1V/ms^{-2}$	0.2 Hz	1 kHz	BK4370
9	$1V/ms^{-2}$	0.2 Hz	1 kHz	BK4370
10	1V/mm	1 Hz	1 kHz	BK4370
11	1V/mm	1 Hz	1kHz	BK4370
12	$0.956V/ms^{-2}$	-	-	K8304B2
13	$1V/ms^{-2}$	0.2 Hz	1 kHz	BK4371
14	$1V/ms^{-2}$	0.2 Hz	1 kHz	BK4371
15	$0.963V/ms^{-2}$	-	-	K8304B2
16	$1.027V/ms^{-2}$	-	-	K8304B2

Table B.3: *Data sheet 3.*

Data sheet no. 4.

Frame:	AAU1
Date:	281096-041196
Sampling rate:	150 Hz
Number of points:	6000

Valid for the files:	
	sm1_25a.dat

Ch.	Amp.	LFL	UFL	Comments
1	10V/63kN	-	-	
2	10V/20mm	-	-	
3	$1V/ms^{-2}$	0.2 Hz	1 kHz	BK8306
4	$1V/ms^{-2}$	0.2 Hz	1 kHz	BK8306
5	$1V/ms^{-2}$	0.2 Hz	1 kHz	BK8306
6	$1V/ms^{-2}$	0.2 Hz	1 kHz	BK4370
7	$1V/ms^{-2}$	0.2 Hz	1 kHz	BK4370
8	$1V/ms^{-2}$	0.2 Hz	1 kHz	BK4370
9	$1V/ms^{-2}$	0.2 Hz	1 kHz	BK4370
10	0.1V/mm	1 Hz	1 kHz	BK4370
11	0.1V/mm	1 Hz	1kHz	BK4370
12	$0.956V/ms^{-2}$	-	-	K8304B2
13	$1V/ms^{-2}$	0.2 Hz	1 kHz	BK4371
14	$1V/ms^{-2}$	0.2 Hz	1 kHz	BK4371
15	$0.963V/ms^{-2}$	-	-	K8304B2
16	$1.027V/ms^{-2}$	-	-	K8304B2

Table B.4: *Data sheet 4.*

Data sheet no. 5.

Frame:	AAU1
Date:	281096-041196
Sampling rate:	150 Hz
Number of points:	6000

Valid for the files:	
	sm1_50a.dat
	sm1_75a.dat

Ch.	Amp.	LFL	UFL	Comments
1	10V/63kN	-	-	
2	10V/20mm	-	-	
3	$1V/ms^{-2}$	0.2 Hz	1 kHz	BK8306
4	$1V/ms^{-2}$	0.2 Hz	1 kHz	BK8306
5	$1V/ms^{-2}$	0.2 Hz	1 kHz	BK8306
6	$1V/ms^{-2}$	0.2 Hz	1 kHz	BK4370
7	$1V/ms^{-2}$	0.2 Hz	1 kHz	BK4370
8	$1V/ms^{-2}$	0.2 Hz	1 kHz	BK4370
9	$1V/ms^{-2}$	0.2 Hz	1 kHz	BK4370
10	0.0316V/mm	1 Hz	1 kHz	BK4370
11	0.0316V/mm	1 Hz	1kHz	BK4370
12	$0.956V/ms^{-2}$	-	-	K8304B2
13	$1V/ms^{-2}$	0.2 Hz	1 kHz	BK4371
14	$1V/ms^{-2}$	0.2 Hz	1 kHz	BK4371
15	$0.963V/ms^{-2}$	-	-	K8304B2
16	$1.027V/ms^{-2}$	-	-	K8304B2

Table B.5: *Data sheet 5.*

Data sheet no. 6.

Frame:	AAU2
Date:	051296-121296
Sampling rate:	150 Hz
Number of points:	5000

Valid for the files:	
	fd2_b01.dat
	fd2_b02.dat
	fd2_b03.dat
	fd2_b04.dat
	fd2_b05.dat
	fd2_b06.dat
	fd2_b07.dat
	fd2_b08.dat

Ch.	Amp.	LFL	UFL	Comments
1	10V/63kN	-	-	
2	10V/20mm	-	-	
3	$1V/ms^{-2}$	- Hz	-	BK8306
4	$1V/ms^{-2}$	- Hz	-	BK8306
5	$1V/ms^{-2}$	0.2 Hz	1 kHz	BK4370
6	$1V/ms^{-2}$	0.2 Hz	1 kHz	BK4370
7	$1V/ms^{-2}$	0.2 Hz	1 kHz	BK4370
8	$1V/ms^{-2}$	0.2 Hz	1 kHz	BK4370
9	$1V/ms^{-2}$	0.2 Hz	1 kHz	BK4370
10	-	-	-	-
11	$1.027V/ms^{-2}$	-	-	K8304B2
12	$0.963V/ms^{-2}$	-	-	K8304B2
13	$0.956V/ms^{-2}$	-	-	K8304B2
14	$1.008V/ms^{-2}$	-	-	K8304B2
15	$0.963V/ms^{-2}$	-	-	K8304B2
16	$0.963V/ms^{-2}$	-	-	K8304B2

Table B.6: *Data sheet 6.*

Data sheet no. 7.

Frame:	AAU2
Date:	051296-121296
Sampling rate:	150 Hz
Number of points:	6000

Valid for the files:	
	wm2_ta05.dat
	wm2_tb05.dat
	wm2_tc05.dat
	sm2_20a.dat
	sm2_40a.dat

Ch.	Amp.	LFL	UFL	Comments
1	10V/63kN	-	-	
2	10V/20mm	-	-	
3	$1V/ms^{-2}$	- Hz	-	BK8306
4	$1V/ms^{-2}$	- Hz	-	BK8306
5	$1V/ms^{-2}$	0.2 Hz	1 kHz	BK4370
6	$1V/ms^{-2}$	0.2 Hz	1 kHz	BK4370
7	$1V/ms^{-2}$	0.2 Hz	1 kHz	BK4370
8	$1V/ms^{-2}$	0.2 Hz	1 kHz	BK4370
9	$1V/ms^{-2}$	0.2 Hz	1 kHz	BK4370
10	-	-	-	-
11	$1.027V/ms^{-2}$	-	-	K8304B2
12	$0.963V/ms^{-2}$	-	-	K8304B2
13	$0.956V/ms^{-2}$	-	-	K8304B2
14	$1.008V/ms^{-2}$	-	-	K8304B2
15	$0.963V/ms^{-2}$	-	-	K8304B2
16	$0.963V/ms^{-2}$	-	-	K8304B2

Table B.7: *Data sheet 7.*

FRACTURE AND DYNAMICS PAPERS

PAPER NO. 64: P. S. Skjærbæk, S. R. K. Nielsen, A. Ş. Çakmak: *Assessment of Damage in Seismically Excited RC-Structures from a Single Measured Response.* ISSN 1395-7953 R9528.

PAPER NO. 65: J. C. Asmussen, S. R. Ibrahim, R. Brincker: *Random Decrement and Regression Analysis of Traffic Responses of Bridges.* ISSN 1395-7953 R9529.

PAPER NO. 66: R. Brincker, P. Andersen, M. E. Martinez, F. Tallavó: *Modal Analysis of an Offshore Platform using Two Different ARMA Approaches.* ISSN 1395-7953 R9531.

PAPER NO. 67: J. C. Asmussen, R. Brincker: *Estimation of Frequency Response Functions by Random Decrement.* ISSN 1395-7953 R9532.

PAPER NO. 68: P. H. Kirkegaard, P. Andersen, R. Brincker: *Identification of an Equivalent Linear Model for a Non-Linear Time-Variant RC-Structure.* ISSN 1395-7953 R9533.

PAPER NO. 69: P. H. Kirkegaard, P. Andersen, R. Brincker: *Identification of the Skirt Piled Gullfaks C Gravity Platform using ARMAV Models.* ISSN 1395-7953 R9534.

PAPER NO. 70: P. H. Kirkegaard, P. Andersen, R. Brincker: *Identification of Civil Engineering Structures using Multivariate ARMAV and RARMAV Models.* ISSN 1395-7953 R9535.

PAPER NO. 71: P. Andersen, R. Brincker, P. H. Kirkegaard: *Theory of Covariance Equivalent ARMAV Models of Civil Engineering Structures.* ISSN 1395-7953 R9536.

PAPER NO. 72: S. R. Ibrahim, R. Brincker, J. C. Asmussen: *Modal Parameter Identification from Responses of General Unknown Random Inputs.*ISSN 1395-7953 R9544.

PAPER NO. 73: S. R. K. Nielsen, P. H. Kirkegaard: *Active Vibration Control of a Monopile Offshore Structure. Part One - Pilot Project.* ISSN 1395-7953 R9609.

PAPER NO. 74: J. P. Ulfkjær, L. Pilegaard Hansen, S. Qvist, S. H. Madsen: *Fracture Energy of Plain Concrete Beams at Different Rates of Loading.* ISSN 1395-7953 R9610.

PAPER NO 75: J. P. Ulfkjær, M. S. Henriksen, B. Aarup: *Experimental Investigation of the Fracture Behaviour of Reinforced Ultra High Strength Concrete.* ISSN 1395-7953 R9611.

PAPER NO. 76: J. C. Asmussen, P. Andersen: *Identification of EURO-SEIS Test Structure.* ISSN 1395-7953 R9612.

PAPER NO. 77: P. S. Skjærbæk, S. R. K. Nielsen, A. Ş. Çakmak: *Identification of Damage in RC-Structures from Earthquake Records - Optimal Location of Sensors.* ISSN 1395-7953 R9614.

PAPER NO. 78: P. Andersen, P. H. Kirkegaard, R. Brincker: *System Identification of Civil Engineering Structures using State Space and ARMAV Models.* ISSN 1395-7953 R9618.

PAPER NO. 79: P. H. Kirkegaard, P. S. Skjærbæk, P. Andersen: *Identification of Time Varying Civil Engineering Structures using Multivariate Recursive Time Domain Models.* ISSN 1395-7953 R9619.

PAPER NO. 80: J. C. Asmussen, R. Brincker: *Estimation of Correlation Functions by Random Decrement.* ISSN 1395-7953 R9624.

FRACTURE AND DYNAMICS PAPERS

PAPER NO. 81: M. S. Henriksen, J. P. Ulfkjær, R. Brincker: *Scale Effects and Transitional Failure Phenomena of Reinforced concrete Beams in Flexure. Part 1.* ISSN 1395-7953 R9628.

PAPER NO. 82: P. Andersen, P. H. Kirkegaard, R. Brincker: *Filtering out Environmental Effects in Damage Detection of Civil Engineering Structures.* ISSN 1395-7953 R9633.

PAPER NO. 83: P. S. Skjærbæk, S. R. K. Nielsen, P. H. Kirkegaard, A. Ş. Çakmak: *Case Study of Local Damage Indicators for a 2-Bay, 6-Storey RC-Frame subject to Earthquakes.* ISSN 1395-7953 R9639.

PAPER NO. 84: P. S. Skjærbæk, S. R. K. Nielsen, P. H. Kirkegaard, A. Ş. Çakmak: *Modal Identification of a Time-Invariant 6-Storey Model Test RC-Frame from Free Decay Tests using Multi-Variate Models.* ISSN 1395-7953 R9640.

PAPER NO. 85: P. H. Kirkegaard, P. S. Skjærbæk, S. R. K. Nielsen: *Identification Report: Earthquake Tests on 2-Bay, 6-Storey Scale 1:5 RC-Frames.* ISSN 1395-7953 R9703.

PAPER NO. 86: P. S. Skjærbæk, S. R. K. Nielsen, P. H. Kirkegaard: *Earthquake Tests on Scale 1:5 RC-Frames.* ISSN 1395-7953 R9713.

PAPER NO. 89: P. S. Skjærbæk, P. H. Kirkegaard, S. R. K. Nielsen: *Shaking Table Tests of Reinforced Concrete Frames.* ISSN 1395-7953 R9704.

PAPER NO. 91: P. S. Skjærbæk, P. H. Kirkegaard, G. N. Fouskitakis, S. D. Fassois: *Non-Stationary Modelling and Simulation of Near-Source Earthquake Ground Motion: ARMA and Neural Network Methods.* ISSN 1395-7953 R9641.

PAPER NO. 92: J. C. Asmussen, S. R. Ibrahim, R. Brincker: *Application of Vector Triggering Random Decrement.* ISSN 1395-7953 R9634.

PAPER NO. 93: S. R. Ibrahim, J. C. Asmussen, R. Brincker: *Theory of Vector Triggering Random Decrement.* ISSN 1395-7953 R9635.

PAPER NO. 94: R. Brincker, J. C. Asmussen: *Random Decrement Based FRF Estimation.* ISSN 1395-7953 R9636.

PAPER NO. 95: P. H. Kirkegaard, P. Andersen, R. Brincker: *Structural Time Domain Identification (STDI) Toolbox for Use with MATLAB.* ISSN 1395-7953 R9642.

PAPER NO. 96: P. H. Kirkegaard, P. Andersen: *State Space Identification of Civil Engineering Structures from Output Measurements.* ISSN 1395-7953 R9643.

PAPER NO. 97: P. Andersen, P. H. Kirkegaard, R. Brincker: *Structural Time Domain Identification Toolbox - for Use with MATLAB.* ISSN 1395-7953 R9701.

PAPER NO. 98: P. S. Skjærbæk, B. Taşkin, S. R. K. Nielsen, P. H. Kirkegaard: *An Experimental Study of a Midbroken 2-Bay, 6-Storey Reinforced Concrete Frame subject to Earthquakes.* ISSN 1395-7953 R9706.

PAPER NO. 99: PAPER NO. 98: P. S. Skjærbæk, S. R. K. Nielsen, P. H. Kirkegaard, B. Taşkin: *Earthquake Tests on Midbroken Scale 1:5 Reinforced Concrete Frames.* ISSN 1395-7953 R9712.

Department of Building Technology and Structural Engineering
Aalborg University, Sohngaardsholmsvej 57, DK 9000 Aalborg
Telephone: +45 9635 8080 Telefax: +45 9814 8243